Statistical analysis of body surface electrocardiographic maps in ischemic heart disease

by

Anthony James Bell MB BS FRACP

Faculty of Medicine and Pharmacy

Department of Medicine

submitted in fulfillment of the requirements

of the degree of

Doctor of Medicine

University of Tasmania

August 1993

This thesis contains no material that has been accepted for the award of any other higher degree or graduate diploma in any tertiary institution, and this thesis contains no material constructed by another person except where acknowledged.

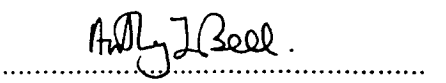

Anthony James Bell

Preface

After becoming interested in body surface mapping in the coronary care unit I came to realize that diagnosis of acute myocardial damage by body surface map was simple and appeared more accurate than with standard 12 lead electrocardiography. This applied especially late at night in the coronary care unit, when recorded maps lead to rapid accurate diagnosis. In fact, in a small number of patients with completely normal standard electrocardiograms, the body surface map showed a myocardial infarction. The method of body surface mapping was quick, efficient and clearly better than the standard methods in some cases. The body surface mapping method developed by Drs David Kilpatrick and Stephen Walker in the University of Tasmania clearly had clinical potential. Drs Kilpatrick and Walker taught me computer methods and provided the background knowledge to proceed with this thesis. This thesis attempts to demonstrate the clinical usefulness of body surface mapping.

The thesis is composed of 13 chapters. Chapters 1 to 5 are introductory in nature and outline the history and concept of body surface mapping, the changes in the standard electrocardiogram related to myocardial infarction, and summarize the statistical methods used in this thesis. After each chapter is an appendix which contains tables then the figures relevant to that chapter.

The clinical study chapters - 6 through 12 - have the same format. There is an introduction reviewing the clinical problem followed by a brief methods section. The results are presented then discussed with reference to the literature on the subject. Each chapter is followed by an appendix section containing the tables and then the figures for that chapter.

Chapters 6, 7 and 8 study patients with acute inferior wall myocardial

infarction. Chapter 6 is a combined effort of Dr S. J. Walker, Dr M. G. Loughhead, Dr D. Kilpatrick and myself. The initial idea of the interpretation of the ST segment body surface maps was conceived by Dr M. G. Loughhead and Dr D. Kilpatrick. The study subgroups patients with acute inferior wall myocardial infarction and relates the body surface map appearance to the prognosis in a learning and test set of patients. The data has been published as two papers. (Walker SJ, Bell AJ, Loughhead MG, Lavercombe PS, Kilpatrick D: Spatial distribution and prognostic significance of ST segment potentials in acute inferior infarction determined by body surface mapping. Circulation 1987;76:289-297 and Bell AJ, Loughhead MG, Walker SJ, Kilpatrick D: Prognostic significance of ST potentials determined by body surface mapping in inferior wall acute myocardial infarction. Am J Cardiol 1989;64:319-323)

Chapter 7 studies the natural history of the body surface map in inferior wall myocardial infarction and relates the natural history to the prognosis. This study has been published. (Bell AJ, Walker SJ, Kilpatrick D: Natural history of ST-segment potential distribution determined by body surface mapping in patients with acute inferior infarction. J Electrocardiol 1989;22:333-341)

Chapter 8 relates the ST segment body surface map to the loss of QRS complex voltage in acute inferior wall myocardial infarction. This study is derived from work by Dr D. Kilpatrick and myself in which Dr Kilpatrick is the major author. The chapter is included for completeness. The work has been published. (Kilpatrick D, Bell AJ: The relationship of ST elevation to eventual QRS loss in acute inferior myocardial infarction. J Electrocardiol 1989;22:343-348)

Chapter 9 studies the body surface map in acute anterior wall myocardial infarction and relates the map to prognosis.

Chapter 10 examines the relationship of the ST segment map to the loss of QRS

voltage in acute anterior wall myocardial infarction. (Bell AJ, Nichols P, Briggs C, Kilpatrick D: Prognostic significance of ST potentials determined by body surface mapping in anterior wall acute myocardial infarction. J Electrocardiol (1993 in press))

Chapter 11 studies the body surface map in patients with a normal electrocardiogram with or without coronary artery disease. The patients all underwent coronary angiography to determine the presence or absence of coronary artery disease. The studies determined if detailed analysis of the body surface map would detect coronary artery disease in patients with no history of myocardial damage. The mathematics and computer program for the Eigenvector method was developed in the University of Tasmania by Ms Lydia Piggot specifically for this purpose

Chapter 12 is a study of the accuracy of the body surface map and the inverse transformation in predicting the loss of myocardial cells as measured by thallium scanning. (Bell AJ, Ryan A, Ware R, Walker SJ, Kilpatrick D: Derived epicardial ST segment potential distribution compared to the resting distribution of thallium scintigraphic defect in acute myocardial infarction. Am J Noninvas Cardiol 1991; 5: 273-279). This chapter leads into a new area of body surface mapping, the clinical application of the inverse transformation.

Chapter 13 summarizes the thesis and plans new directions and applications for body surface mapping.

The list of references used is documented after chapter 13.

The appendix after the bibliography contains the more recent papers published on body surface mapping by myself and Dr. Kilpatrick.

These studies would not have been possible without the assistance of the consultant and resident staff of the Royal Hobart Hospital and the nursing staff of

the Coronary Care Unit in the Department of Critical Care Medicine. Special thanks are due to the dedicated "mappers" Dr A. Duffield, Dr W. Herbert, Sr J. Walsh and Sr C. Briggs.

Dr David Kilpatrick has been outstanding as my supervisor in the project and I give him special thanks. Dr. Stephen Walker deserves special thanks for teaching me that computers are useful. Many thanks to my family especially Suzanne.

Abstract

Body surface electrocardiographic mapping is a technique for recording the thoracic electrical potentials generated by the cardiac cycle and transmitted to the body surface. The body surface map emphasizes the spatial distribution of the cardiac electrical potentials rather than the time magnitude relationship of the standard electrocardiogram. The body surface map contains more information than the standard electrocardiogram and in a different format. This thesis addresses the following questions:

1. is the additional information contained in the body surface map of clinical significance in myocardial infarction ?
2. is the display format and thus the application of topographical statistics of clinical benefit in myocardial infarction?
3. is the addition information able to detect coronary artery disease in patients presenting with chest pain ?

Detailed analysis of the body surface map in acute inferior wall myocardial infarction predicted the clinical course of the patient, one map pattern being associated with a high mortality and morbidity, giving a guideline to immediate therapy. The area of ST segment elevation corresponds to the the area of eventual Q wave formation in acute inferior wall myocardial infarction. Thus the body surface map may be useful in assessing reperfusion by thrombolytic agents in acute myocardial infarction.

In acute anterior wall myocardial infarction the body surface map was diagnostic but only moderately predictive of the eventual outcome. Again the area of ST segment elevation matched the area of Q wave formation and thus the body surface map may be of value in assessing reperfusion.

The body surface mapping was unable to differentiate patients with and without coronary artery disease who had normal standard electrocardiograms. The body surface map was useful in differentiating patients with acute or old myocardial infarction from normal patients but did not detect coronary artery disease in the absence of myocardial damage.

The information content of the body surface is increased if an accurate inverse transformation can be used to calculate the epicardial potentials in the clinical situation. To prove that epicardial potentials are accurately calculated, comparison of the area of myocardial damage to the calculated epicardial area of ST segment elevation was made using thallium scanning. This demonstrated a good correlation demonstrating that the inverse transformation was accurate. The technique is adding a new dimension to the understanding of the origin of the electrocardiogram.

Body surface mapping is an easily performed clinical investigation that adds information in the assessment of the patients with myocardial infarction.

Table of Contents

Table of Contents

Chapter 1

History of and introduction to body surface electrocardiographic mapping

A brief history of body surface electrocardiographic mapping

The electrocardiogram has been a major tool in the diagnosis of coronary artery disease for over 75 years. Since the initial recording of the human electrocardiogram by Waller in 1887 [Waller 1887], the development of the string galvanometer in 1913 [Einthoven 1913] and the advancement of the PQRST terminology to describe the electrocardiogram by Einthoven [Cooper 1986] enabled the electrocardiogram to become a standard tool in clinical cardiology.

As early as 1888 Waller had sketched the electrical potential over the entire thoracic surface of man. The recording and displaying of the entire thoracic electrocardiographic potential became known as body surface mapping. The first simultaneous recording over the thoracic surface was by Nahum et al. in 1951 [Nahum 1951]. In 1965, Taccardi and his team at the University of Parma, Italy, published hand drawn isopotential maps of the surface distribution during the QRS complex [Taccardi 1963]. These workers had manually recorded 80-600 electrocardiographic leads in patients then constructed hand drawn isopotential maps. Horan et al. developed a belt system [Horan 1963], derived from the work of Nelson [Nelson 1957], to record the potentials of the torso of a dog, and used a small computer to plot isopotential body surface maps.

In recent years with the introduction of multi-channel recorders, computerized data analysis and graphics, the methods of body surface electrocardiographic map recording have become simpler. Many groups have now studied body surface electrocardiographic maps in relationship to normal cardiac physiology and cardiac pathophysiology. Normal atrial activation and recovery [Mirvis 1980, Taccardi 1966, Spach 1969], ventricular activation [Eddlemon 1968, Taccardi 1966, Olliff 1972, Young 1974], and ventricular repolarization [Green 1985, Taccardi 1966,

Spach 1979a, Spach 1979b, Abildskov 1976] have been well described. The body surface map in myocardial infarction has been described by many workers [Flowers 1976a, Vincent 1977, Flowers 1976b, Toyama 1980, Pham-Huy 1981], but the early map changes in acute myocardial infarction have been less well studied [Muller 1978, Maroko 1972, Muller 1975, Selwyn 1977, Mirvis 1977] . The early studies of the body surface map changes in acute myocardial infarction used maps recorded hours after the onset of acute myocardial infarction. For example, the study of Montague et al. recorded maps from patients a mean of 76 hours after the onset of acute myocardial infarction [Montague 1983]. The early changes of acute myocardial infarction, although well described for the 12 lead (standard) electrocardiogram, have never been examined in detail in large numbers of patients.

The concept of the body surface electrocardiographic map

The body surface electrocardiographic map is the measurement of the heart's electrical activity as manifest on the surface of the body. The body surface electrocardiographic map is displayed as the contours connecting identical potentials on the body surface occurring at a certain time point in the cardiac cycle. The potentials are all referred to a reference potential commonly Wilson's central terminal. A time component is added by using a series of body surface electrocardiographic maps each showing the entire thoracic surface recording at each time over the total cardiac cycle. On the other hand the standard electrocardiogram records the electrical potentials at 12 sites on the body surface and displays the potential over time. The concept that the body surface electrocardiographic map shows the complete body surface potential generated by the heart at a single time, as compared to the standard electrocardiogram which shows the potential generated at a particular site on the thorax over the whole cardiac cycle, is important for

understanding the body surface map. The body surface map is a spatial electrocardiogram with the emphasis on the distribution of potentials. The standard electrocardiogram is a time magnitude recording of the cardiac electrical field at particular body surface sites.

Advantages of body surface electrocardiographic map

Mirvis has recently reviewed the presumed advantages of body surface mapping over standard electrocardiography [Mirvis 1987]. These include the following features:

1: analysis of spatial as well as temporal features of the cardiac electrical cycle;

2: detection of information not projected to localized torso regions; and

3: the close correlation of body surface map information and epimyocardial events [Myerburg 1989].

In spite of the theoretical and practical advantages of body surface mapping in chronic myocardial infarction and exercise testing, body surface mapping has not become the clinical gold standard in electrocardiography. Indeed the acceptance of body surface mapping has been limited [Mirvis 1987].

The aim of this study

The aim of this research is to describe accurately the clinical usefulness of the body surface map in ischemic heart disease. The studies set out to describe the initial body surface map in inferior wall and anterior wall acute myocardial infarction including the clinical correlations. The studies test the capability of the body surface map to differentiate patients with coronary artery disease from patients without coronary artery disease and to detect myocardial infarction in the initial body surface map. The thesis examines future methods of improving interpretation of the body

surface map using the inverse transformation [Spach 1979a].

These studies provide the answer to the more general question regarding body surface mapping: is body surface mapping of value in clinical medicine?

Chapter 2

Electrocardiographic changes

in acute myocardial infarction

Introduction to the electrocardiogram

The electrocardiogram is a measurement on the body surface of the electrical activation and the electrical recovery of the heart. The electrical potentials measured by the electrocardiogram are generated by the heart and are due to cellular membrane ion fluxes. The ion flux generates a current which in turn generates extracellular fields within and on the surface of the body. The cardiac current flow causes the electrocardiographic potentials on the skin surface, measured by the electrocardiogram. Each electrocardiographic measurement is the potential difference between two points on the skin surface measured over a complete cardiac cycle of depolarization and repolarization. In humans the heart is usually in a constant position in the thorax, has a constant structure and generates a consistent current flow, and therefore the electrocardiogram is of a uniform nature. By using consistent body surface sites to measure the cardiac generation of electrical potentials, an electrocardiogram of constant pattern is obtained. Alterations in the heart tissue lead to changes in the electrical current generated by the heart. The electrical potential changes are measured by the electrocardiogram and correlate to changes in the heart structure and function. Over the last 100 years studies correlating the changes in the electrocardiogram with types of heart disease have developed the electrocardiogram into a powerful diagnostic tool. For example, the initial and characteristic changes in the electrocardiogram during acute myocardial infarction are used to diagnose and plan treatment for the patient.

The standard electrocardiogram measures 12 potentials on the body surface. The body surface electrocardiographic map measures between 36 and 196 potentials on the surface of the body. Thus the body surface map details the cardiac generated electrical potentials over the thorax to a much greater extent than the standard electrocardiogram.

Terminology describing the electrocardiogram

The electrocardiogram consists of 12 measurements of electrical potential differences. Each measurement is between two points on the skin surface. Each site of measurement is called an electrocardiographic lead. The various features of an electrocardiographic lead are named as shown in figure 1. The initial wave, the P wave, is the electrical potential measure at the time of atrial depolarization. The QRS deflection is the electrical depolarization of the ventricular muscle: the Q wave is an initial negative deflection in the QRS deflection; the R wave is the initial positive deflection in the QRS complex; and the S wave is a negative deflection after a positive deflection. An R' is a second positive deflection. An S' is a further negative deflection following a previous S wave. The T wave is the repolarization of the ventricular muscle. The segment of the electrocardiogram between the P wave and the QRS deflection is the PR interval. The segment between the QRS deflection and the T wave is the ST segment. The segment between the T wave and the P wave of the next beat is the TP segment. The J point is the point at which the QRS deflection becomes the ST segment.

The baseline or zero potential of the electrocardiogram

The true baseline (zero potential) of the electrocardiogram occurs when all the myocardial fibres are at rest and thus potential differences between areas of the heart are absent. This condition occurs in normal hearts when the cell membranes are polarized and awaiting depolarization in the TP segment. There is no absolute reference value for the baseline in the electrocardiogram because the measured electrocardiogram is recorded by alternating current amplifiers. This gives the potential difference between two points on the skin with the elimination of the direct

current electrical component. The use of alternating current amplifiers means that the signal is recorded about zero and that actual potential differences existing during the TP, PQ, and ST intervals cannot be derived. The difference between the steady levels, for example the ST-TP difference, can be measured but whether the difference is due to primary ST elevation or TP depression would require direct current amplifiers to elicit. This has relevance for this thesis in which ST changes are of major importance.

The generation of the cardiac electrical field

Electrocardiographic potentials arise from ion fluxes that occur during depolarization and repolarization of myocardial cells. The alteration of the electric potentials is known as the action potential. The action potential of a single myocardial cell is shown in figure 2. These intracellular ionic currents generate extracellular potential fields on and around the heart and thus on the surface of the body. A complete discussion of the generation of the electrocardiogram is beyond the scope of this thesis.

The measured potentials of the body surface electrocardiogram are influenced by many factors. The initial factor is the generation of the cardiac current flow known in total as the cardiac generator as shown in figure 3 [Mirvis 1988].

The action potential of the heart cells is caused by movement of ions across the cell boundaries resulting in potential differences between the inside and outside of the cell. During cardiac excitation intracellular potentials exist between electrically connected cells. Each cell is surrounded by a relatively impermeable high resistance membrane. This cell structure favours conduction through one end of the cell to the end of the next cell. Thus current flow is along the direction of the fibre. With cell excitation extracellular potential gradients exist. The depolarized cell has a less

negative potential than the neighbouring cells in the rest phase. Current flows in the intracellular space through the cell connections from regions of higher to regions of lower potential. The intracellular current flow determines the extracellular potentials [Spach 1979a]. The extracellular potentials are transmitted to the body surface as a potential of about 1% of the amplitude of the transmembrane voltages. The transmitted potentials have a relationship to the cardiac events although the relationship is influenced by factors that alter the transmission to the body surface (figure 3) [Mirvis 1988a].

The QRS complex in the electrocardiogram

The QRS complex arises from the excitation of the ventricular muscle. In the normal heart the cardiac electrical conducting system causes the cardiac muscle to be excited almost simultaneously at a number of right and left ventricular sites. Each muscle fibre undergoes an electrical discharge known as the action potential. The QRS complex of the electrocardiogram represents the depolarization of all the ventricular muscle with each electrocardiographic lead recording at that body surface site the sum of the electrical potential differences generated by cellular depolarization. The general pattern of the QRS complex is dependent on the heart geometry, depolarization sequence, body tissue conduction and the shape of the body surface (figure 3).

The ST segment in the electrocardiogram

The ST segment is a quiescent period after the QRS deflection (depolarization) and before the T wave deflection (repolarization). The ST segment represents the phase of slow repolarization of the cardiac muscle cells. The isoelectric course of the ST segment is caused by the relatively long flat slope of ventricular repolarization as

shown in the action potential of a single muscle fibre (figure 2). The absence of ST segment deviation from the baseline implies the absence of significant current flow during slow ventricular repolarization. This condition is not always fulfilled. If there is a slight difference between cells in the timing of the end of the QRS complex then there is J point deviation and early deviation of the ST segment. As a result the ST segment deviation is usually measured 80 milliseconds from the J point.

The duration of the ST segment tends to parallel the duration of the action potential. Rate dependent changes in the duration of the ST segment reflect rate dependent changes in the duration of the ventricular action potential [Lepeschkin 1953]. The duration of the ST segment may vary with disorders of calcium, thyroid activity and catecholamine levels.

Normal values for the deviation of the ST segment from the TP segment (the zero potential reference) are less than 20 μV for the limb leads and higher in the precordial leads. The normal precordial lead values range from lead V1 averaging 50 ± 30 μV, lead V2 averaging 100 ± 60 μV to lead V6 averaging 10 ± 10 μV.

The T wave in the electrocardiogram

The T wave is caused by the repolarization of the action potential between cells. The T wave pattern is directly related to the activation sequence of the heart, the intrinsic cardiac properties and the transmission factors. Although repolarization is a nonpropogated phenomenon there is a link to depolarization, that is, the activation sequence of the heart determines to some extent the recovery pattern of the heart. The net result is that repolarization forces are a result of activation sequence and intrinsic repolarization properties [Abildskov 1971, Horan 1978].

The electrocardiogram in acute myocardial infarction

QRS changes

In myocardial infarction there is a loss of myocardial tissue. The loss of tissue, with replacement of the electrically active tissue by electrically inert tissue, alters the QRS complex. The loss of tissue results in the loss of the electrical forces in the region of the infarction. A recording electrode may record an alteration in electric potentials. The summation of all the electrical forces remaining may be negative, causing the initial deflection of the recording to be negative and creating the initial Q wave characteristic of acute myocardial infarction. However if the summation of the remaining voltages remains positive a reduced voltage is recorded. Thus loss of R wave height is a marker of myocardial infarction on the standard electrocardiogram. The most obvious sign of acute myocardial infarction is the development of new Q waves, while reduction in the R wave magnitude is a less obvious sign of acute myocardial infarction [Horan 1971]. Distinguishing a normal R wave from a reduced R wave in acute myocardial infarction is difficult, especially when a pre-infarction electrocardiogram is not available.

The loss of QRS complex is related to the site and the size of the myocardial damage [Bar 1984]. There may be associated loss of conduction through damage to specialized cardiac electrical conduction system fibres, with further distortion of the QRS complex. The classical standard 12 lead electrocardiogram finding of pathological Q waves occurs when the infarction involves tissue which is depolarized in the first 40 milliseconds of the onset of the QRS complex. Otherwise the infarction pattern is found as a notching of the R wave or loss of R wave voltage. The position of the lead showing the loss of R wave or Q wave development has a relationship to the area and size of the myocardial damage.

Unfortunately the situation is not clear-cut. In non-transmural acute myocardial

infarction Q wave formation occurs though the Q wave formation may not be detected by the standard 12 lead electrocardiogram; but it may be detected by body surface mapping [Montague 1986]. This is thought to be due to delayed activation of the area of damaged muscle such that the area was electrically silent at the onset of the QRS complex [Miller 1978, Daniel 1971].

ST segment changes

ST segment displacement is due to either systolic or diastolic injury currents or both. The systolic injury current is due to the shortening and decreased amplitude of the action potential after injury. This causes intracellular systolic currents to flow from the normal to ischaemic areas, a true ST segment elevation. Secondly loss of resting membrane potential produces a diastolic injury current flow in the intracellular spaces from the ischaemic to the normal cells, which is true TP depression but registers on the standard electrocardiogram as ST segment elevation. TP segment depression is recorded on the electrocardiogram as ST segment elevation because the TP segment is the baseline (zero) potential against which other potentials are measured.

The course of the true ST segment elevation component is different from the initial ST segment elevation due to TP depression. The systolic component (true ST segment elevation) is initially present, peaks at around 5 minutes after arterial occlusion then recovers after 1 hour [Kleber 1978, Janse 1981]. The result is a rapid onset of ST segment elevation. At 2 hours after arterial occlusion the systolic (true ST segment elevation) and diastolic (TP depression) components are approximately equal [Kleber 1978, Cohen 1975]. The ST segment elevation then declines due to a decrease in the current flow, return of excitability and cellular uncoupling with total loss of cellular electrical activity.

The type of ST segment deviation that occurs with myocardial injury varies with the site of the injury. The usual explanation for this phenomenon is that in subendocardial damage in the anterior wall of the heart the current flow is away from the recording electrode on the anterior chest wall and thus there is ST segment depression. If the injury involves the epicardial surface then the current flow during the ST segment is towards an overlying electrode and ST segment elevation is seen [Macfarlane 1989].

Associated with ischaemia there is a conduction velocity decrease and activation of the ischaemic myocardial is delayed. Repolarization of damaged tissue is altered, with the differences between the ischaemic and non-ischaemic action potentials causing secondary T wave changes. The delayed activation may cause the T wave inversion.

ST segment change indicates the area of infarction and size of infarction

Although there is a general relationship between the cardiac site of a myocardial infarction and the site of the abnormal standard electrocardiogram leads, the localization of the site of a myocardial infarction by standard electrocardiograms is poor. This relates to the variability of the arterial supply to the heart, to the presence or absence of collateral vessels, and to differences in the shape of the heart, lungs and thorax in different people. For example, angioplasty studies have shown that occlusion of the left anterior descending artery can produce ST segment elevation if the collateral flow is poor and ST segment depression if the collateral flow is good [MacDonald 1986]. There should be a relationship between the ST segment change and the QRS change after myocardial infarction [Klainman 1987]. A rough correlation has been shown with anterior wall acute myocardial infarction in the standard 12 lead electrocardiogram [Selwyn 1978, Henning 1978, Essen 1980,

Zmyslinski 1979].

Reciprocal ST segment changes

ST segment depression always occurs in the presence of ST segment elevation and can be either the result of the process which caused the injury current responsible for the ST segment elevation (true reciprocal ST segment depression), or due to the presence of an additional area of injury in another location in the heart causing primary ST segment depression. There has been debate about the prognostic value of detection of reciprocal change in the ST segment for acute inferior wall myocardial infarction [Roubin 1984, Wasserman 1983, Croft 1984, Shah 1980. Cohen 1984, Ferguson 1984, Goldberg 1981, Gibson 1982, Gelman 1982. Lembo 1986, Stafford 1986, Hlatky 1985] and for acute anterior wall myocardial infarction [Myers 1949, Pichler 1983, Haraphongse 1984, Quyyumi 1986].

Persistent ST segment elevation after myocardial infarction

In 60% of acute anterior wall myocardial infarction and 5% of acute inferior wall myocardial infarction there is persistent ST segment elevation [Shah 1980]. The ST segment elevation is related to an area of the myocardium with asynergy [Bar 1984]. The persistence of the ST segment elevation relates to dyskinesis [Arvan 1984]. The aetiology of the persistent ST segment elevation is unknown.

Further clinical causes of ST segment elevation

The usually encountered cause of ST segment elevation is acute full wall thickness myocardial infarction. Other causes include normal variant ST segment elevation, subepicardial injury, full thickness myocardial ischaemia (angina variant). conduction defects and pericarditis [Macfarlane 1989].

Secondary ST segment deviations

These deviations relate to changes in the uniformity of depolarization and repolarization that can occur with conduction delays. Such changes are usually associated with T wave variation due to the lack of uniformity in the repolarization of the heart muscle [Macfarlane 1988].

Normal variant ST segment elevation

This implies that the ST segment shift is due to the shortening of the ventricular action potentials in some epicardial regions. The condition is found in normal people, more so in blacks, and is not associated with a worse prognosis in the individual [Kambara 1976, Spodick 1976]. Isoproterenol and exercise may abolish the ST segment elevation by abolishing the differences between action potentials [Spodick 1976, Morace 1979].

Pericarditis

Pericarditis is similar to normal variant ST segment elevation but the inscription of the QRS has not returned to the normal baseline by the start of the ST segment [Spodick 1976, Surawicz 1970]. The ST segment elevation in pericarditis is usually present in both limb leads and pericardial leads. The electrocardiographic record of normal variant angina usually shows a regional distribution due to the regional alteration in blood flow. The extent of the ST segment elevation in pericarditis is a clue to the diagnosis [Spodick 1976].

Summary

The electrocardiographic changes related to myocardial cell ischaemia and infarction are well described. The aetiology of the changes is not well described or understood and is beyond the scope of this thesis.

Figure 1 : Terminology used to describe the normal electrocardiogram wave forms

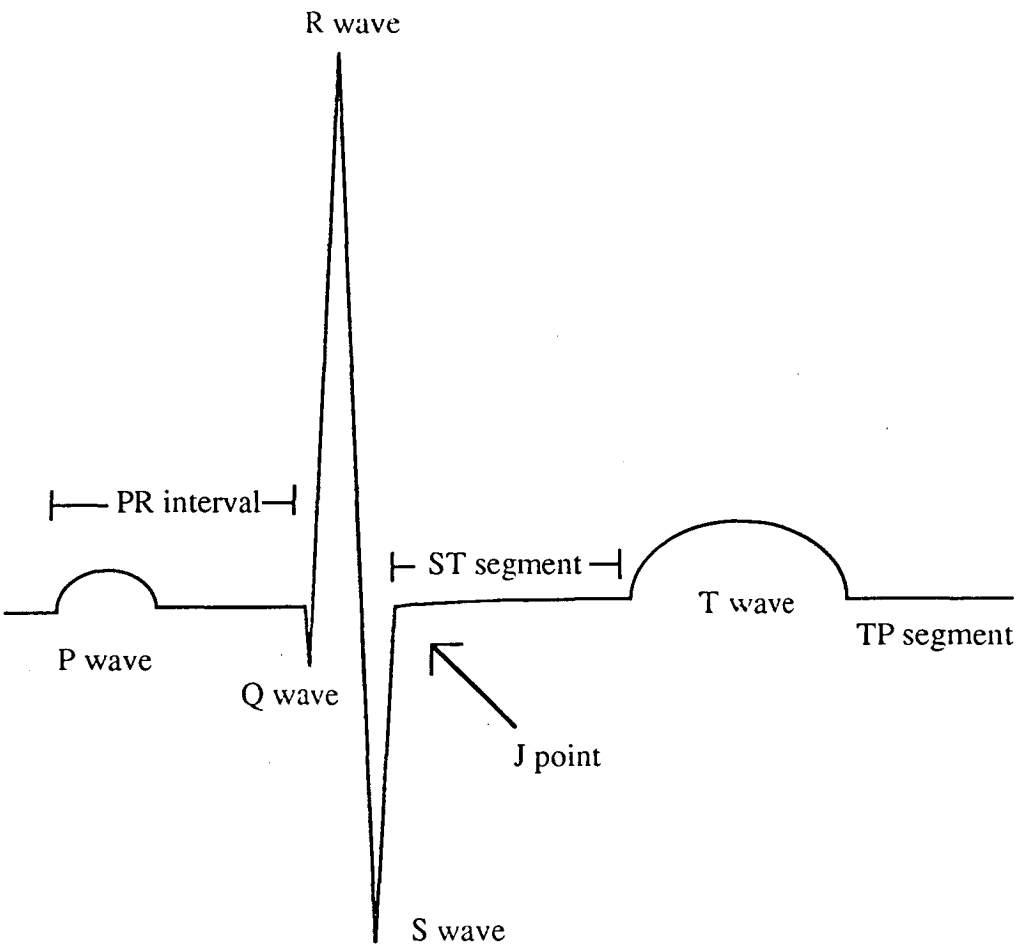

The standard terminology applied to the electrocardiogram over a single cardiac cycle. The P wave is atrial depolarisation, the QRS complex ventricular depolarisation, the t wave ventricular repolarisation. The Q wave is an initial negative deflection in the QRS complex. The R wave is an initial positive deflection in the QRS complex. The S wave is a non initial negative deflection in the the QRS complex. The J point is where the QRS complex changes to the ST segment.

Figure 2 : Action potential of a single cardiac muscle fibre

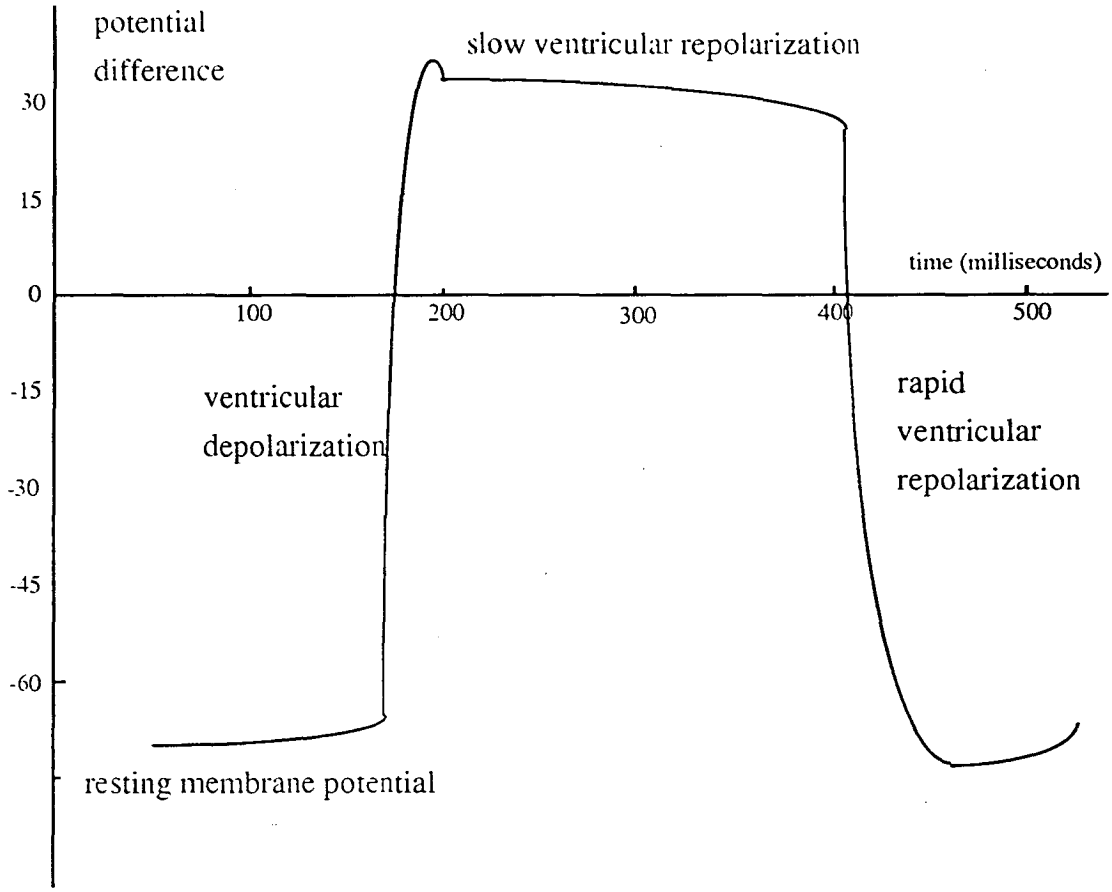

The x axis is time in milliseconds. The y axis is the potential difference between the inside of the myocardial cell and the outside of the myocardial cell.

Figure 3: Generation of the body surface electrocardiographic map

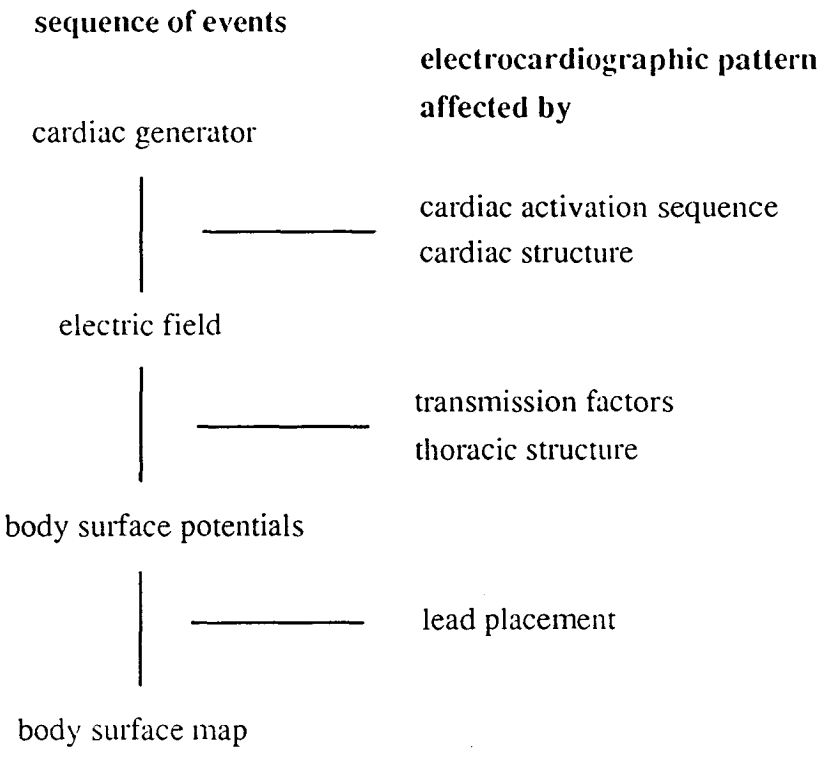

Generation of the body surface map is dependent on a number of factors including the structure of the heart, transmission factors and the recording device's position [from Mirvis 1988].

Chapter 3

Data collection in body surface electrocardiographic mapping

Introduction to body surface mapping methods

Data collection in body surface mapping is more difficult than in standard twelve lead electrocardiography. Where the standard electrocardiogram has 9 electrodes applied at 9 body sites collecting 12 potential differences, our body surface map has 50 electrode sites measuring 50 potential differences. The increased electrode application and the increased data collected creates problems with the recording and analysis of the data. This chapter discusses the problems of electrode positioning and data collection in body surface mapping.

The electrode position

The major factor in body surface mapping is the electrode coverage of the thorax. The electrode array must record all relevant electrical potentials on the body surface. To conduct studies on seriously ill patients, the electrode application must be simple and able to be performed with a minimum of discomfort to the patient. Data must be recorded rapidly to avoid interference with patient care. Different approaches that avoid interference with patient care are possible. One solution is to use a comprehensive lead system where 125 to 250 electrodes are applied. This electrode system covers the torso with electrodes at a high density. The data recorded has a large redundancy of information, and failure of data collection from one or many of the electrodes is not critical. Though the data collected from multiple electrodes may have greater detail [Arisi 1983] the question of a clinical advantage has not been studied. For example there is little qualitative difference between the body surface map appearance recorded from 121 and from 85 recording electrodes [Yamada 1978]. The disadvantages of systems with large numbers of electrodes are the time required for application and the discomfort to the patient associated with the application. The large amount of data recorded with a

high degree of redundancy makes analysis of the information difficult.

A second approach is to use lead subsets. This involves the application of fewer electrodes with electrode placement in selected sites. This method is based on the assumption that comprehensive lead systems have a large amount of redundant data, and that all non-redundant data can be captured by selected lead placement. Several methods have been described [Horan 1980, Barr 1983, Spach 1971]. By principal component analysis Barr and coworkers developed an electrode system with 24 electrodes of a 150 electrode lead system [Barr 1983, Spach 1971]. The analysis allows calculation of the 150 leads from the 24 measured leads by linear combinations of the measure voltages at each of the 24 leads. Green and coworkers used a data reduction algorithm to reduce a measured 192 electrode array to a 32 electrode array body surface map [Green 1987]. When a 32 electrode array was used to record and body surface map and compared to the 192 lead array body surface map, the root-mean-square error between the two maps was low, and the correlation between the two maps was extremely high. The conclusion is that the available data can be recorded using a 32 lead array of electrodes provided the electrodes are placed appropriately. Interestingly, in a companion study Lux, Green and coworkers used different sets of 30 electrodes including a set with no back electrodes [Lux 1979]. All sets of 30 electrodes produced estimates little different from the 192 lead body surface electrocardiographic map. Thus 30 electrodes appear to be adequate for the measurement of most of the information contained in the cardiac electrical potentials on the surface of the body.

In our system, a 40 to 50 electrode system has been used. The electrode positions are shown in figure 1. The use of 50 electrodes is sufficient to record accurately potentials on the thorax and allows for some electrodes to fail without loss of information, but this number is substantially greater than the 24-32 electrodes

required to record the fine detail of the map [Lux 1979, Lux 1978]. Fifty electrodes allows collection of potentials from sites not recorded by the standard 12 lead electrocardiogram. Using 50 electrodes reduces the technical burden of clinical mapping and allows ease of computation. In our mapping system the 50 electrodes are spaced around the torso with a greater density over the left precordium as shown in figure 2. This array is better than a tightly packed left precordial electrode system [Lux 1979] and standard electrocardiographic lead positions [Lux 1979]. The packing system used corrects for the eccentric position of the heart in the chest cavity. Thus the angle subtended by each electrode around the heart is approximately equal (figure 2).

The electrical reference point

The potential sensed by the electrode is the difference between the reference electrode and the recording electrode. Our system uses a calculated reference electrode. The calculation is designed to calculate the electrocardiographic reference electrode known as Wilson's central terminal [Wilson 1932]. In fact the choice of reference electrode is not important as the shape and location of the contour lines do not change [Spach 1979, Taccardi 1962]. The choice of Wilson's central terminal, the reference point for standard electrocardiography, allows comparison with standard 12 lead precordial electrocardiography. Using Wilson's central terminal allows standard interpretation of the body surface maps.

The isoelectric (zero) baseline

The isoelectric baseline is important to the interpretation of body surface maps. The selected baseline is the zero potential, and all other voltages are quantitative in relationship to the baseline. The system in these studies used the T-P segment as

baseline [Taccardi 1962]. This is the usual practice in standard electrocardiography.

The QRS complex onset (zero time)

The continuous nature of the cardiac electrical cycle means that a zero time point is required. The onset of the QRS complex is taken as the zero time reference point. The QRS onset is automatically picked by a computer algorithm and checked manually. The data is differentiated and the location of the first value to exceed a specific threshold derivative is found. From this point the position where the derivative next becomes negative is found. If this position is less than 6 milliseconds on from where the threshold value was exceeded, it is assumed that a noise spike has been found and the search continues. Otherwise it is assumed that the point reached is near the QRS complex peak. If no peak is found then the search is continued with a lower threshold value. Once a point near the peak of the QRS complex is found a search is continued backwards until the undifferentiated data reaches the baseline noise level. This point is the designated QRS onset. The onset of the QRS complex is difficult to pick to the nearest millisecond. The reason for this inaccuracy is the noise in the system and the gradual onset of the electrical potential. In theory the onset starts with a single myocardial fibre depolarizing and then spreading to other myofibrils. The electrical onset is a hyperbolic curve and the moment of onset is difficult to pick from the background noise [Macfarlane 1989]. In practice this means that onset picking between maps may vary by up to ±10 milliseconds, in our experience. Figure 3 represents an expanded electrocardiogram lead trace. The problem is to pick the exact time when the electrocardiogram starts. The potential inaccuracy in timing the QRS makes the use of specific times after the onset of the QRS an irrational concept. In these studies an integral body surface map is used. The integral map takes a time period and calculates the average map per unit time

over a given time period. This concept is illustrated in figure 4. Using integral maps over a short time periods, for example 20 milliseconds, makes some correction for the variation in the QRS onset. Some loss of information in integral maps is unavoidable and the clinical significance of such loss is unclear. The use of integral maps is more rational than the use of instantaneous maps. Integral maps reduce noise, especially 50 Hertz noise from mains electricity.

A second problem with the onset picking is that the QRS onset may vary by up to 40 milliseconds depending on which lead is used to pick the QRS onset [Ikeda 1985]. In our body surface mapping method the onset is picked on an average of all electrodes and the lead 12, a central thorax lead. By using a consistent reference electrode and standard method of determining the QRS onset, the variation in the QRS onset picking in minimized.

Description of body surface mapping method

The system used was built and developed in the University of Tasmania by Drs D. Kilpatrick and S. J. Walker [Walker 1983]. A jacket with the fixed array of 50 electrodes (figure 1) was wrapped around the patient starting from a position 7.5 cm to the right of the sternum, so that the second column of electrodes was on the mid-sternal line. The number of electrodes in contact with the patient varied with the size of the patient. The overlap of electrodes enables virtually all patients to be studied. Fifty electrode positions around the patient were calculated from the distance separating the electrodes and the degree of overlap of the jacket recorded at the time of mapping. Nickel plated brass drawing pins are used to contact the skin. These produce a low skin contact potential. Each electrode is active using an Analog Devices AD 544 wired as a buffer. The input impedance is of the order of 10^{11} ohms. The buffers eliminate the need for electrode jelly. Although electrode

positioning varied between patients, body surface maps comparable between patients were produced by using an interpolation scheme which took into account the size of each patient. A spline interpolation method was used which produces 32 columns, each of 12 values evenly distributed around the thoracic surface for the map displays. The reference electrode was a simulated Wilson central terminal calculated from the raw map data. This format is comparable to that used by other groups [Barr 1983]. There is a greater density of electrodes over the left precordium as the heart is in an asymmetrical position in the thorax (figure 2). The asymmetrical electrode placement allows for an even rotation angle from the centre of the heart to each electrode (figure 2). The recording is made for 4 seconds at 1000 Hz with 1 second of data stored. The signal from each electrode is passed through a differential amplifier with a gain of 1000. DC offsets single order high pass filter with 3dB point at 0.05Hz. The high frequency range is limited by a third order low pass filter with 3dB point at approximately 500 Hz. Although this implies that some noise at frequencies approaching the sampling rate will be passed by the filter, in practice it is found that the amount of noise with frequencies above 500 Hz present in the signals is very small. Electronic noise associated with the amplifiers is approximately 10 μV peak to peak with respect to amplifier input. The amplifier outputs are connected through a 64 channel multiplexer to a high speed analog to digital converter. The analog to digital converter has a resolution of 10 bits and is set up to digitise a range of -5 to +5 volts, giving a resolution of 10 μV with respect to amplifier input. A bedside display of the sampled electrocardiographic signals enabled an immediate check on the quality of the data and the recording was repeated if there was inadequate data acquisition. If there were only 1 to 5 bad electrode recordings, the inadequate electrode recordings were deleted and replaced by interpolation from the surrounding leads. Linear baseline drift was corrected

by interpolation between baseline points picked manually in successive TP (baseline zero reference) segments. Baseline wander was reduced by attention to patients having normal quiet respiration at the time of recording. Complete recordings were usually made within five minutes of approaching the patient. Map displays were available within five minutes of recording the data.

To comply with patient electrical isolation standards, the jacket, amplifiers, multiplexer and analog to digital converter are battery powered. Digital signals output from the analog to digital converter and all control systems are optically isolated. Low voltage circuitry is used in the jacket and the input buffer circuits are individually potted in epoxy resin.

Data display

The data display of a body surface map is intrinsically different from the display of a standard electrocardiogram. The standard electrocardiogram displays the electrical potential changes over time between two points on the thorax. The body surface map displays the total thoracic electrical potentials compared to a reference electrode at a single time, and successive maps show the change in time at all points on the thorax. Thus the display is different; the conventional body surface map is a representation of the thoracic surface with the potentials at the various sites displayed.

In this system linear interpolation is used to create columns of data between the original electrode columns which were spaced 15 cm apart. The neck and reference electrode values are expanded out to form a row of identical values along the top and the bottom of the map respectively. A copy of the first column of values is placed after the last column so that the maps appear to wrap horizontally. These procedures produce an array of voltage values with 7 rows and a variable number of columns

depending on the size of the patient. This data format can be use to plot map types and fed into statistical packages. The display format may be contour lines of equal potential, the isopotential map (figure 5), or a perspective map (figure 6). The isopotential or contour maps shows the overall spatial pattern and magnitudes of the potentials. Perspective maps accentuate the gradient between adjacent regions. In these studies the isopotential contour map display has been used. The display form is simple and complements the data analysis used in these studies. This format is the most commonly used in body surface electrocardiography. The data format is displayed on the unwrapped thorax. The left edge of the display is the right mid-axillary line, the centre of the display is the left mid-axillary line, and the right edge is also the right mid-axillary line. The left half of the display is the anterior thorax and the right half of the display is the posterior thorax (figure 7). With each display the maximum voltage, the minimum voltage and the site of maximum and minimum voltage are automatically calculated. The zero contour line is a bold continuous line. The positive contour lines are continuous plain lines, and the negative contour lines are dashed lines.

A time component in body surface mapping is added by producing multiple maps over the time period. In the extreme form this can be a "map movie" where say 1 millisecond maps are displayed rapidly on the computer screen and the changing pattern of the map pattern watched in real time.

The display format for this thesis is consistent with the above description of isopotential body surface maps.

Figure 1 : The configuration of the electrode jacket.

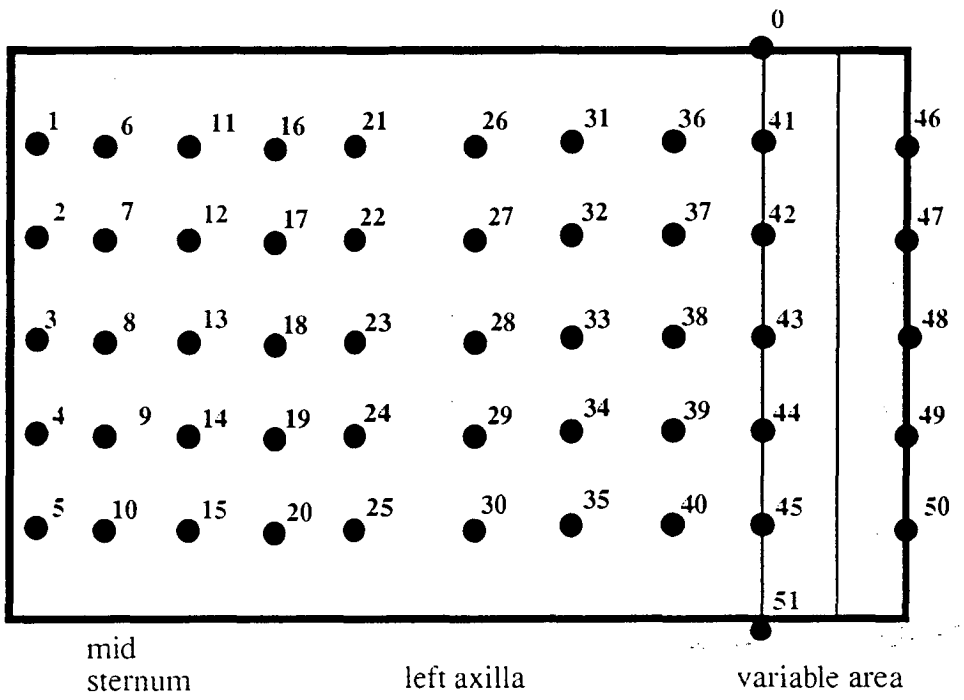

The left edge of the jacket represents the electrodes positioned 7.5 cm to the right of the sternum so that the second column of electrodes is always over the mid-sternum. The neck electrode (0) is placed on the right side of the neck. The reference electrode (51) is placed on the right anteriorsuperior iliac spine. The overlap of the jacket varies with patients' size.

Figure 2 : Position of the electrodes around the thorax in relation to the heart position

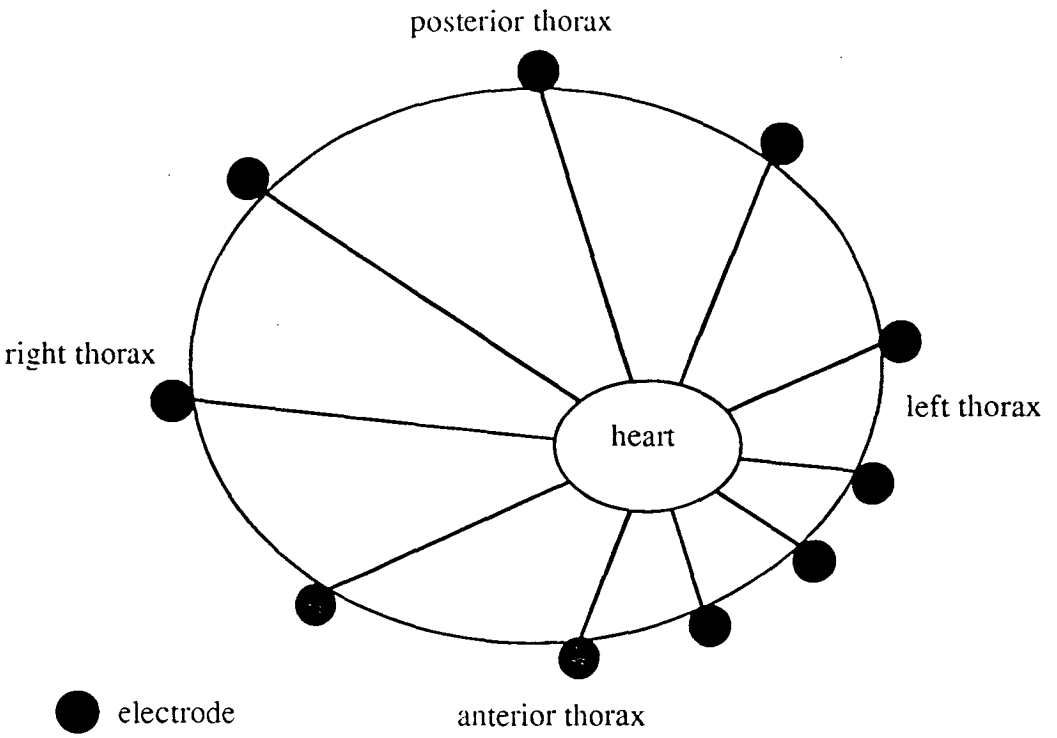

A representation of the body surface map electrode position around the outside of the thorax. The electrode density is increased over the anterior to left thorax to compensate for the eccentric position of the heart in the thorax. Thus the angle subtended by all electrodes is nearly equal.

Figure 3 : Expanded electrocardiogram trace and problems with onset picking

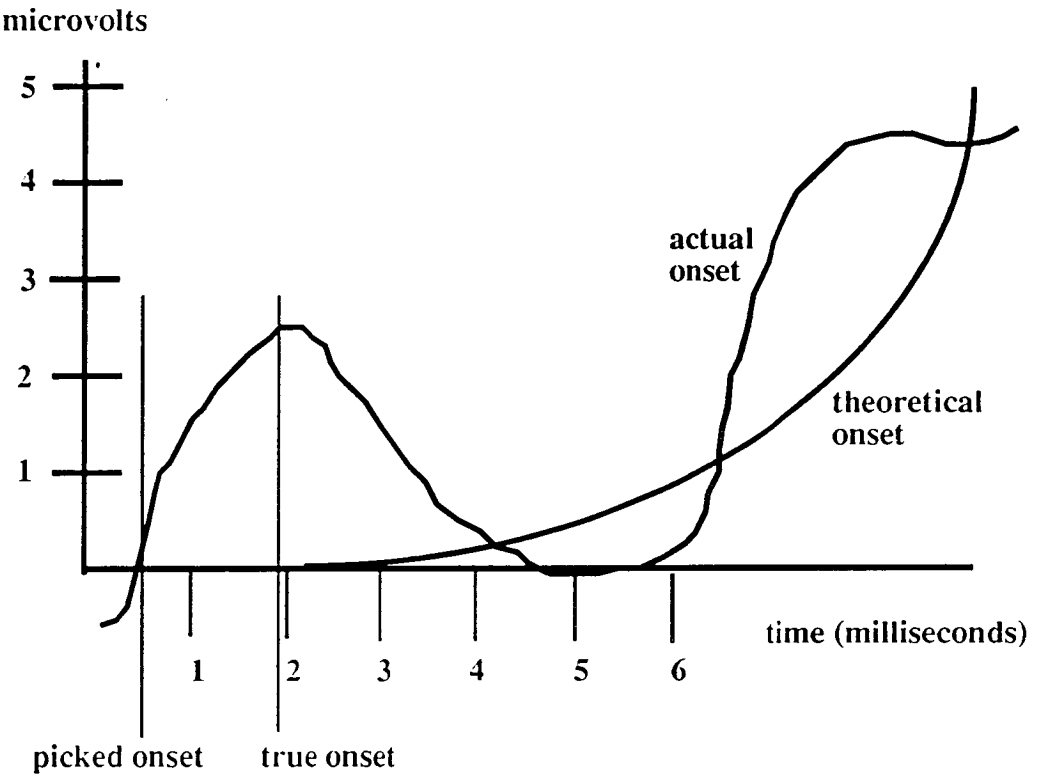

The smooth line is a theoretical representation of the electrocardiogram trace. The curving line is the usual situation. The usually recorded electrocardiographic signal has added background noise. In this situation the onset picking loses accuracy as shown by the difference between the true onset and the picked onset.

Figure 4 : The concept of the integral body surface map

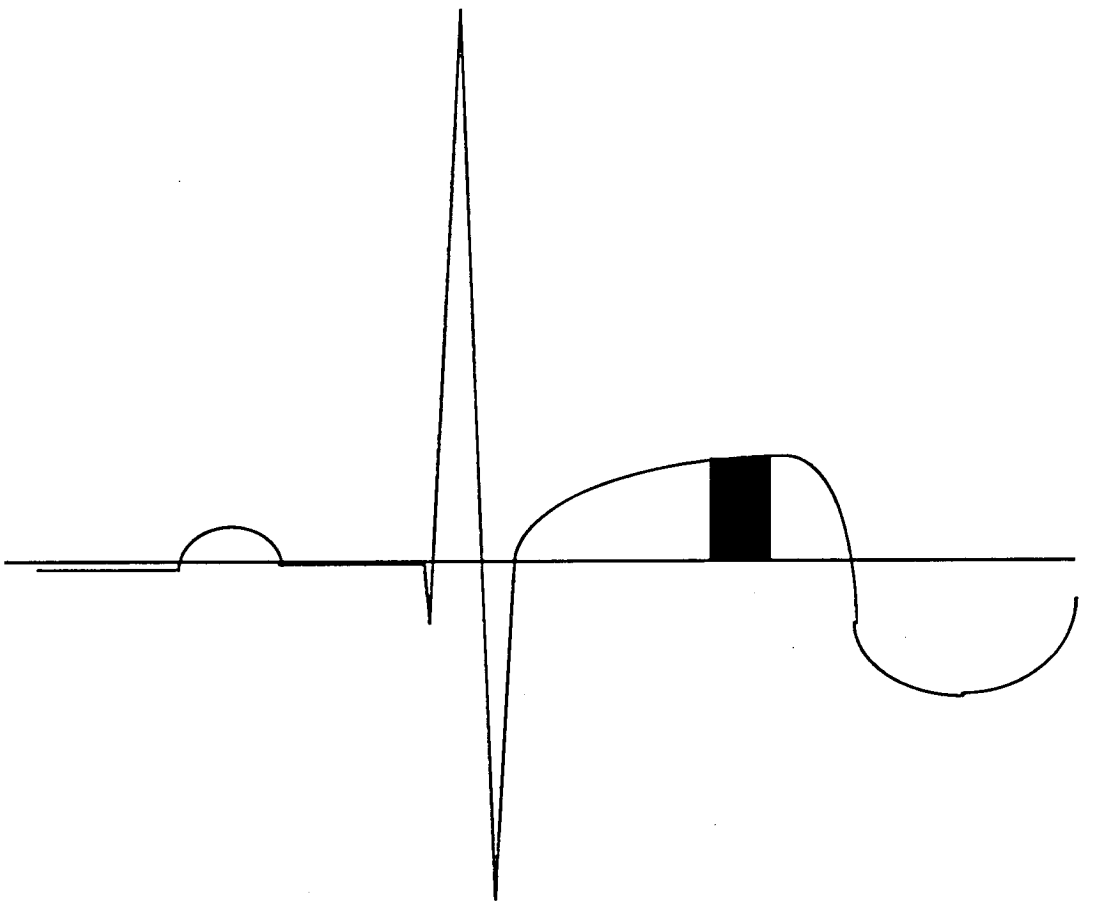

The area represented by the black shading represents the portion of the ST segment used to create an integral ST segment body surface map.

Figure 5 : Contour or isopotential body surface maps

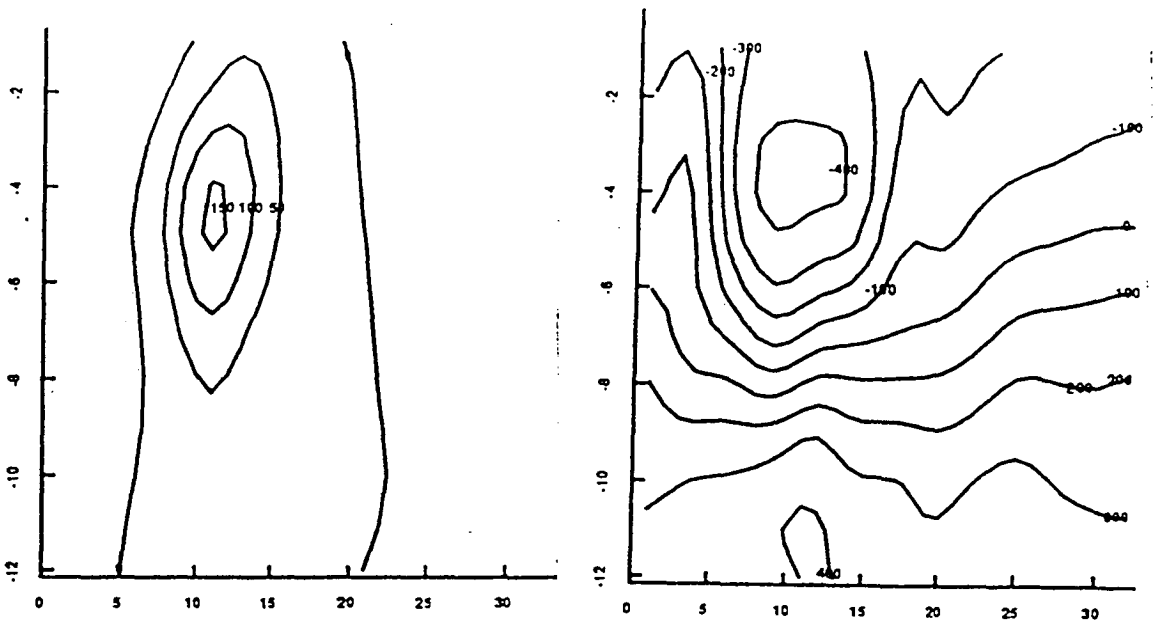

The figures represent the ST segment isopotential body surface map from a normal patient on the left and an acute inferior wall myocardial infarctio patient on the right.

Figure 6 : Perspective views of body surface maps

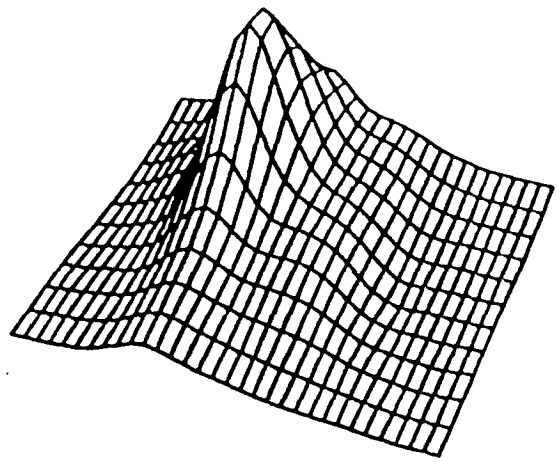

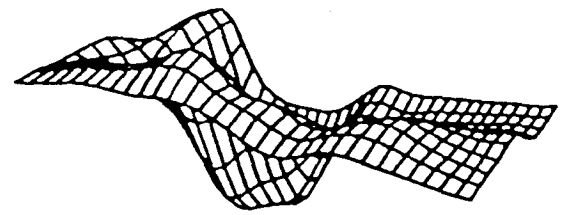

The figures represent the ST segment isopotential body surface map, displayed as a perspective body surface map from a normal patient on the left and an acute inferior wall myocardial infarction patient on the right.

Figure 7 : Contour body surface map display

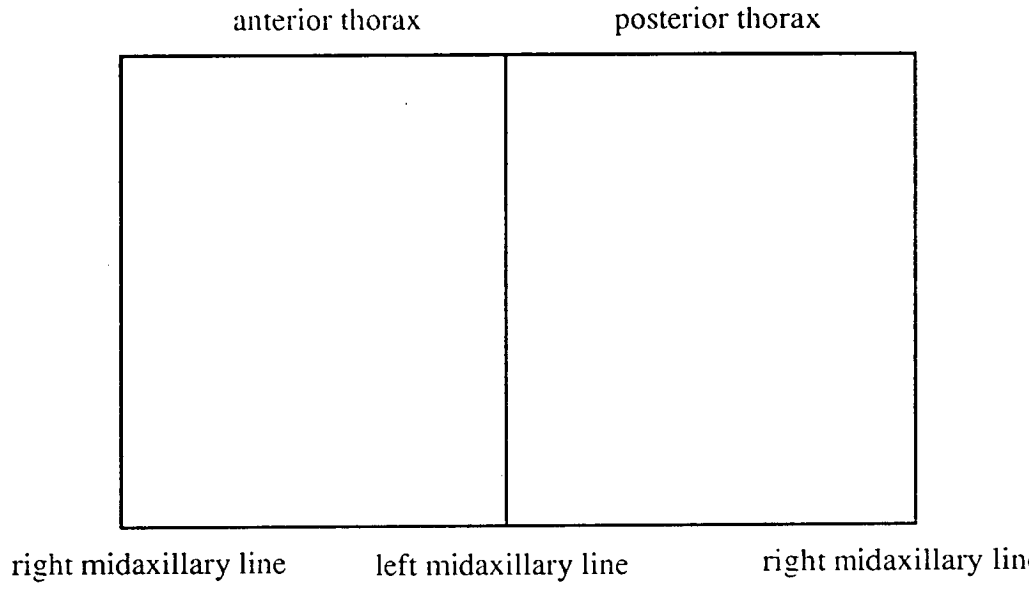

The body surface map display used in map analysis. The thorax is opened along the right midaxillary line.

Chapter 4

Data analysis in body surface electrocardiographic mapping

Methods of data analysis

Visual inspection

The simplest method of body surface map analysis is visual inspection, as per the standard electrocardiogram. The ability of visual inspection to group map patterns, and to determine the significance of patterns, was tested. In these studies all maps were inspected visually. Map differences between normal patients and patients suffering myocardial infarction are obvious. The subgroups of map patterns in patients with acute myocardial infarction were not apparent, although other researchers have claimed the opposite [Pham-Huy 1981]. Failure to recognise subgroups is due to the inability of visual inspection to group patterns uniformly and to disregard minor variations in the patterns. For example, using inferior wall myocardial infarction body surface maps, visual grouping was difficult due to the continuum of body surface maps in the condition [Walker 1987]. Although certain patterns are distinguished, a number of patterns fall in between the major patterns and could be matched to either group [Bell 1989]. This problem of classification represents a problem in the biological sciences. Problems associated with intermediate patterns preventing classification are difficult to circumvent [Everitt 1974].

Difference maps

Using a subtraction map - that is, the map pattern produced when an initial map is subtracted from a follow up map - gives information about the nature of the change due to the events in the intervening time (figure 1). The method is simple: each voltage at each electrode site is subtracted from the corresponding site voltage in the second map and the resultant voltage used to construct a new body surface map. The subtraction map is displayed as an isopotential map in the same manner as recorded

maps. The method removes subject to subject variation, and corrects for different magnitudes of potentials recorded in different subjects. Difference maps have been used in longitudinal studies of body surface electrocardiographic change over time, such as the changes occurring after acute myocardial infarction [Montague 1983, Montague 1984, Montague 1986]. Unfortunately a body surface electrocardiographic map recorded before acute myocardial infarction is rare and generally unavailable in the clinical setting. In 7 years of mapping most patients admitted to the coronary care unit only two patients have pre-event maps. This factor limits the use of difference maps where the initial event occurs before a body surface map has been recorded. The time course of electrocardiographic changes occurring after an index map can be monitored by this method.

Departure maps

A departure map displays the difference between an individual map and an average map of a control group [Flowers 1976a, Flowers 1976b, Mirvis 1981]. This method requires a suitable control population, either normal body surface maps, or abnormal body surface maps representing a particular condition. The control body surface maps are averaged at each electrode point. The confidence limits or standard deviation about the mean are calculated for each electrode. Each individual electrocardiographic body surface map can be compared to the population group. The voltage at each lead site is compared to the mean and standard deviation of the corresponding control map lead and if the voltage falls within the two standard deviations (or other limits as determined) then the result is zero. If at a particular electrode the measured voltage is outside the predetermined range then the measured value is recorded at the appropriate site. Comparing all 50 electrodes creates a new map called a departure map. The result can be displayed as an isopotential body

surface map using zeros and the outlying values. A second method of displaying a departure map is to use the number of standard deviations from the mean value of each lead and build a contour map using the number of standard deviations from normal instead of voltages. The standard deviation departure map created can have zero substituted for standard deviations less than a predetermined cut off number.

The departure map is a method of comparing the individual body surface map to a control population body surface map where the individual cannot act as the control, that is, where the event or intervention has taken place before the data are recorded. The departure map is analogous to the reference range in any clinical laboratory. In these studies the normal range was considered to be the range of plus or minus two standard deviations from the mean. This method has been used to compare body surface maps in clinical studies [Flowers 1976a, DeAmbroggi 1986a, DeAmbroggi 1986b, Ohta 1981, Suzuki 1984].

Statistical comparisons

The above methods of body surface map comparison essentially produce another body surface map showing the difference between the original map and a control map. In statistical comparison the difference between body surface maps is reduced to a single numerical value. The body surface maps can be compared by this single numerical value and, based on the value, body surface maps can be grouped into categories [Mirvis 1988]. When comparing body surface maps there are two factors to consider, the magnitude of the maps and the spatial pattern of the maps. Different statistical methods emphasize different aspects of the body surface map. Using percentage error calculation or lead error calculation (described below) emphasizes the voltage magnitude of the body surface maps being compared. The correlation coefficient emphasizes the spatial distribution of the body surface maps. The

calculations are straightforward and easily applied to body surface maps. The major question is whether such methods are clinically applicable to detect important differences in body surface maps.

Percentage error

The percentage error is calculated as follows:

$$\text{percentage error} = 100 \times (\Sigma (p_{1i} - p_{2i})^2 / \Sigma(p_{1i})^2)$$

where p_{1i} and p_{2i} are potentials at the i^{th} electrode of maps 1 and 2 respectively. The smaller the percentage error the more similar the maps [Mirvis 1988].

Lead error

The lead error is also known as the root-mean-squared error and is calculated by the formula:

$$\text{lead error} = \sqrt{(\Sigma [(p_{1i} - p_{2i})^2 / N])}$$

where p_{1i} and p_{2i} are potentials at the i^{th} electrode of maps 1 and 2 respectively and where N is the total number of electrodes. The smaller the lead error the closer the maps are related [Mirvis 1988].

Both of these methods are primarily concerned with magnitude comparison between body surface maps, although the body surface map pattern plays some role in the final comparative value.

Correlation coefficient

The correlation coefficient is concerned with the spatial similarities or differences between body surface maps. The magnitude of the electrical potentials

does not vary the result; for example if two body surface maps are compared and the result gives a correlation coefficient of 0.87, then even if the values in one of the body surface maps are multiplied by a factor of 10 the correlation coefficient remains 0.87. The correlation coefficient relates the zero potential line of one body surface map to another and correlates the positive areas versus positive areas and the negative areas versus negative areas. The correlation coefficient is a measure of the closeness of a relationship between two sets of variables (or more exactly the closeness of a linear relationship); in this case the variables are body surface maps.

The correlation coefficient can be applied to the body surface map matrix with the following justification known as the law of Cosines. If vectors a_1, a_2 and $a_1 - a_2$ form a right angle triangle and:

$$| a_1 - a_2 |^2 = |a_1|^2 + |a_2|^2$$

also $|a_1 - a_2|^2 = t(a_1 - a_2)(a_1 - a_2)$

$= (t(a_1) - t(a_2))(a_1 - a_2)$

$= t(a_1)\, a_1 - t(a_1)\, a_2 - t(a_2)\, a_1 + t(a_2)\, a_2$

$= |a_1|^2 + |a_1|^2 - 2t(a_1)\, a_2$

and a_1 and a_2 need not be perpendicular and t is a variable.

If a_1 and a_2 are perpendicular then $t(a_1)\, a_2 = 0$ and this is the orthogonality condition.

If the result is extended, where a_1 and a_2 form an angle μ (that is, a_1 and a_2 are not perpendicular), then the Pythagorean theorem can be replaced by the law of cosines;

then

$$|a_1 - a_2|^2 = |a_1|^2 + |a_2|^2 - 2\,|a_1|\,|a_2| \cos \mu$$

$$t(a_1)\, a_1 = |a_1|\,|a_2| \cos \mu$$

Thus the inner product of two vectors a_1 and a_2 is equal to the product of 3 factors : the absolute value of a_1 and a_2 and the cosine of the angle between the two vectors;

thus $\cos \mu = a_1 . a_2 / |a_1||a_2|$

and in three dimensions

$\cos \mu = a_1 . a_2 / |a_1||a_2|$

with a_1 a three dimensional vector, and continued to the n^{th} dimension [modified from Batschelet 1971].

Computation of the correlation coefficient

In these studies the correlation coefficient is calculated by considering the 2 maps as vectors and calculating the dot product of the two maps then dividing by the sum of the magnitudes of each vector.

Properties of the correlation coefficient

The correlation coefficient has the following properties. The correlation coefficient r is a pure number without units or dimensions. The correlation coefficient r is always $-1 \leq r \leq 1$. The value of r estimates the closeness of the linear relationship between two variables X and Y [Snedecor 1980, Armitage 1987, Altman 1991].

The correlation coefficient squared, r^2, may be described approximately as the estimated proportion of the variance of Y that can be attributed to its linear regression on X while $(1 - r^2)$ is the proportion free from X. Thus if $r \leq 0.5$ then only a minor portion of the variation in Y is due to X. At $r = 0.7$ about half the variation of Y is due to X, and at $r = 0.9$ about 80% of Y is due to X. When correlation coefficients are used the correlation coefficient is often associated with a p value [Snedecor 1980]. The use of the p value is that if the probability or p value < 0.05 then this indicates a non-zero relationship and nothing else. The p value indicates a relationship greater than would be expected by chance but is of no use in describing the extent of the relationship. The p value thus tests the negative question about the chance of a relationship existing and does not address the question of degree of a relationship thus the p value is not useful in grouping body surface maps.

The correlation coefficient calculation is the spatial analog of the standard regression analysis. The magnitude of map values plays little role in the calculation of the correlation coefficient and maps of very different magnitudes may have very similar correlation coefficients. As with standard correlation coefficients, a correlation coefficient of greater than 0.70 is excellent, greater than 0.3 good, equal to 0.0 no correlation and less than -0.70 an excellent correlation with the pattern but with the positive and negative areas reversed. To use correlation coefficients as a measure of the magnitude of a relationship the correlation coefficient squared, r^2 can be used. When the value of r^2 is not zero the distribution of r becomes skew thus does not reflect the degree of relationship between between maps. The solution to this problem is to use the Fisher transformation of r to z, a normally distributed variable [Snedcor 1980]. With 50 data points from each of two samples the z value confidence limits for significant relationship between the two samples is an r value of 0.30 to 0.68. Thus a relationship exists between maps correlated at an r value of 0.30

or more. A r value of 0.68 or more is associated with a relationship over two standard deviations from the mean. Thus the correlation coefficient can be used to compare the spatial distribution of body surface maps but care must be taken in interpretation of the meaning of the p value and r correlation coefficient. Once the correlation coefficient is calculated for all combinations of a number of body surface maps then cluster analysis may be used to group maps with similar spatial distribution.

Methods of grouping electrocardiographic body surface maps

Cluster analysis

Cluster analysis is a general term for methods of grouping individuals according to a single characteristic or multiple characteristics. Cluster analysis methods are used to group data, reduce data, test hypotheses and generate hypotheses. The methods intrinsically do not add information but allow an interpretation and integration of information. In body surface mapping cluster analysis may reduce the large amount of information to meaningful amounts without significant loss of information. Cluster analysis methods may allow automatic diagnosis [Kendall 1980].

These studies use hierarchical clustering techniques with agglomerative methods for fusing body surface maps into groups of similar maps [Everitt 1974]. Several methods were tried and developed into automated cluster analysis programs. Methods using the correlation coefficient between maps as the basic grouping tool were the most successful. Attempts at using percentage error and lead error as measures of map similarity were not sucessful. The method that classified maps into clinically applicable groups and was consistent was the furthest neighbour method also known as the complete linkage method. The method matches single individuals

by the highest correlation coefficient. Once a group has formed the match is based on the lowest correlation coefficient within the group with the "to be" fused individual or group. If two groups are considered then the groups are fused only when the lowest correlation coefficient between the individual group members is the highest correlation coefficient in the analysis. Higher correlation coefficients between the two groups are not counted. This is the standard grouping method used in these studies.

The nearest neighbour method using the correlation coefficient as a measure of the similarity of the maps. This method, also known as the single link method, fused individuals according to the highest correlation coefficient. When a group has formed, the next fusion is between the highest correlation coefficient between two individuals, and if the individuals are within groups then the groups are fused. This method produced groups with a wide variety of maps in single groups; thus although the highest map correlations are high, there is a problem with the correlation drift between early incorporated maps and later incorporated maps in the same group.

A third method is to use the group average correlation coefficient between all pairs of individuals in the groups. Although this method superficially appears satisfactory, it is not suitable for use with correlation coefficients [Lance 1966]. The technique produces unpredictable results. In strict statistical terms averaging of correlation coefficients is not an acceptable method.

A further method used is similar to the group average method but avoids the problem of averaging correlation coefficients. By recalculating the correlation coefficient matrix after each fusion, from an updated group average map, correlation coefficients are not averaged. Thus each step consists of fusion of two individuals to create a group, averaging the two maps into a single map and recalculating the correlation coefficients between the new map and all other maps and fusing the

highest correlation coefficient. The cycle is then repeated. The method tends to group all individuals into a single group, the mean map pattern. The method determines outlying map patterns, but is insensitive in detecting subgroups.

Grouping can also be done by divisive methods. These methods split the whole group based on the removal from the group of the most distant neighbour. This method is not used in these studies.

In all grouping methods eventually all maps would be grouped into a single group and thus at some point the process is stopped. The decision when to stop grouping is a difficult one, and has been discussed in detail [Everitt 1974]. In these studies cluster analysis was stopped around a correlation coefficient of 0.50 to 0.30, corresponding to the 0.05 % confidence limits and the dendrogram and map patterns considered. Members of each group were combined into an average map pattern.

The individual map patterns of a group were correlated with the average map pattern of that same group and a mean correlation coefficient calculated. If the mean correlation coefficient was greater than 0.75, then clustering was considered adequate.

Interestingly, in the procedure an individual map, map "a", may be placed into group "A" by the initial cluster analysis, but when compared to the average map patterns created from the cluster analysis that individual map "a" may have a higher correlation coefficient with the average map pattern of group "B". This occurred with some 10% of map patterns using the cluster analysis furthest neighbour method but with 5% using cluster analysis and recalculation of the correlation coefficients. After this reclassification was done, new average map groups were calculated from the correlation between the individual maps and the average map patterns produced by cluster analysis. Comparing individual maps with the secondary average map patterns again 6% of the individual maps changed groups. Even after some 6

reclassifications some 6% of the maps were still changing groups. The mean correlation coefficient for all the maps against the group average map did not vary by more then 0.06, and peaked after 2 reclassifications.

Thus there appears to be no method of completely classifying maps on the basis of pattern. This is due to the problem of classification where lines separating groups are drawn arbitrarily across a continuous spectrum of map patterns, when slight change will reclassify border maps into different groups. In these studies the original average map patterns produced by cluster analysis were used. There was no apparent benefit in multiple averaging and reclassification methods.

Display methods for cluster analysis

The dendrogram can be used to display the grouping procedure. Figure 2 shows the grouping of 123 body surface map patterns using correlation coefficients. The cluster analysis is displayed as a dendrogram. The method used was the furthest neighbour method with the y axis representing 1-correlation coefficient. The use of dendrograms is an excellent visual method for determining when to stop the analysis. Any horizontal line drawn on the dendrogram shows at a glance the number of groups formed at any correlation coefficient value, and the number of groupings about to occur.

Combined methods of analysis

The methods of cluster analysis can be applied to the body surface map patterns created by subtraction mapping or by departure mapping. Using departure mapping with cluster analysis is an attempt to group body surface maps on the basis of a change from normal rather than grouping on the maps' basic patterns. This method is applicable to acute anterior wall myocardial infarction where the abnormal ST

segment maps and the normal ST segment maps are very similar in shape but different in voltage. In such cases the correlation coefficient may be high as the spatial distribution is similar, but the correlation coefficient between the departure map and the normal is very low. This combined use of methods appeared satisfactory and overcomes the problems of the correlation coefficient not considering magnitude.

Multivariate analysis of body surface maps

Eigenvectors and coefficients

The methods of body surface analysis described use static maps representing a single time integral body surface map. In reality the body surface map is continuously altering over time. To overcome the limitations of static map analysis a method of representing the complete body surface map as 72 coefficients of eigenvectors was developed, based on the work of the Salt Lake City researchers [Evans 1981, Lux 1981]. The eigenvector principle is similar to that of feature extraction by Fourier transformation, that is representation of the spatial and temporal data patterns as coefficients of standard base functions (patterns), known as eigenvectors. The standard eigenvectors were derived from 1352 maps representing all electrocardiographic varieties seen in the patients admitted to the coronary care unit over a 5 year period. These included body surface maps of patients with patients with acute anterior wall myocardial infarction (355 maps), acute inferior wall myocardial infarction (345), chronic anterior myocardial infarction (43), chronic inferior wall myocardial infarction (104), non-Q wave acute anterior wall myocardial infarction (80), non-Q wave acute inferior wall myocardial infarction (21), and normal electrocardiogram (404). Each map was reduced to 72 coefficients of which 12 were spatial vectors and 6 were temporal vectors. The 72 coefficients are

independent variables and contain most of the data from the first 400 milliseconds of each body surface map.

To test the reproducibility of the eigenvector data compression, 503 body surface maps were reduced to the 72 coefficients. The body surface maps were recreated using the coefficients at each 1 millisecond through the first 400 milliseconds of the body surface map. Each original millisecond by millisecond body surface map was compared to the reproduced corresponding millisecond body surface map using correlation coefficients. Thus 201,200 comparisons were made to test the accuracy of the method. Figure 3 shows the histogram of the correlation coefficients against the number of comparisons fitting that correlation coefficient. Figure 4 shows the boxplot of the time after the QRS onset point (zero time) on the x-axis and the correlation coefficient on the y-axis for all 503 body surface maps. This shows that the coefficients represent the total data of the body surface map, although at certain times the accuracy is not as great as desired. This occurs especially at the QRS onset, the QRS offset and the ST segment. The advantageous of this approach are of data reduction and removal of redundancy.

Application of eigenvector data reduction in body surface mapping

As the 72 coefficients are independent variables, multivariate analysis can be used to analyse the data. We have used the multivariate analysis, discriminant function analysis, to analyse body surface map data. Discriminant function analysis has two major functions. The first is interpretive. Interpretive analysis describes the characteristics of groups. The interpretive function indicates the degree of separation of the groups and the characteristics that are powerful separators of the groups. The second function of discriminant analysis is classification including automated classification. In this thesis the question posed by discriminant function analysis is

whether two sets of objects vary from each other. The discriminant analysis aims to construct linear combination of, in this case, the coefficients of eigenvectors that best discriminates the groups. The linear combination is a derived mathematical function for the purpose of classification and the equation has no meaning in concrete terms. By analysing a learning set of data and applying the derived discriminant function to a test set of data the accuracy of the separation of groups can be determined. Unfortunately in discriminant function analysis the equation has no meaning in concrete terms; it is a linear combination of the eigenvectors that best separate the learning groups and is not directly related to the original body surface map data. The method is useful as a technique for automatic diagnosis of patients' body surface maps [Altman 1991, Armitage 1987].

Variables for discriminant function analysis must have the following properties: the number of variables must be less than the number of cases by at least two; no variable may be a linear combination of another variable; no variable may be perfectly correlated with another variable; and each group is drawn from a population which has a multivariate normal distribution. As the Eigenvector coefficients follow these rules, the Eigenvector coefficients are suitable variables for discriminant function analysis.

The discriminant function analysis was performed by a standard method [Armitage 1987]. We calculated the eigenvectors. The coefficients of the patients under study were calculated from the eigenvectors. The patients were divided into two groups, the learning group and the test group. The learning group was used to develop the discriminant function analysis linear equation using the program S [Becker 1984]. The linear equation was applied to the test set to determine the test set classification. The calculated test set classification was compared to the true test set classification. The comparison was displayed as scatter plots of the groups, by

density function graphs, and by chi squared testing [Becker 1984]. Examples of the scatter plot and density function are given in figures 5 and 6 respectively. In the example the separation of the graphs is clear, and this is confirmed by the density function graph. The density function is the estimated probability density, also known as the theoretical relative frequency distribution [Snedecor 1980, Wegman 1972]. To determine the probability of the occurrence of events located between any two points on the dimension, the density function is integrated between these points. The best known example of a density function is the normal distribution. The graphic display method allows rapid assessment of the probability distribution and displays the nature of the relationship. The density function is similar to a histogram but is a continuous distribution.

Figure 1: Difference isopotential body surface maps

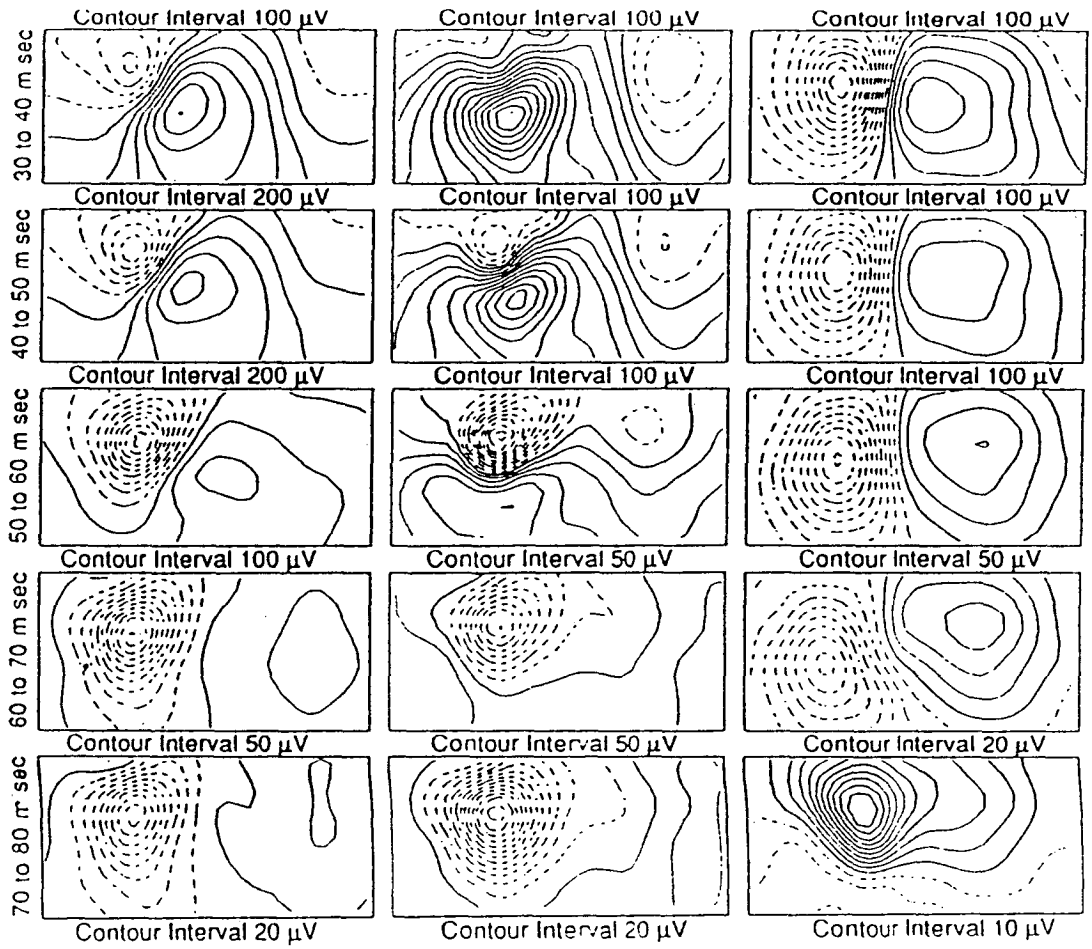

The pre-event maps are in the right hand column. The post event maps are in the left hand column. The middle column displays the difference maps showing the changes over time after an acute anterior myocardial infarction. The left hand column numbers are the integral times for the maps in milliseconds after the onset of the QRS complex.

Figure 2: Dendrogram showing map grouping by cluster analysis

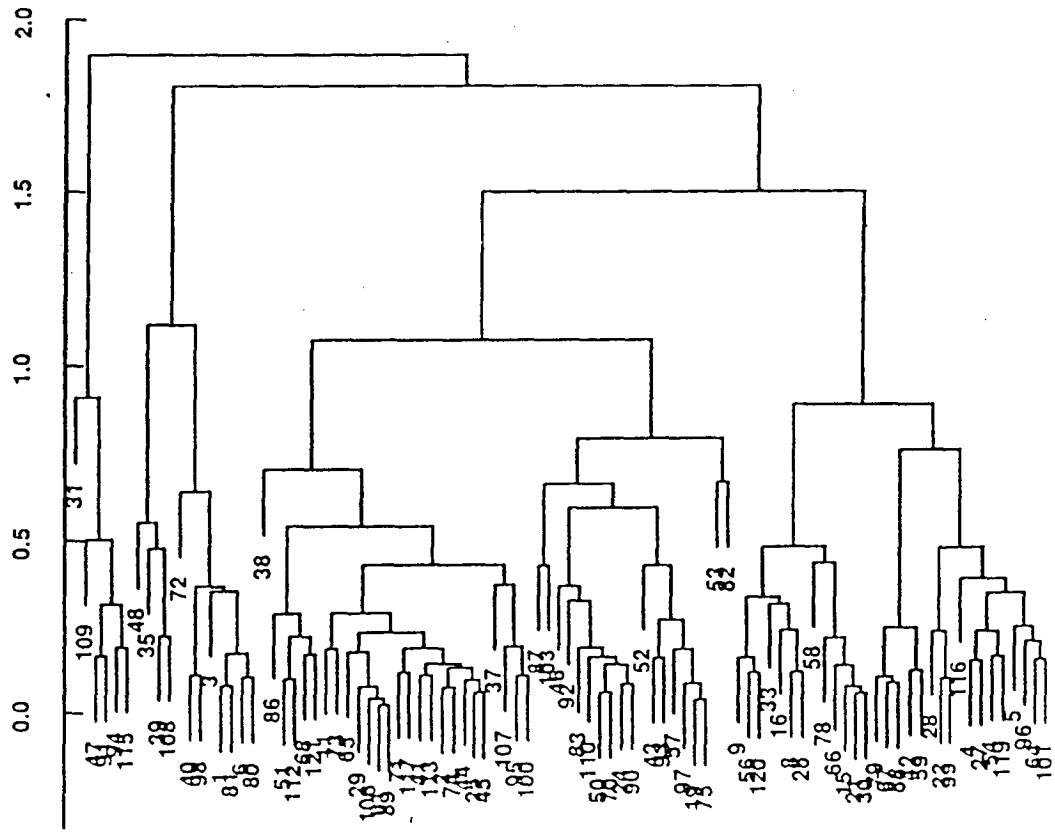

The x-axis numbers represent the body surface map number. The y-axis the 1-correlation coefficient between each map. The cluster analysis method is the single linkage method.

Figure 3: Histogram of correlation coefficients between the original and recreated body surface maps

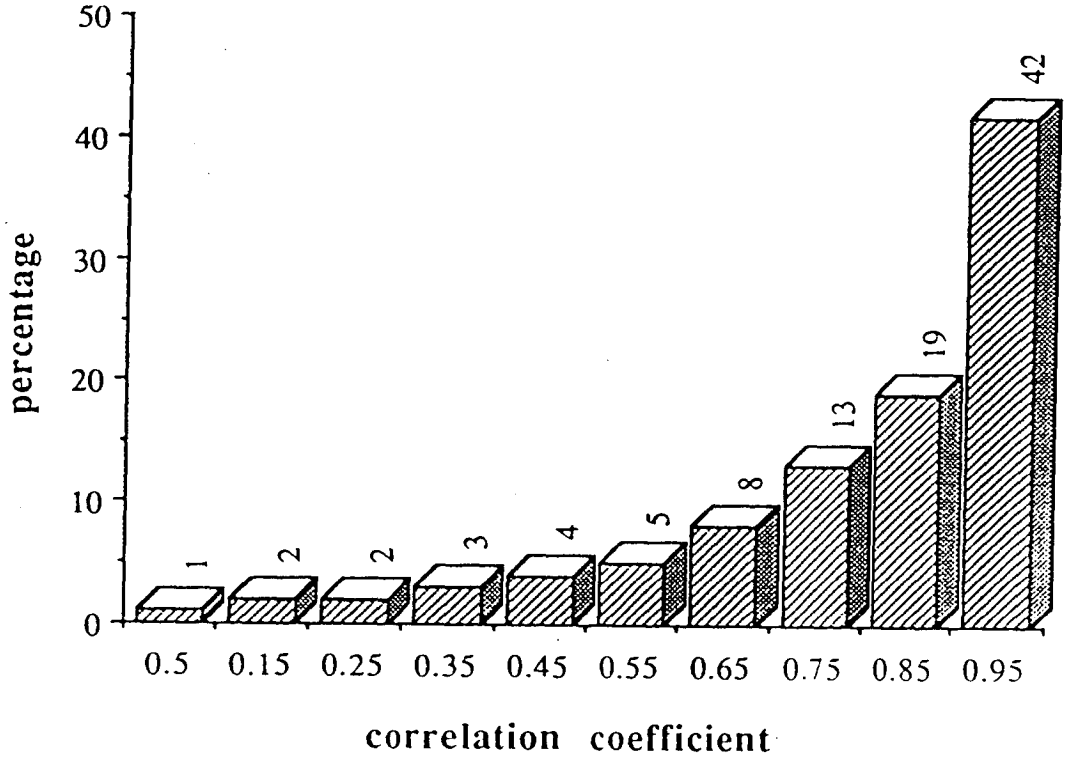

The x-axis of the histogram is the correlation coefficient in 0.10 intervals. The y-axis is the fraction of the total number of comparisons. The correlation coefficients are between the original body surface map and the recreated body surface map. The total number of comparisons is 201,200 comparisons.

Figure 4: Boxplot of correlation coefficients between the original and recreated body surface maps

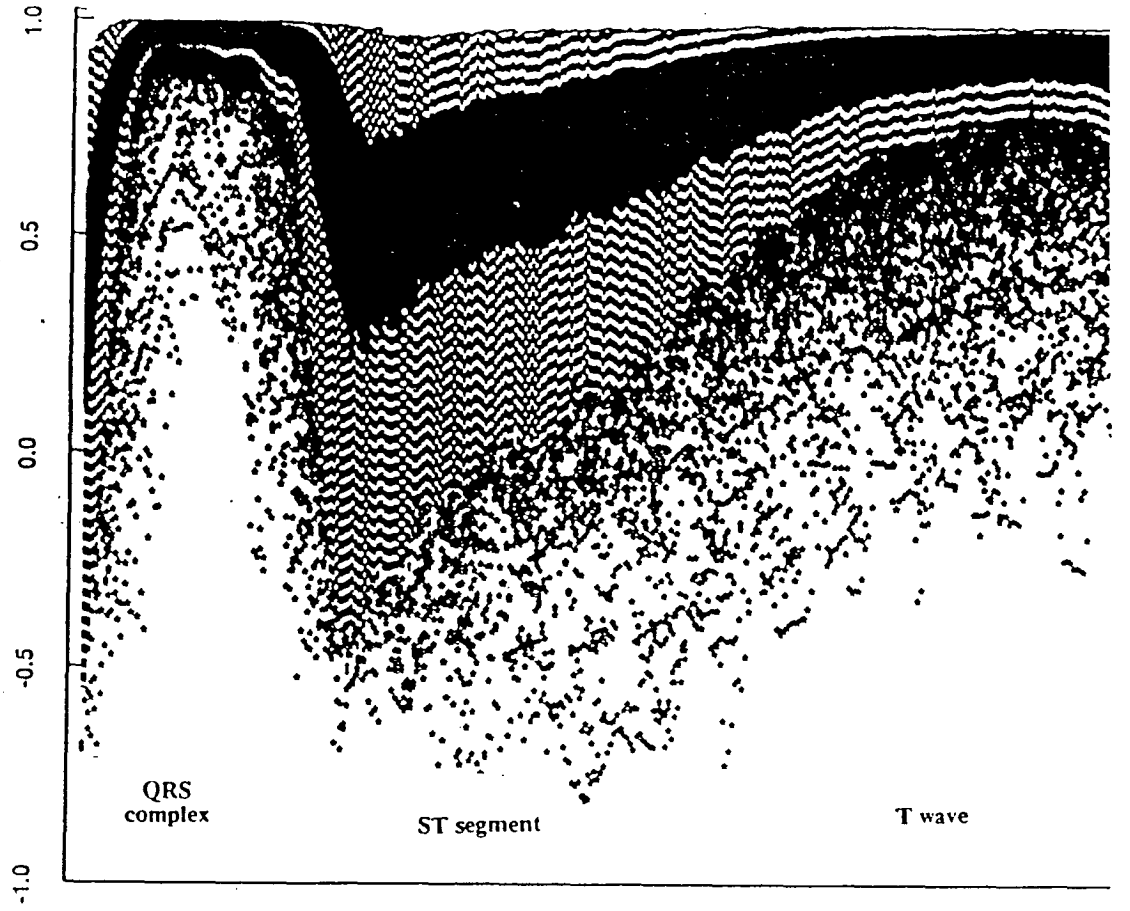

The x-axis is time from the QRS onset from 0 to 400 milliseconds, labeled as the significant electrocardiographic segments. The Y-axis is the correlation coefficient values. The dark areas represent the 75% confidence limit, the striped area the 95% confidence limit and the asterisk the outliner values.

Figure 5: Scatter plot of the first and second discriminant variables separating patients with and without coronary artery disease

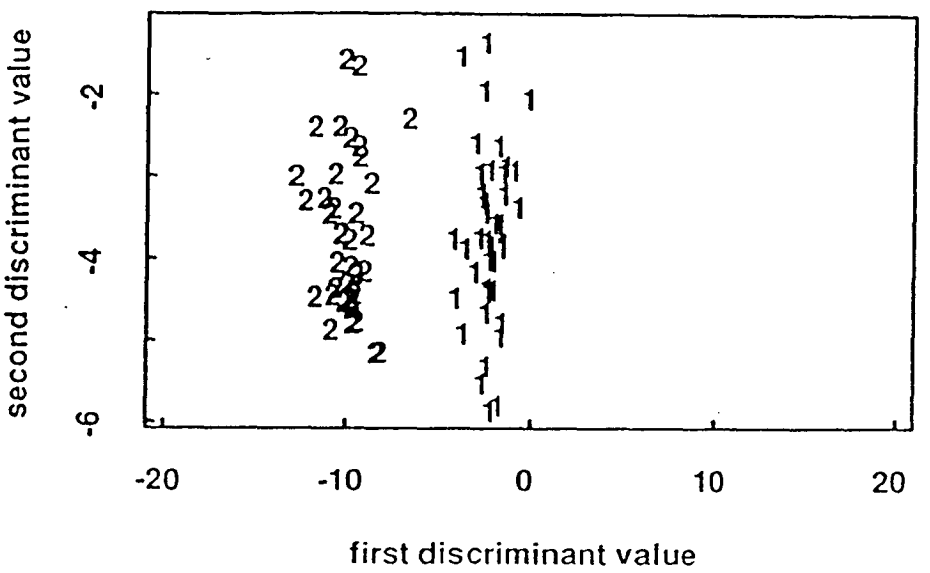

Each 1 represents a patient with normal coronary arteries. Each 2 represents a patient with coronary artery disease. The x-axis is the first discriminant variable. The y-axis is the second discriminant variable.

Figure 6: Density function plot of the first discriminant variable separating patients with and without coronary artery disease

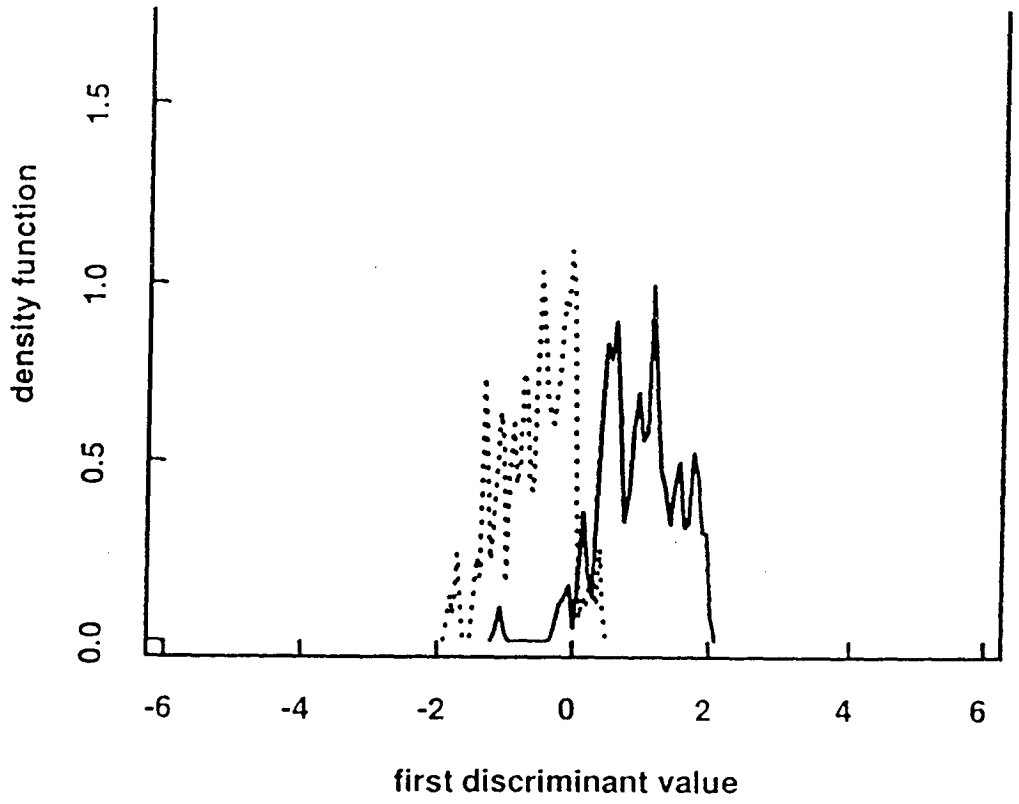

The x-axis is the first discriminant variable. The y-axis is the density function. The solid line is the normal patients density function line. The dotted line is the patients with coronary artery disease density function line.

Chapter 5

Data collection

Data collection for myocardial infarction studies

In May 1983 clinical body surface electrocardiographic mapping commenced at the Royal Hobart Hospital. Patients with acute myocardial ischaemic pain admitted to the Coronary Care Unit had body surface maps recorded as soon after admission as possible. The time of anginal pain onset was recorded at the time of the initial body surface map. The body surface electrocardiographic map was repeated each day until the patient was discharged from the Coronary Care Unit. The time of the recording of the body surface map was recorded at the time of data entry. Patients where invited to attend by letter each year for follow up body surface electrocardiographic mapping.

The collection of the body surface map information was rapid, usually less than 5 minutes, and did not interfere with the clinical care of the patients. The rapid method allowed collection of data even on patients with severe complications of acute myocardial infarction.

Detailed medical records of were kept independent of any knowledge of the body surface map. Total creatine kinase was measured every 8 hours for 48 hours and the peak creatine kinase measured level was used in the study as an approximation of infarct size. Patients were classified as having ventricular fibrillation after one or more episodes of ventricular fibrillation. Patients were classified as having ventricular tachycardia only if it was sustained or recurrent and warranted cardioversion or continuing drug therapy. Left ventricular failure was diagnosed if a chest x-ray showed pulmonary venous engorgement with interstitial oedema and the notes on the patient indicated evidence of clinical left ventricular failure. Right ventricular infarction or ischemia was diagnosed clinically if the jugular venous pressure was elevated and rose further on inspiration in the absence of other known cardiac or pulmonary causes. Right ventricular infarction or ischemia was diagnosed

by investigations if nuclear imaging demonstrated right ventricular dyskinesis and/or a diminished right ventricular ejection fraction compared with that for the left ventricle. The selected endpoints were used as these endpoints are well defined events and thus measurable without major difficulty in interpretation.

Standard electrocardiograms were kept and reported by a Hospital consultant cardiologist or experienced general physician and myself. The diagnosis of acute anterior or lateral wall myocardial infarction diagnosed on the basis of cardiac pain typical of acute myocardial infarction, anterior or antero-lateral ST segment elevation of at least 0.2 milliVolts in the 12 lead electrocardiogram with subsequent q wave formation and a rise and fall of creatine kinase consistent with myocardial infarction. All patients with a history of previous myocardial infarction, with bundle branch block or a QRS duration of greater than 0.11 seconds on the initial 12 lead electrocardiograms were excluded from the diagnosis of acute infarction.

All patients diagnosed as having acute inferior wall myocardial infarction had at least 0.1 milliVolts ST segment elevation in leads III or aVF of the standard electrocardiogram. Anterior ST segment depression was considered present if there was ST segment depression of at least 0.1 milliVolts on one or more of the standard 12 lead electrocardiogram leads V_1 to V_6. Both ST segment depression and elevation were measured by caliper at 140 millisecond after QRS onset with the use of the TP segment as zero baseline.

Gated heart pool scanning was performed in the department of Nuclear Medicine and the results reported by Dr R. Ware. Data included the the right and left ventricular ejection fraction and in the thallium scans a detailed analysis of the position of the myocardial infarction on the surface of the heart.

Coronary angiography was performed by the Hospital cardiologists and the results checked by Dr. David Kilpatrick.

Deaths after discharge were determined by telephone contact with the patients local medical officer or with the surviving patients or by inspection of the State registrar of deaths.

All studies were performed prospectively.

Data collection of angiogram controlled studies

All patients referred to the Cardiology unit of the Royal Hobart Hospital for coronary angiography were considered for the studies. The patients were screened for a past history of acute myocardial infarction, and if present were excluded from the study. Patients with angina or atypical chest pain having angiography for the assessment of coronary artery disease were entered into the study. The patients had a standard 12 lead electrocardiogram performed and reported by two consultant cardiologists not involved in the studies.

Basic demographic data and brief histories were obtained from all patients and recorded. The patients underwent standard coronary angiography in the Royal Hobart Hospital. The angiography was reported by the consultant cardiologists without regard to the patients entry into the study. The angiograms were recorded on a diagram of the coronary arteries showing 13 subdivisions of the coronary arteries and the percentage of the vessel diameter occluded by the disease. Left ventricular end diastolic pressure was recorded.

Patients underwent body surface electrocardiographic mapping either in the 24 hours before coronary arteriography or within 24 hours after coronary arteriography.

The results of nuclear medicine scanning, measurement of left and right ventricular ejection fractions, and exercise thallium testing were recorded.

The results of exercise testing were recorded, including the amount of exercise possible, the reason for the test stopping, electrocardiographic changes, changes in blood pressure and pulse rate.

The studies were performed prospectively.

Chapter 6

Analysis of the ST segment potential distribution in acute inferior wall myocardial infarction

Introduction

Anterior ST segment potential depression often accompanies acute inferior wall myocardial infarction, but the mechanism and prognostic significance have been debated. Most investigators have concluded that anterior ST segment depression is a reciprocal effect of inferior and/or posterior ST segment elevation [Wasserman 1983, Croft 1982, Perloff 1964]. This conclusion has been challenged by others who attribute anterior ST segment depression to anterior wall myocardial ischaemia [Roubin 1984, Shah 1980]. Since the spatial distribution of ST segment potentials in a large series of patients with acute inferior wall myocardial infarction has not been previously described, all of these studies have discussed anterior ST segment potential depression without detailed knowledge of the spatial distribution of ST segment potentials.

Some authors have concluded that there are no important differences in prognosis between patients with and without anterior ST depression [Wasserman 1983, Cohen 1984, Ferguson 1984], whereas others have concluded that patients with anterior ST depression have larger infarcts [Roubin 1984, Goldberg 1981, Gibson 1982, Stafford 1986], more complications [Perloff 1964, Roubin 1984, Shah 1980, Gelman 1982] or multivessel disease [Roubin 1984, Shah 1980].

The prognosis after recovery from acute inferior wall myocardial infarction is determined independently by the degree of left ventricular dysfunction, the degree of residual ischemia, and the frequency of occurrence of ventricular arrhythmias [Bigger 1984]. If anterior ST depression is a marker of larger infarcts, or of anterior wall myocardial ischaemia remote from the infarction site, or both, one possible explanation for the disparate results of previous studies is that the standard electrocardiography is an insensitive tool for quantifying the degree of anterior ST depression because of limited chest wall sampling.

In this study body surface maps recorded at the time of admission to the coronary care unit were analysed to determine if detailed measurement of body surface map ST segment potentials and the distribution of the ST segment potentials would predict those patients at high risk of death or major complications.

Methods

Study population

One hundred and ninety-eight patients all with first acute inferior wall myocardial infarction admitted to the coronary care unit of the Royal Hobart Hospital had body surface electrocardiographic maps recorded as soon as practicable after admission. The first 100 patients with a diagnosis of acute inferior wall myocardial infarction formed a learning set and the next 98 patients a testing set. The diagnosis of inferior wall myocardial infarction was based on a history of myocardial ischaemic pain, changes in the standard electrocardiogram (0.1 mV ST segment elevation in leads III or aVF of the standard electrocardiogram) and elevation of cardiac enzymes. The diagnosis was confirmed by echocardiography, arteriography, and nuclear imaging. All patients with bundle branch block (QRS duration greater than 0.11 seconds), or previous acute myocardial infarction were excluded. All patients gave informed consent and mapping did not interfere with the clinical management. No patient was excluded because of age, shock, left ventricular failure or arrhythmias. Clinical management and investigations were carried out by the patient's physician independently of any data acquired by mapping.

Clinical observation

Detailed records were kept independent of any knowledge of the body surface

map. Total creatine kinase was measure every 8 hours for 48 hours and the peak creatine kinase measured level was used in the study as an approximation of infarct size. Patients were classified as having ventricular fibrillation after one or more episodes of ventricular fibrillation. Patients were classified as having ventricular tachycardia only if it was sustained or recurrent and warranted cardioversion or continuing drug therapy. Left ventricular failure was diagnosed if a chest x-ray showed pulmonary venous engorgement with interstitial oedema and the medical record of the patient indicated evidence of clinical left ventricular failure at anytime during the hospital course. Right ventricular infarction or ischaemia was diagnosed clinically if the jugular venous pressure was elevated and rose further on inspiration in the absence of other known cardiac or pulmonary causes at anytime during the hospital course. Right ventricular infarction or ischaemia was diagnosed by investigations if nuclear imaging demonstrated right ventricular akinesis and/or a diminished right ventricular ejection fraction compared with that for the left ventricle.

Deaths after discharge were determined by telephone contact with all surviving patients and inspection of the State register of deaths.

Body surface mapping

Body surface maps were recorded as described previously. For this study only the ST segment maps were used. The ST segment distribution maps were constructed from data averaged over a 20 millisecond interval centered on a point 140 milliseconds after the QRS onset.

Grouping of map patterns

The learning set of 100 patients was grouped using the correlation coefficient

between all maps, using the complete linkage method of cluster analysis described in chapter 4. Each patient's body surface map in the testing set was placed into the learning set group with which the body surface map had the highest correlation coefficient.

Statistical analysis

After the patients were separated into groups by cluster analysis, data were analysed by Students t test or chi squared values with Yeats correction for small values when appropriate. The Mann-Whitney U test for ordered categories [Moses 1984] was used to examine the significance of variables with regard to associations with mortality or complications. A finding was considered significant when the p value was less than or equal to 0.05.

Results

The learning study population of 100 patients was made up of 77 men and 23 women with a mean age of 61 years. The median time between the onset of symptoms and the recording of the body surface map was 8.3 hours. Thirty-five patients had the diagnosis of acute inferior wall myocardial infarction confirmed by either angiography, echocardiography or nuclear medicine scanning.

The test study population of 98 patients was made up of 62 men and 36 women, with a mean age of 61 years. The median time between the onset of symptoms and the recording of the body surface maps was 6.5 hours. The median follow up time was 14 months. In 48 patients additional investigations (gated heart pool scan, coronary arteriography and post mortem) confirmed the diagnosis of inferior wall acute myocardial infarction.

Maximum negative ST segment measurement and prognosis of the learning set

Twenty-six patients had no ST segment depression on the body surface map, that is, the peak negative voltage was less than 0.1 mV, and 74 patients had ST segment depression. Table 1a compares major complications, death, and maximum creatine kinase in patients with a maximum negative potential less than 0.1 mV and those with ST segment depression. Patients with a maximum negative ST segment potential less than 0.1 mV had the same complication rate (apart from a lower occurrence of atrioventricular block) as patients with a maximum negative potential greater than 0.1 mV. When the complications, death, and creatine kinase peak value were analysed against increasing maximum negative potential there was a significant increase in the incidence of ventricular tachycardia, atrioventricular block, left ventricular failure, and death. There is also a relationship between increasing peak creatine kinase value and increasing maximum negative ST potential.

Maximum negative ST segment measurement and prognosis of the testing set

Table 1b compares the major clinical features of patients with increasing values of maximum ST depression. Ventricular tachycardia, atrioventricular block, left ventricular failure and death all have an increased rate of occurrence with increasing maximum ST depression identical to the initial set of patients. The peak creatine kinase values did not relate to the maximum negative ST potential. At a maximum ST depression over 0.2 millivolts there was a 25% mortality rate. Of the 4 patients who died with low maximum ST depression values, 1 died of cardiac rupture proven by autopsy, 1 died suddenly in hospital, and 2 died suddenly months after discharge. Of the patients who died with a high maximum ST depression, 7 died of left ventricular failure, 1 of myocardial rupture proven by autopsy, 1 of

sudden death and 1 of disseminated laryngeal carcinoma 8 months after the index myocardial infarction.

Maximum positive ST segment measurement and prognosis of the learning set

Table 2a shows the the relationship between complications, deaths and peak creatine kinase with maximum positive ST potential. There was a significant increase in the occurrence of left ventricular failure with increased maximum positive ST potential. There was a weak relationship between high values of maximum positive ST potentials and high creatine kinase peak values.

Maximum positive ST segment measurement and prognosis of the test set

Table 2b compares the major clinical features in patients with increasing values of maximum ST segment elevation. There was no consistent relationship for any clinical feature in the test set.

Clinical correlation with body surface map patterns

The learning set patients were clustered into 5 groups (denoted groups 0,1,2,3 and 4). The mean body surface ST segment maps for each group are shown in figure 1. Group 4 consisted of only 2 patients with poor quality, low level body surface ST segment maps that correlated poorly with those of all other patients. Data from this group have been excluded. Table 3 lists the mean values for maximum positive and negative ST segment potential for all groups.

Groups 0 and 1 had similar mean ST segment negative and positive potentials. The maximum negative ST potential occurred on the upper left front of the thorax in both these groups. However, in group 0, the maximum positive potential occurred on the lower right front of the thorax, whereas in group 1 it was located more to the

left and back. In group 2 the maximum positive potential was located in a similar position to that in group 0, although somewhat higher on the thorax. Group 2 had significantly lower mean maximum positive and negative ST potential values compared with those in the other groups. The median time between the onset of symptoms and mapping was significantly longer in group 2 than in the other groups.

The mean map pattern for group 3 was characterized by anterior ST depression and a significantly higher maximum negative ST potential than the other groups. The mean value for maximum positive ST potential is significantly lower in group 3 than in groups 0 and 1.

Groups 1 and 2 seemed to be low risk groups with a virtual absence of ventricular fibrillation, ventricular tachycardia, atrioventricular block, left ventricular failure, or right ventricular infarction or ischemia (table 3). Group 2 had a significantly lower mean peak creatine kinase compared to the other groups. Mortality was low in group 2 and no patient died in group 1. Group 3 had a significantly higher mortality compared with the other groups either singly or combined. There was no significant difference in peak creatine kinase values or in time from onset of symptoms to mapping between group 3 and groups 0 or 1. Overall, group 0 was an average risk group, groups 1 and 2 were low risk groups, and group 3 was a high risk group.

Table 4 shows the major clinical features of the 4 map pattern groups of the test set patients. The mean correlation coefficient for individual maps against the average maps was 0.790 and the median value 0.832. The mean body surface ST segment maps for each of the 4 groups are shown in figure 2. The body surface map patterns are virtually identical to the patterns from the learning set and the correlation coefficients between equivalent group average maps is greater than 0.98. Groups 0 and 1 have similar mean maximum ST segment elevation and maximum

ST depression values. Group 2 has both a significantly lower mean maximum ST depression value. The mean map pattern for group 3 is characterized by anterior ST depression, and a significantly higher mean maximum ST depression and lower maximum ST segment elevation values compared to the other groups. Group 3 has a significantly higher rate of left ventricular failure than the other groups, as found in the learning set. The average left ventricular ejection fraction for group 3 is less than in other groups.

Figure 3 shows the combined mortality and coronary artery bypass grafting survival curve for the 4 groups. Each group has an early morbidity. Group 3 has a significantly higher combined risk of death or coronary artery bypass grafting than the other groups ($p < 0.01$). On the other hand group 2 is a low risk group with a 92 % complication free survival at 15 months although this does not reach statistical significance ($p = 0.10$). This is consistent with the findings in the learning set of patients from whose data the map patterns were derived.

Relationship of ST segment body surface maps to coronary artery anatomy

In an attempt to relate coronary artery anatomy to the body surface map, the 42 patients who had coronary artery anatomy examined at angiography or at post mortem examination were examined in detail. In the high risk group (group 3), 13 patients were examined and 11 had significant triple vessel disease or left anterior descending artery disease. Two patients had single vessel disease. Of the 29 patients examined in the low risk groups (groups 1 and 2), 23 patients had no or trivial left anterior coronary artery disease. One patient had both right coronary artery disease and left circumflex disease. Four patients had right coronary artery disease and left anterior descending disease, 2 of whom were studied 9 and 11 months after mapping, and after the onset of new anginal symptoms.

Discussion

Body surface mapping

This study details the body surface distribution of ST segment potentials in 198 patients with acute inferior wall myocardial infarction. The 2 patients in group 4 were excluded as noted. Examination of the body surface potential distributions indicate that the presence or absence of anterior ST segment depression on the standard 12 lead electrocardiogram depends heavily on where those leads are placed and the overall shape of the body surface potential distribution. In patients with inferior wall myocardial infarction the standard chest leads generally fall on an area of the thorax where there is a steep voltage gradient, as shown by figures 1 and 2. Thus, observation of anterior ST segment depression is highly sensitive to the location of standard electrocardiographic leads. Such unreliability appears to be reflected in the recently published results on the significance of anterior ST depression in acute inferior wall myocardial infarction [Wasserman 1983, Roubin 1984, Shah 1980, Gibson 1982, Montague 1984]. Body surface mapping removes the unreliability resulting from lead placement because the entire surface of the thorax is sampled in detail.

The variation in distribution of ST segment potentials is probably due to one or more of the following factors: (1) variation in the anatomy of the coronary arteries, (2) which artery is occluded, (3) where in the course of that artery the occlusion has occurred, (4) the presence or absence of ischemia in other territories, and (5) the variation in the overall thoracic geometry [Stanley 1986].

These data suggest that the body surface map gives an indication of the involved artery or arteries. Certainly mean maps showing ST segment elevation on the right thorax (groups 0 and 2) appear associated with right coronary artery involvement.

Also, findings such as those in group 3 patients are associated with left anterior descending artery disease. It is unfortunate that arteriography results were not available in all patients as the angiograms were performed for clinical reasons with no reference to the body surface map and thus the patients undergoing angiography is a selected subset of the patients. Thus the limited number of patients studied may not be representative of the whole group.

Prognosis determined by body surface mapping

Early identification of patients at high risk after acute inferior wall myocardial infarction is required if a more aggressive therapeutic approach aimed at reducing the risk is to be successful. Reinfarction and death in patients who have left hospital after acute myocardial infarction are most common soon after hospital discharge [Bigger 1984]. If ischaemia remote from the infarct site is contributing to the left ventricular dysfunction and subsequent increased likelihood of death, then it should be identified promptly. Coronary arteriography and myocardial nuclear imaging both present considerable logistic difficulties in attempting to assess all patients with acute myocardial infarction. Standard 12 lead electrocardiography is a simple technique and has been previously shown to identify some patients at risk after infarction [Roubin 1984, Shah 1980, Gelman 1982]. Body surface mapping techniques rapidly measure the maximum ST depression and maximum ST elevation over the whole thorax. Increasing magnitudes of maximum ST depression were strongly correlated with death, ventricular tachycardia, atrioventricular block, left ventricular failure and a rising peak creatine kinase level. The ST distribution rapidly identified these high risk patients.

The grouping of the map patterns was done on the basis of correlation coefficients, which are independent of the overall magnitude of the maps. This

method also separated the patients into groups with important clinical differences. The patients in groups 1 and 2 were at very low risk of ventricular fibrillation, ventricular tachycardia, atrioventricular block, left ventricular failure, right ventricular infarction or ischemia, or death. On the other hand, patients in group 3 had a high complication rate in the test set of patients. Severe left anterior descending artery disease was demonstrated in most of the group 3 patients for whom angiographic or autopsy results were available. The high death rate of group 3 in the learning set (37%) was not present in the test set. In this study there were more deaths in other groups due to cardiac rupture and sudden death in hospital. In the test set, of the 10 deaths outside group 3, 4 patients died of sudden cardiac death, 4 patients died with proven single vessel disease, of whom 2 had autopsy proven cardiac rupture. In the learning set most patients died of left ventricular failure. The progressive mortality of the group 3 patients over the 15 month follow up period confirms that this is indeed a high risk group. The lack of a high early death rate may reflect alteration in management of patients following inferior wall myocardial infarction with increased use of thrombolytic therapy, converting enzyme inhibitors as therapy and early coronary arteriography and aggressive management by surgery.

Body surface mapping and angiogram appearance

Of the 29 patients in the low risk groups for whom angiographic data were available only 4 had left anterior descending artery disease (stenosis greater than 70%) and two of these patients had angiography months after the index myocardial infarction. Of the group 3 patients who had coronary angiography 11 of 13 patients had left anterior descending disease. Thus there is a strong association with left coronary artery disease and the group 3 body surface map pattern. The potential

distributions defining group 3 are dominated by a large area of marked ST segment depression anteriorly. It is tempting to speculate that in patients in this group, the degree of ST segment depression is due to anterior wall ischemia as well as the ST segment depression that would be associated in a reciprocal manner with the ST elevation associated with inferior wall myocardial infarction. This concept of distal ischemia in acute myocardial infarction has been previously discussed [Schuster 1980].

Body surface isopotential electrocardiographic map patterns

As each individual map pattern in this study had a high correlation coefficient with one of the average map patterns from the learning set of 100 patients, this study confirms that the method of producing groups is valid and that there are 4 major patterns of ST potential distributions in inferior wall acute myocardial infarction. There is a suggestion that the group 0 patients have increased rate of right ventricular infarction (tables 3 and 4). This did not reach statistical significance in the test group. This may be due to there being no association, the inaccuracy of measuring the presence or absence of right ventricular infarction or a combination of both factors.

In the clinical setting the presence of a group 0 body surface map pattern would lead to consideration of right ventricular infarction as a cause of say low blood pressure, while a group 3 pattern would lead to consideration of left ventricular failure as a cause of hypotension. This consideration would lead to different therapy for the patient while definite investigations were performed.

Conclusion

Patients suffering an initial inferior wall myocardial infarction are not a

homogeneous group [Goldberg 1981]. There is a subset at low risk in whom aggressive interventional therapy is not warranted. In the group at high risk aggressive interventional management, including an attempt at immediate thrombolysis followed by angiography is warranted. The body surface map is a method of rapid risk stratification. A standard 12 lead electrocardiogram is unable to differentiate the map patterns due to the limited thoracic sampling. Using the chest leads, V leads of the standard electrocardiogram, at various levels improves detection of the ST segment depression but not as efficiently as the body surface map. Also, although ST depression is detected, the maximum magnitude of ST depression may not be determined. This may explain why attempts to relate the standard electrocardiogram to prognosis in inferior wall acute myocardial infarction has produced disparate results [Wasserman 1983, Croft 1982, Roubin 1984, Shah 1980, Gelman 1982]. The use of multiple electrocardiograms over time may improve the prognostic ability [Lembo 1986] as may the use of multiple body surface maps in an individual patient.

Table 1a: Clinical significance of maximum ST segment depression in learning set

	maximum ST segment depression (milliVolts)					
	[0.0,0.1)	[0.1,0.2)	[0.2,0.3)	[0.3,0.4)	≥0.4	p value[a]
number	26	28	17	9	20	
VF	0	0	2	0	2	NS
VT	0	0	2	1	4	<0.006
AVB	1[b]	4	4	2	10	<0.006
LVF	3	1	1	3	9	<0.004
Deaths	1	1	1	2	6	0.0014
peak CK	1046	1132	1557	1591	2272	
(IU/L)	±870[c]	±514[c]	±909	±1340	±1567	

Note: [x,y) means the range of values between x and y including x but not y, as per standard mathematical notation.
VF = ventricular fibrillation. VT = ventricular tachycardia, AVB = atrioventricular block,
LVF = left ventricular failure. peak CK = creatine kinase peak value (IU/L)

[a] p value for analysis of complication rate against increased ST segment depression by Mann-Whitney U test

[b] p value < 0.05 for different rate of occurrence in patients with maximum ST segment depression <0.01 and patients with ST depression ≥ 0.1 mV.

[c] p value < 0.05 by one way analysis of variance and students t test versus maximum ST segment depression ≥ 0.4

Table 1b: Clinical significance of maximum ST segment depression in test set

	magnitude of anterior ST segment depression (milliVolts)					
	[0.0,0.1)	[0.1,0.2)	[0.2,0.3)	[0.3,0.4)	≥0.4	p value[a]
number	30	28	16	14	10	
VF	2	1	1	1	3	NS
VT	5	4	6	4	3	0.047
AVB	4	7	9	3	5	0.007
LVF	2	5	4	3	4	0.007
Deaths	4	0	3	3	4	0.015
peak CK[b]	1573[c]	1973[c]	2444	1806[c]	3098	
(IU/L)	± 1108	± 1971	± 1575	± 1256	± 1789	

Note: [x,y) means the range of values between x and y including x but not y, as per standard mathematical notation.
VF = ventricular fibrillation, VT = ventricular tachycardia, AVB = atrioventricular block,
LVF = left ventricular failure, peak CK = creatine kinase peak value (IU/L)

[a] p value for analysis of complication rate against increased ST segment depression by Mann-Whitney U test

[b] $p = 0.079$ by one way analysis of variance for differences in creatine kinase values

[c] p value < 0.05 by students t test versus maximum ST segment depression ≥ 0.4

Table 2a: Clinical significance of maximum ST segment elevation in learning set

	maximum ST segment elevation (mV)					
	[0.0,0.1)	[0.1,0.2)	[0.2,0.3)	[0.3,0.4)	≥0.4	p value[a]
number	20	37	20	8	15	
VF	1	2	0	0	1	NS
VT	0	1	2	2	2	NS
AVB	2	5	5	2	7	NS
LVF	2	3	3	2	7	<0.0009
Deaths	2	4	2	1	2	NS
peak CK	1166 ± 591[b]	1328 ±1113[c]	1124 ±616[b]	2000 ±1077	2278 ±1641	

Note: [x,y) means the range of values between x and y including x but not y, as per standard mathematical notation.
VF = ventricular fibrillation, VT = ventricular tachycardia, AVB = atrioventricular block,
LVF = left ventricular failure, peak CK = peak creatine kinase level

[a] p value for analysis of complication rate against increased ST segment depression by Mann-Whitney U test

[b] p value < 0.05 students t test versus maximum ST segment elevation ranges [0.3,0.4) and ≥0.4 mV.

[c] p value < 0.05 by one way analysis of variance and students t test versus maximum ST segment elevation ≥ 0.4

Table 2b: Clinical significance of maximum ST segment elevation in test set

	maximum ST segment elevation (mV)					
	[0.0,0.1)	[0.1,0.2)	[0.2,0.3)	[0.3,0.4)	≥0.4	p value[a]
number	30	35	21	5	7	
VF	3	1	2	0	2	NS
VT	8	4	4	3	3	NS
AVB	4	8	9	3	4	NS
LVF	8	7	2	0	1	NS
Deaths	3	5	3	1	2	NS
peak CK[b]	1983 ± 2102	1631 ± 1135	2453 ± 1342	2305 ± 556	2528 ± 1588	

Note: [x,y) means the range of values between x and y including x but not y, as per standard mathematical notation.
VF = ventricular fibrillation, VT = ventricular tachycardia, AVB = atrioventricular block,
LVF = left ventricular failure, peak CK = peak creatine kinase level

[a] p value for analysis of complication rate against increased ST segment depression by Mann-Whitney U test

[b] p = 0.321 by one way analysis of variance for differences in creatine kinase values

Table 3 : Clinical characteristics of map pattern groups in learning set

	Group 0	Group 1	Group 2	Group 3
patient numbers	45	22	12	19
time between symptoms and map (hours)	14.1 ± 15.6	8.5 ± 10.7	37.7 ± 32.6[a]	14.4 ± 14.5
maximum ST depression (μV)	281 ± 195	210 ± 175	77 ± 47[a]	465 ± 436[a]
maximum ST elevation (μV)	284 ± 175	210 ± 132	127 ± 34[c]	174 ± 139[c]
VF	2	0	0	2
VT	5	0	0	2
AVB	11	0[b]	1[b]	5
LVF	10	0[b]	1[b]	5
RVI	11	0[b]	0[b]	5
Deaths	3	0	1	7[d]
peak creatine kinase	1606 ± 1206	1395 ± 949	772 ± 578[a]	1592 ± 1225

VF = ventricular fibrillation, VT = ventricular tachycardia, AVB = atrioventricular block,
LVF = left ventricular failure, RVI = right ventricular infarction by clinical detection

[a] p value < 0.05 different from all other groups by Student's T test

[b] p value < 0.05 chi squared test, groups 1 and 2 combined versus groups 0 and 3 combined

[c] p value < 0.05 different from groups 0 and 1 by Student's T test

[d] p value < 0.005 chi squared test versus all other groups

Table 4 : Clinical characteristics of map pattern groups in test set

	Group 0	Group 1	Group 2	Group 3
patient numbers	32	14	25	27
time symptoms to map (hrs)	12.8 ± 16.1	7.7 ± 7.7	16.3 ± 16.6	20.1 ± 22.9
maximum ST depression (mV)	240 ± 180	198 ± 262	100 ± 70[a]	318 ± 238[b]
maximum ST elevation (mV)	222 ± 188	217 ± 173	195 ± 96[a]	112 ± 66[a]
VF	4	2	0	2
VT	9	3	4	6
AVB	15	3	2[c]	8
LVF	4	3	0	11[c]
RVI	10	1	4	2
Deaths	5	3	2	4
peak creatine kinase (IU/L)	1619 ± 1161	2344 ± 1083	1767 ± 1177	2494 ± 2252
Ejection fraction (%)	54 ± 10	59 ±6	58 ± 5	48 ± 13
no. patients having ejection fraction measured	10	3	5	9

VF = ventricular fibrillation, VT = ventricular tachycardia. AVB = atrioventricular block,
LVF = left ventricular failure, RVI = right ventricular infarction by clinical detection

[a] p value = 0.02 by one way analysis of variance against the other groups

[b] p value = 0.002 by one way analysis of variance against the other groups

[c] $p < 0.002$ different from all other groups

Figure 1: Average integral ST segment body surface maps for patients with acute inferior wall myocardial infarction in the learning set

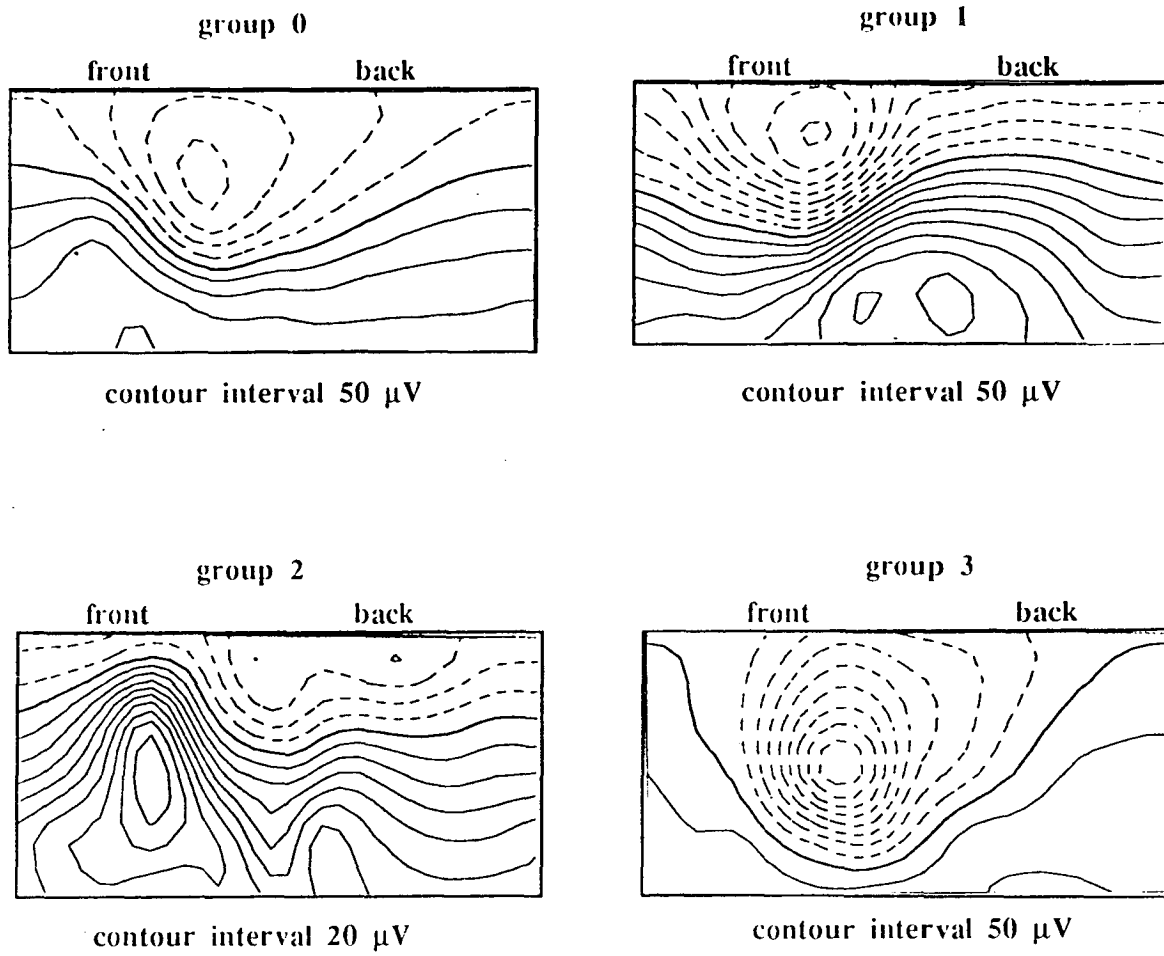

The display is the standard format. The contour interval is in microvolts.

Figure 2: Average integral ST segment body surface maps for patients with acute inferior wall myocardial infarction in the test set

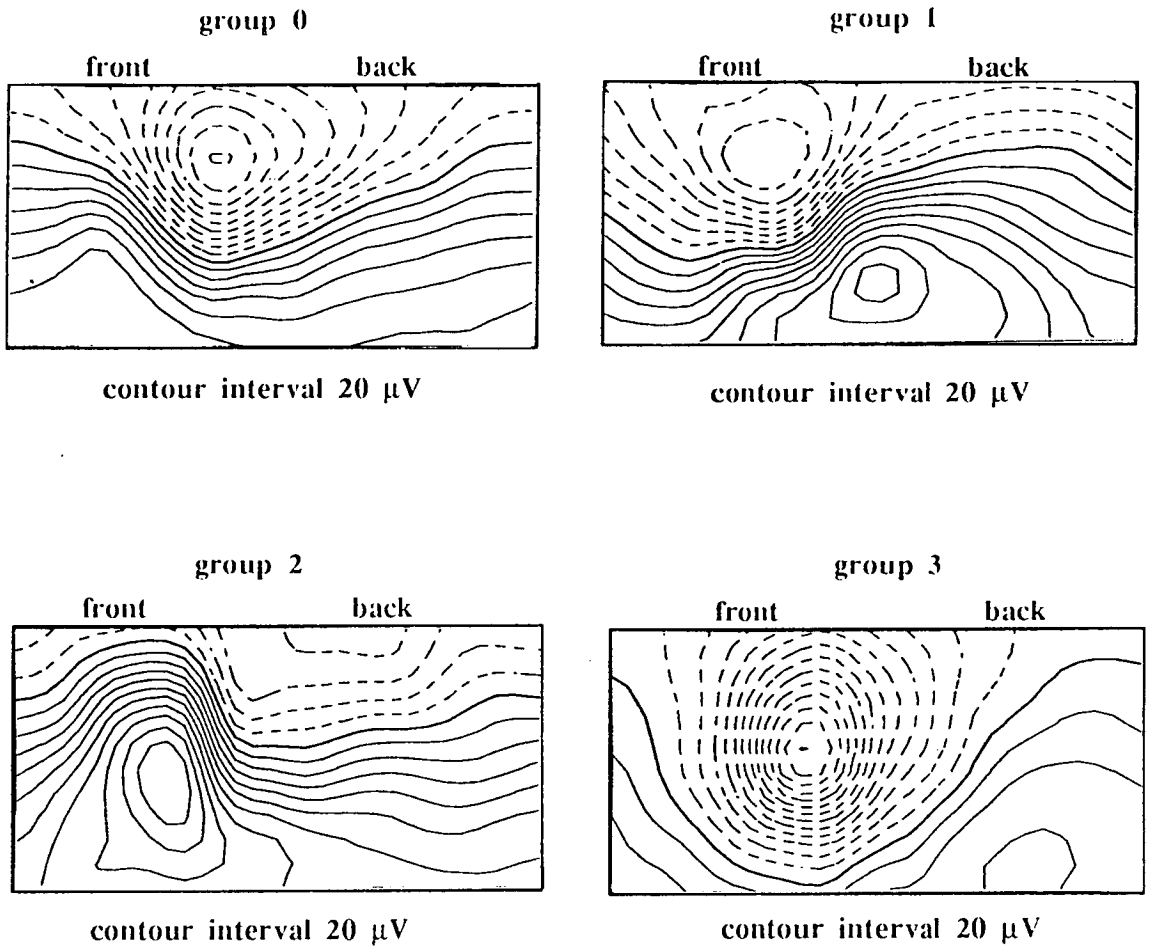

The display is the standard format. The contour interval is in microvolts.

Figure 3 : Patient survival rate free of death and coronary artery bypass grafting

A

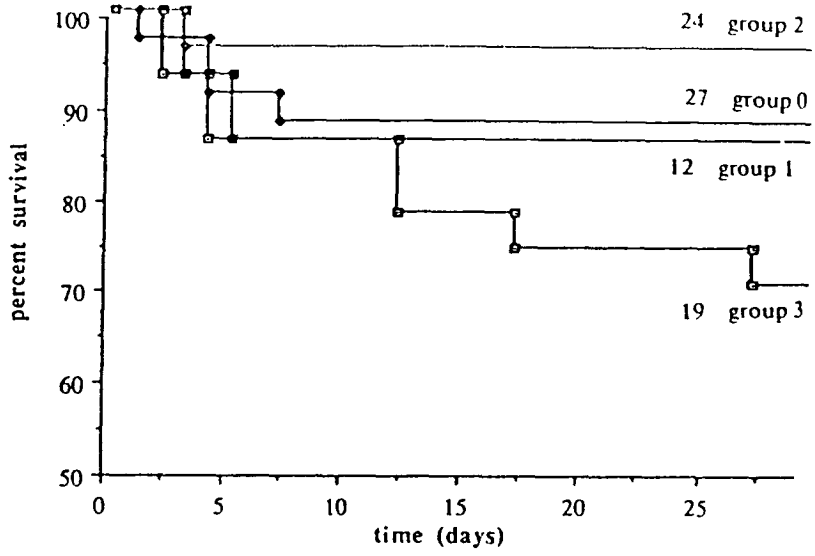

B

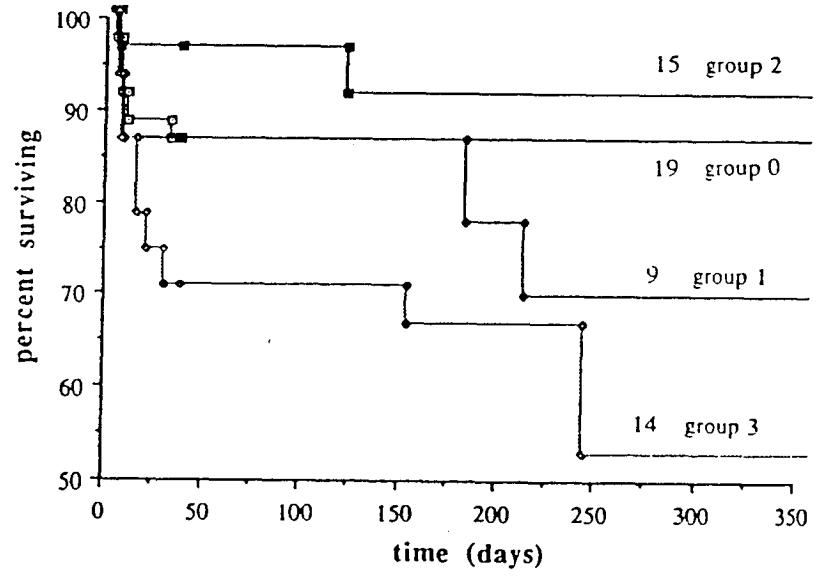

Patient survival rate free of coronary artery surgery after inferior wall myocardial infarction. Graph A - first 30 days. Graph B - 1 year follow up. Numbers on lines represent the number of patients under observation in each group at the 25 days (graph A) and 270 days (graph B).

Chapter 7

Natural history of ST segment potential distribution determined by body surface mapping in patients with acute inferior infarction

Introduction

The prognostic significance of precordial electrocardiographic (ECG) ST segment depression during acute inferior infarction is controversial. Some studies suggest its presence defines a high risk group [Roubin 1984, Shah 1980, Goldberg 1981, Gibson 1982, Stafford 1986, Gelman 1982] where as others claim that it has little relationship to long term prognosis [Wasserman 1983, Cohen 1984, Mills 1975]. Two factors are relevant to this controversy. Firstly most studies have attempted to relate prognosis to the magnitude of the ST segment depression on the earliest recorded ECG. Precordial ST depression is more common in ECGs recorded soon after symptom onset and studies have shown that initial ST depression resolves rapidly in the majority of patients [Mills 1975, Klainman 1987]. Persistent ST depression has been reported to indicate a high risk group [Lembo 1986] which suggests that the time of ECG recording may influence any possible relationship to prognosis. Secondly the choice of ECG leads to define precordial ST depression varies between studies. The technique of body surface mapping, by sampling from the entire thorax, overcomes the problem of variation in the choice of leads. In the previous chapter and published studies we have described the body surface distribution of ST segment potentials in patients with acute inferior wall myocardial infarction [Walker 1987, Bell 1989], and showed that the precordial leads were positioned over an area of steep voltage gradient. Hence the observation of precordial ST segment depression is very sensitive to the location of the chest leads. By sampling from the entire thorax this potential source of error is diminished.

There have been few sequential electrocardiographic mapping studies on the early evolutionary phase of myocardial infarction. Recent studies on the temporal evolution of the body surface map pattern in acute infarction have focused on changes occurring between days and months after the infarction [Montague 1984,

DeAmbroggi 1986]. In this study we sought to examine the changes in ST segment potentials both during the initial 72 hours of an inferior myocardial infarction and over subsequent months. In particular we analysed the ST segment distributions and their relationship to death, or ongoing coronary ischemia requiring hospital admission or coronary artery bypass grafting.

Methods

Study population

All patients admitted to our coronary care unit with acute myocardial infarction had electrocardiographic body surface maps recorded as soon after admission as practicable. All patients in the study had the diagnosis of acute inferior myocardial infarction on the basis of a history of myocardial ischaemic pain, changes in the 12 lead electrocardiogram and enzymatic methods. All patients with a history of previous myocardial infarction were excluded. Patients who received thrombolytic therapy were excluded. All patients with bundle branch block or a QRS duration of greater than 0.11 seconds on the initial or subsequent electrocardiograms were not included in the analysis. All patients gave informed consent and mapping did not interfere with clinical management of the patients. No patient was excluded because of age, shock, left ventricular failure or arrhythmia. Clinical management and investigations were the responsibility of the patient's attending physician.

Patients in this study consisted of two groups. Both groups were a subset of all patients admitted to the coronary care unit with acute inferior wall myocardial infarction. The total number of patients admitted to the coronary care unit over the period of data collection was 198 patients described in chapter 6. All patients who met the selection criteria for this study were included. Patients were excluded if they did not have a further body surface map performed due to death, early transfer from

the coronary care unit, refusal to participate in the study and map machine failure. The first group (group A) comprised 91 patients who were mapped within 24 hours after the onset of symptoms and who had a subsequent body surface map performed in the next 48 hours. The second group (group B) consisted of 61 patients who were mapped within 24 hours after the onset of symptoms and who returned for repeat body surface mapping at least 6 months after acute inferior infarction. All potential study candidates were approached. Patients with further infarction or coronary artery by-pass grafting were excluded. Thirty patients are in both groups A and B.

Clinical observation

Detailed medical records were kept. Total creatine kinase levels were measured every 8 hours for 48 hours and the peak measured level was used in this study as an approximation of infarct size. Patients were classified as having ventricular fibrillation (VF) if they left hospital alive after one or more episodes of ventricular fibrillation. Patients were classified as having ventricular tachycardia (VT) only if it was sustained or recurrent and warranted cardioversion or continuing drug therapy. All patients with either second degree or complete heart block were classified as having atrioventricular block (AVB). Left ventricular failure (LVF) was diagnosed if a chest X-ray showed pulmonary venous engorgement with interstitial oedema and the patients notes recorded evidence of clinical left ventricular failure. Right ventricular infarction or ischemia was considered diagnosed if the jugular venous pressure was elevated and rose further on inspiration in the absence of other known cardiac or pulmonary causes. Patients were classified as having died if they died within 3 years of the index myocardial infarction. Patients were regarded as having significant long term morbidity if they were readmitted to the coronary care unit within 18 months of acute infarction with either new infarction or angina.

Kaplan-Meier survival curves were based on the full follow up period. Patient status was determined at the time of follow up mapping; the Canadian Heart Class classification of angina [Campeau 1976], the New York Heart Association classification of left ventricular failure [New York Heart Association 1973] and the medical history were recorded. The status of all surviving patients was determined by interview with the patient or local medical officer.

Body surface mapping

The ST segment isopotential maps used in this study were each constructed from data averaged over a 20 millisecond interval centered on a point 140 milliseconds after the QRS onset.

Grouping of map patterns

All patients were categorized into map pattern groups based on the highest correlation coefficient of their body surface ST segment potential distribution to four previously described ST segment distributions in acute inferior infarction as shown in chapter 6 [Walker 1987, Bell 1989] and a normal ST segment distribution based on 576 normal maps kindly loaned by the investigators in Salt Lake City [Green 1985]. The groups are named according to the terminology in the previous chapter and studies [Walker 1987, Bell 1989].

Statistical analysis

Continuous variables were compared by the Student t test. Discrete variables were compared by chi squared test with correction for continuity where appropriate. The distribution of a discrete variable on a continuous variable was analysed by the Mann-Whitney U test. The Kaplan-Meier morbidity curves were compared using the

Mantel-Haenszel test. A p value of 0.05 or less was regarded as significant.

Results

Group A map patterns and magnitude of ST segment potentials

The study group consisted of 91 patients, 20 females and 71 males with a mean age of 63 ± 10 years. Initial body surface maps were performed a mean of 7.9 ± 5.4 hours after onset of acute inferior infarction and a further map a mean of 32.6 ± 21.6 hours post infarction.

The initial map patterns are shown in figure 1 and the map data in table 1. The initial map patterns correlated from the previously described map patterns described in chapter 6 with a correlation coefficient of 0.98 or greater between equivalent groups.

The follow up map patterns are shown in figure 2 and map data in table 2. Each of the individual follow up map patterns correlated well with one of the initial map patterns.

Natural history of map patterns

The changes in map pattern between the initial map pattern group and the follow up map pattern group are shown in table 3 with the clinical data of combined mortality and morbidity. Forty two patients (46%) remained in the same ST segment distribution group at a mean follow up time of 32.6 hours. Twenty-five patients (34% of those patients not in group 2) moved to group 2 and 4 patients (7%) correlated best with the normal ST segment distribution and were included into a normal group. Seven patients went into group 3, of whom 3 died and 2 suffered

morbidity. Patients who at any time had a group 3 map pattern had a 45% chance of death or morbidity compared to the other groups' 13% risk ($p < 0.005$). as shown in figure 3; the mortality and morbidity "survival" curve for the patients in group 3 at any time against patients who were never in group 3.

Group B map patterns and magnitude of ST segment potentials

Sixty-one patients, 46 males and 15 females with an average age of 65 ± 10 years, were studied in group B. The initial maps were done a mean of 15.0 ± 15.8 hours after the onset of symptoms. The follow up maps were recorded a mean of 19.6 ± 13.0 months after the myocardial infarction.

Figure 4 shows the initial map patterns and the map pattern group data are in table 4. The map patterns are virtually identical to the map patterns of group A patients. Table 5 shows the follow-up map data and figure 5 shows the follow up map details. The correlation coefficient of the mean map patterns from initial group to follow up group is greater than 0.96 in all groups. Table 6 shows the initial and follow-up map groups of the 61 patients as well as the morbidity in these patients. Twenty-seven patients, 44% of the total number, correlated best with a normal ST segment distribution. Nineteen patients moved into or remained in the group 2 pattern. Twelve patients (20%) remained outside the normal or group 2 pattern of ST segment distribution. Seven patients had the high risk map pattern group 3 at the time of follow up mapping. Of these seven patients one subsequently died and two have had admissions to the coronary care unit. Six patients had significant angina at the time of follow up with 2 patients in group 2, and 4 patients in group 3 ($p < 0.001$). There were six patients in New York Heart Association class 3, four from group 4 and two from group 2.

Discussion

This study follows the natural history of the ST segment in acute inferior infarction. The ST segment after infarction is thought to return to normal over a 24 to 48 hour period in uncomplicated inferior myocardial infarction [Mills 1975, Klainman 1987]. This study shows that an ST segment distribution pattern clearly recognizable as associated with inferior infarction persists to a mean of 19 months post myocardial infarction in 56% of patients.

At a follow up time of 32.6 hours post symptom onset group 2 is the predominant pattern. At 19 months follow up map patterns that correlate best with a normal ST segment distribution are dominant and the group 2 pattern accounts for 40% of the patients. We believe that the group 2 pattern represents the ST segment distribution associated with resolving uncomplicated inferior infarction. The pattern occurs early after infarction in some patients although group 2 initial maps are recorded a longer time after symptom onset than other groups. These patients have an uncomplicated course generally. At 24 to 72 hours the group 2 pattern is the most common pattern and is associated with few complications. Generally group 2 patients have lower peak creatine kinase value than the other groups. At 19 months, the early group 2 patients ST segment patterns either correlate to a group 2 pattern or correlate with the normal ST segment distribution.

On the other hand patients in the group 3 pattern of ST segment distribution, the pattern dominated by anterior ST segment depression, have a high mortality and morbidity. Though patients having an initial group 3 map pattern in this study do not have a higher mortality or morbidity the selection criteria for the study select against group 3 patients. Previous studies have demonstrated a higher early mortality rate in patients admitted with a group 3 ST segment distribution pattern. Patients who remained in the group 3 pattern continued to have a 33% combined mortality and

morbidity. Patients who moved to the group 3 pattern at 24 - 72 hours had a 33% mortality and a 33% morbidity. At follow up mapping 19 months following the infarction group 3 patients had significantly higher angina scores than other groups.

The aetiology of persistent anterior ST segment depression is not clear. We believe that the best explanation is that the depression is due to inferior infarction with associated anterior myocardial wall ischemia. This explanation for the group 3 pattern was suggested previously. As the peak creatine kinase values are not different between the groups infarct size is probably not different. Also patients with the group 3 pattern at 19 months have angina and not left ventricular failure which suggests the presence of ischemia and not left ventricular failure that is associated with larger infarction size. This suggests that ischemia persists as the cause of the pattern and that the pattern is not related to the size of the infarction. There may be a subgroup of patients with larger infarction in the group 3 pattern but-patients with anterior wall ischemia dominate and lower the peak creatine kinase value. Certainly the number of patients in the group 3 pattern who have left ventricular failure rises in the 24 - 72 post infarction map. Other causes of persistent ST segment depression must be considered. If the anterior ST depression was reciprocal to inferior ST segment elevation then the body surface map would be expected to measure the ST elevation. This may occur in inferior wall ventricular aneurysm formation for example but was not detected in this study. Group 3 patients may have a ventricular conduction defect with alteration of the repolarization forces. A ventricular conduction defect is commonly seen after myocardial infarction but is frequently unclassifiable and its clinical significance is not known.

Patients with ST distribution of group 0 type appear to fall into three types. Four patients developed the type 3 pattern at 24 - 72 hours post infarction, and all these patients either died, 3 patients, or had urgent coronary artery by pass grafting.

Approximately half the group 0 patients remained in the group and half moved to the group 2 pattern. The group 0 ST distribution pattern falls between the group 2 and group 3 patterns. We believe the variability of the follow up ST distribution in this group is a reflection of the continuous distribution of ST segments depending on the circumstances. Pattern grouping methods in continuous distributions are not ideal and have been used here to attempt to order the large quantities of data.

This study demonstrates that the ST segment changes may persist for years after an inferior myocardial infarction in a pattern recognizably associated with inferior myocardial infarction. Pathologically this suggests that the source of ST segment elevation is not only due to acute damage currents, but persists due to changes in repolarization secondary to loss of myocardium. Typically the ST segment voltages return to within normal limits soon after acute inferior myocardial infarction. Failure to return to normal suggests the presence of ventricular aneurysm or a large area of ventricular asynergy [Mills 1975]. Another mechanism for the persistence of ST segment elevation is based on the spatial concordance of Q wave and ST segment patterns [Gewirtz 1979]. The ST elevation observed over the infarcted area may be reciprocal to the ST depression in other areas of the heart. This explanation is analogous to Q wave formation, which is considered to reflect transmural excitation of remote regions of the heart viewed through electrically inactive areas of infarction.

This study describes the persistence of an abnormal ST map pattern which has not previously been described. Although the ST segment voltages do not exceed the normal voltages the pattern is abnormal. Thus we believe this persistence of an abnormal pattern reflects effects of damage to the myocardium and that the most likely cause is an abnormal depolarization and associated repolarization of the ventricle. The other explanations for persistent ST segment elevation are not as applicable.

In any event body surface mapping represents a simple method to assess ST segment changes after acute inferior wall myocardial infarction, and possibly in the assessment of patients with recent undiagnosed chest pain. In our experience the body surface map is quicker to perform than a standard 12 lead electrocardiogram, and the classification by map patterns adds a further assessment dimension not available in 12 lead electrocardiography.

Conclusion

The body surface map in acute inferior infarction is of clinical significance. Regardless of when the map is recorded patients who move into the high risk group 3 are at particular risk of death or ongoing clinically significant ischemia. Long term changes in ST segment patterns after inferior infarction occur and require further analysis, but may be indicators of inferior aneurysm formation.

Table 1: Initial body surface map patterns and map data: Group A

	initial map pattern group			
	0	1	2	3
number of patients	33	21	21	16
time from symptom onset (hrs)	7.5 ± 4.4	5.0 ± 3.7	11.9 ± 6.3[a]	7.5 ± 5.7
correlation coefficient*	0.86 ± 0.10	0.84 ± 0.18	0.81 ± 0.10	0.78 ± 0.16
maximum ST-segment elevation (μV)	261 ± 155[b]	198 ± 147	152 ± 67	122 ± 72
maximum ST-segment depression (μV)	279 ± 192	219 ± 220	102 ± 66	309 ± 194

Table 2: Follow up body surface map patterns and map data: Group A

	follow up map pattern group				
	0	1	2	3	4
number of patients	25	7	39	16	4
time after symptom onset (hrs)	30 ± 6[b]	28 ± 7	41 ± 21	21 ± 18	32 ± 19
correlation coefficient*	0.80 ± 0.14	0.80 ± 0.11	0.77 ± 0.15	0.78 ± 0.16	0.48 ± 0.24
maximum ST-segment elevation (μV)	147 ± 94	143 ± 141	149 ± 79	114 ± 78	116 ± 50
maximum ST-segment depression (μV)	163 ± 87[c]	102 ± 39	87 ± 49	243 ± 101[a]	60 ± 42

* the mean correlation coefficient between each individual map pattern and the average map pattern for the initial map groups

[a] different from all other groups, $p < 0.03$, [b] different from groups 2 and 3, $p < 0.012$

[c] different from groups 2 and 4 , $p < 0.03$

Table 3: Relationship between initial and follow up map patterns and morbidity: Group A

	initial map pattern group			
group	0	1	2	3*
follow-up map group				
0	15 (2)	2	4	4 (1)
1	2	4	1	0
2	11 (1)	11 (4)	14 (2)	3 (1)
3*	4 (4)	2 (1)	1	9 (3)
normal	1	2	1	0

The numbers in parenthesis indicate the number of patients with mortality or morbidity.
* patients in group 3 at any time have a higher morbidity rate

Table 4: Initial body surface map patterns and map data: Group B

	initial map pattern group			
	0	1	2	3
number of patients	20	13	18	10
time from symptom onset (hrs)	12.5 ± 12.9	6.8 ± 8.1	23.8 ± 12.0[a]	11.6 ± 11.1
correlation coefficient*	0.86 ± 0.11	0.82 ± 0.09	0.85 ± 0.07	0.79 ± 0.11
maximum ST-segment elevation (μV)	208 ± 141	200 ± 120	171 ± 55	83 ± 31[b]
maximum ST-segment depression (μV)	218 ± 182	213 ± 112	107 ± 58[c]	251 ± 83

* the mean correlation coefficient between each individual map pattern and the average map pattern for the initial map groups

[a] different from groups 0 and 1 by Students t-test, $p < 0.03$

[b] different from all other groups by Students t-test, $p < 0.012$

[c] different from all other groups by Students t-test, $p < 0.03$

Table 5: Follow up body surface map patterns and map data: Group B

	follow up map pattern group				
	0	1	2	3	4
number of patients	3	1	22	7	28
time after infarction (months)	18 ± 3		14 ± 12	20 ± 14	22 ± 14
correlation coefficient	0.60 ± 0.16	0.53	0.52 ± 0.18	0.51 ± 0.25	0.53 ± 0.20
maximum ST-segment elevation (μV)	102 ± 33	48	139 ± 78	128 ± 124	183 ± 82
maximum ST-segment depression (μV)	166 ± 76	68	69 ± 42	211 ± 96[a]	85 ± 101
angina score >2	0	0	2	4	0
NYHA score ≥ 3	0	0	1	0	4

* the mean correlation coefficient between each individual map pattern and the average map pattern for the initial map groups
NYHA= New York Heart Association score for left ventricular failure
[a] different from groups 2 and 4 by Students t-test, $p < 0.005$

Table 6: Relationship between initial and follow-up map patterns and morbidity: Group B

	initial map pattern group			
group	0	1	2	3
follow up map group				
0	1 (1)	0	2	1
1	0	0	0	1
2	9 (1)	6	4 (3)	4 (1)
3	2 (1)	0	2	3 (2)
normal	7 (1)	6	12 (3)	2 (1)

The numbers in parenthesis indicate the number of patients with mortality or morbidity

Figure 1: Mean initial integral ST segment body surface maps for patients in group A

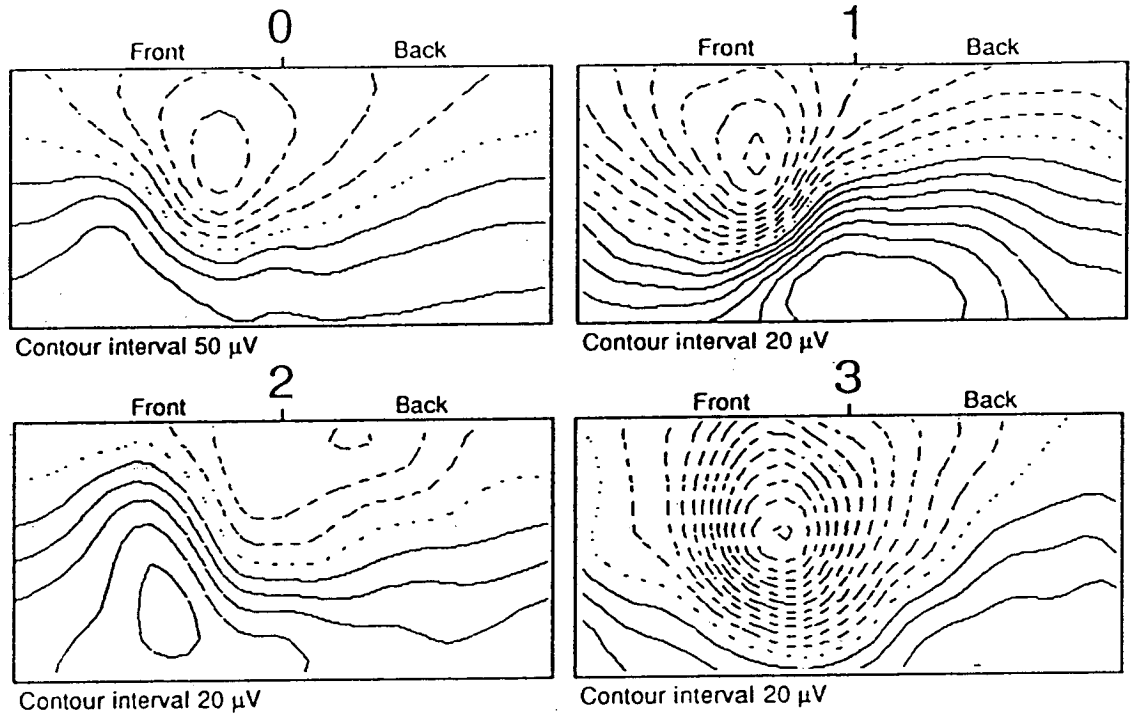

The mean ST segment potential distribution for the initial body surface maps in group A showing groups 0-3. The data format is the standard format. The contour interval is in microvolts and displayed below each map.

Figure 2: Mean follow up integral ST segment body surface maps for patients in group A

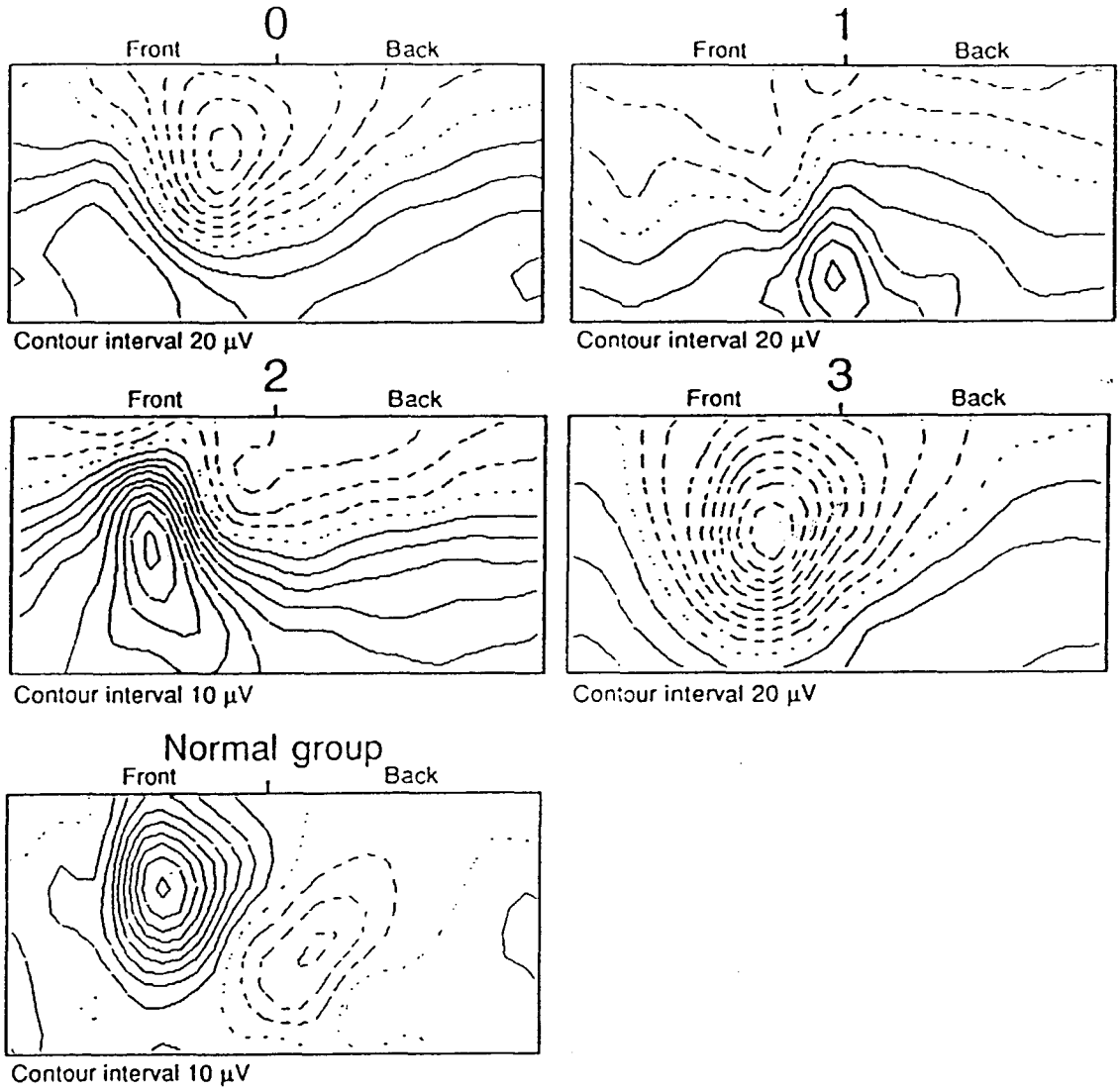

The mean ST segment potential distribution for the initial body surface maps in group A showing groups 0-3 and the normal ST segment matched group. The data format is the standard format. The contour interval is in microvolts and displayed below each map.

Figure 3: Survival curve for patients with and without a group 3 body surface map

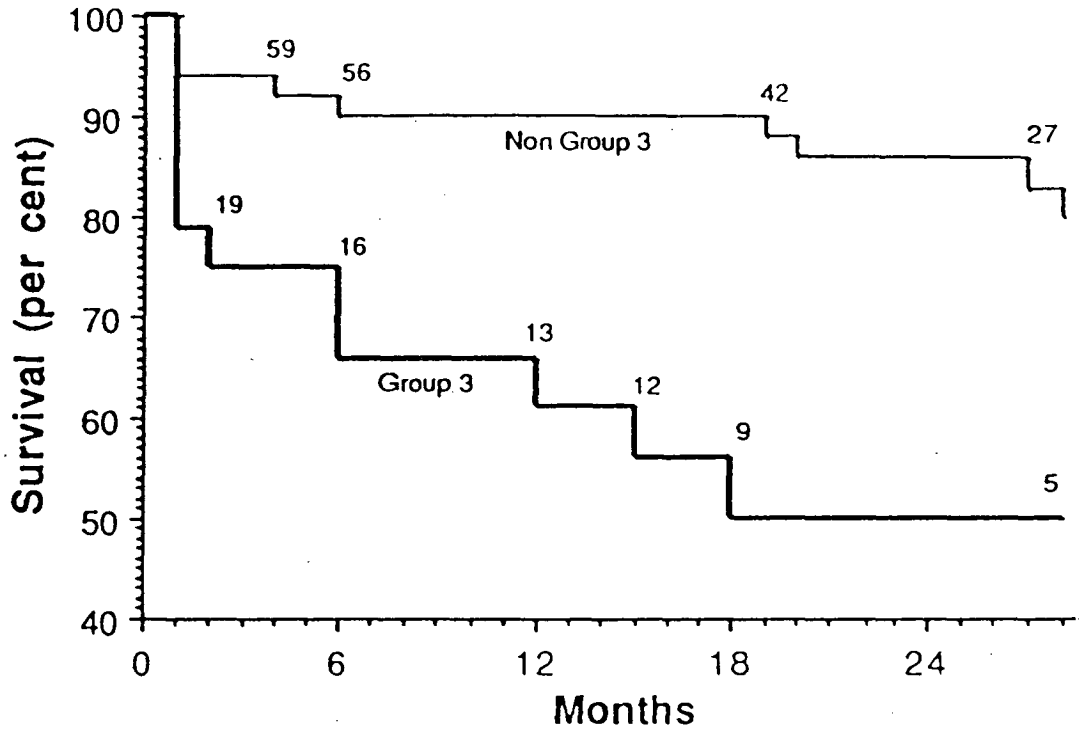

The bold line is the survival curve for patients who have a group 3 map appearance at any time. The plain line is the survival curve for patients who never have a group 3 map appearance. The numbers above the line refer to the number of patients alive at the particular time. Patients with a map pattern of the group 3 type at any time have a higher mortality rate with $P < 0.005$.

Figure 4: Mean initial integral ST segment body surface maps for patients in group B

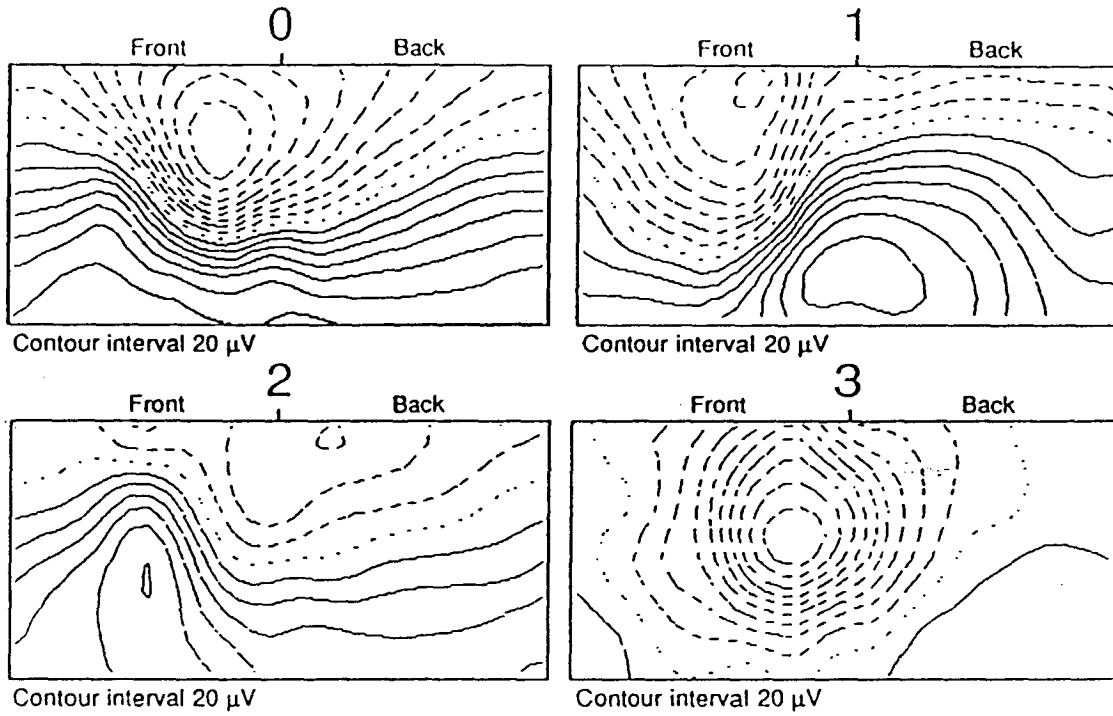

The mean ST segment potential distribution for the initial body surface maps in group B showing groups 0-3. The data format is the standard format. The contour interval is in microvolts and displayed below each map.

Figure 5: Mean follow up integral ST segment body surface maps for patients in group B

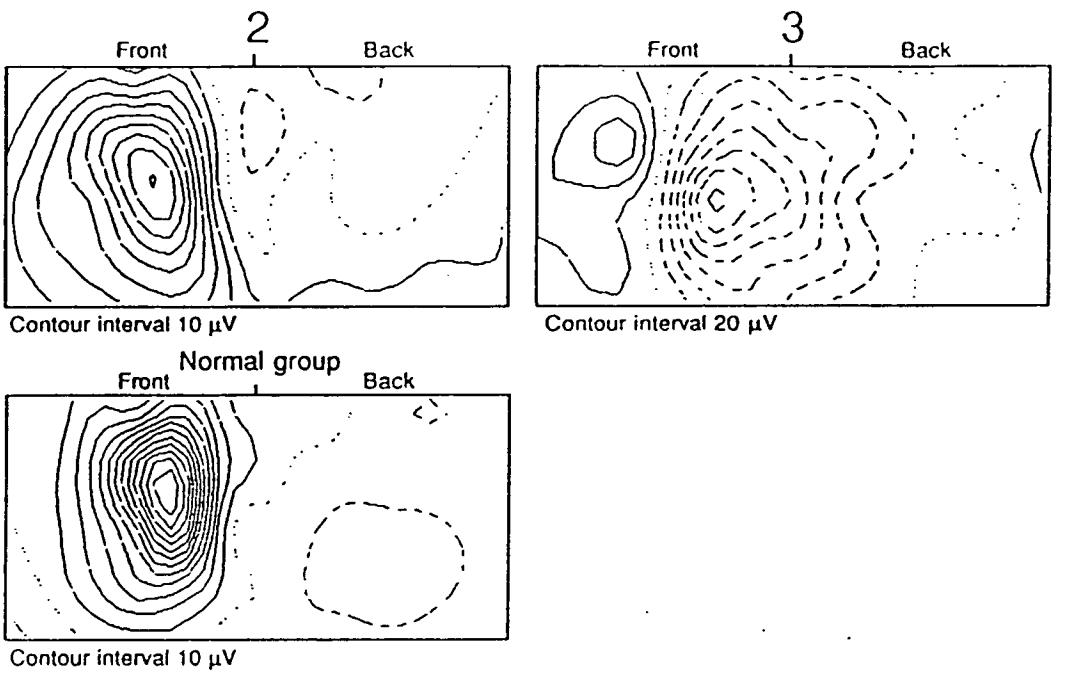

The mean ST segment potential distribution for the follow up body surface maps in group B showing group 2, group 3 and the normal ST segment matched group. The data format is the standard format. The contour interval is in microvolts and displayed below each map.

Chapter 8

The relationship of ST segment elevation to eventual QRS loss in acute inferior myocardial infarction

Introduction

To use the electrocardiogram to assess the effects of therapy in patients receiving thrombolytic therapy the relationship between ST elevation and loss of QRS potentials must be known, so that the eventual outcome as assessed electrocardiographically can be compared to the predicted outcome from the initial ST segment elevation. The relationship between ST elevation and eventual Q wave formation or QRS loss has not been well studied in inferior wall myocardial infarction because of the technical difficulty of adequately collecting map data in acutely ill patients and the limitations of standard 12 lead electrocardiograms. The standard electrocardiogram does not allow adequate quantification of potential distributions, making it necessary to use body surface potential mapping [Selwyn 1978, Henning 1978].

To analyse the natural history of these changes in acute inferior wall myocardial infarction we have isolated those patients with first inferior wall myocardial infarction who might accurately represent the natural history of electrocardiographic change, and analysed the initial ST elevation in relation to the eventual QRS loss in these patients.

Methods

Patient selection

The patients consisted of the 198 patients described in chapter 6 [Walker 1987, Bell 1989]. From this group of patients all patients who had received thrombolytic therapy, had coronary artery bypass grafting or coronary angioplasty or subsequent infarction were excluded. Follow up maps were taken at 6 months and at least 18 months following infarction.

Body surface mapping

The body surface maps were recorded as previously described. This study used the standard ST segment map and the integral 0-80 millisecond QRS map.

Data processing

We constructed the body surface map for the time interval 0 to 80 milliseconds after the onset of the QRS complex to represent the QRS. We include a comparison of each 10 msec interval for a set of 196 patients with inferior wall myocardial infarction to demonstrate that a mean inferior wall myocardial infarction pattern differs from the normal pattern at all intervals from the Q wave to the ST-segment (figure 1). We examined subtraction maps from the normal QRS over the same time interval. The normal QRS is derived from data kindly loaned to us by Drs Green et al. [Green 1985] based on 208 normal men and 173 normal women.

Statistical processing

We used the correlation coefficient to compare the maps. We also performed direct visual comparison of the data by looking at the regions on the map to determine whether the contours defined the same region in the two maps being compared. Correlations were defined as; good - maps in which all regions were predicted; partial - maps in which the ST elevation was inferior, but showed an additional region, such as right sided or posterior ST elevation that was not seen on the final electrocardiogram. The remainder, in which no correlation was observed were defined as bad correlations.

Results

Seventy patients, 54 men and 16 women, met the criteria for entry into the study.

Their mean age was 65 ± 9 years and the mean creatine kinase was 1437 ± 1214 units (normal < 200 units). The initial maps were recorded 13.4 ± 14.8 hours after the onset of symptoms. The early follow up maps were recorded 41.7 ± 25.7 hours after the onset of symptoms, and the long term follow up maps 21.2 ± 14.7 months after infarction.

The QRS maps of the averaged normal, averaged inferior infarction and normal minus inferior wall infarction maps at 10 msec intervals throughout the QRS are presented in figure 1. The difference maps show clearly that the differences are present throughout the QRS.

For all 70 patients we examined the correlation coefficients computed between the initial map and the short term follow up map. The correlation coefficient results are shown in table 1. Thirty-seven patients had both short and long term follow up maps. In 41% the long term maps showed less correlation with the ST segment elevation than did the short term follow up maps, due to recovery of inferior postivity in the final map.

Discussion

These results show that in most patients the region of ST elevation during an acute inferior wall myocardial infarction correlates well with that of the eventual loss of R wave. Subjectively this had been suspected, and several studies showed the relationship of QRS changes to right ventricular infarction [Montague 1983, Essen 1980]. The relationship of body surface ST elevation area and myocardial infarction size has not been studied in inferior wall myocardial infarction, but with anterior wall myocardial infarction a general relationship has been shown to exist.

Our patients included only patients not given thrombolytic therapy. The reasons for not prescribing streptokinase were usually related to the time of presentation.

Our routine practice was to prescribe streptokinase only to highly suitable patients. This may have caused a bias towards patients with later presentations and less ST elevation. In the six patients in whom there was no correlation between QRS loss and ST elevation, the elapsed time between the onset of pain and the initial mapping was long in three but less than 5 hours in three others. Additional confounding factors may include pericardial involvement and non-Q-wave infarction.

The techniques of analysis used in this analysis are complex and involve the use of a normal map average from 381 normals to assess the region of QRS loss. Although this technique does not take into account the variability between individuals, it has been previously used successfully [Flowers 1976a, Flowers 1976b, Yamada 1978, Toyama 1984, Suzuki 1984, Toyama 1982]. Subtraction techniques have also been used by other authors, using the patients own maps for subtraction [Montague 1984]. To do this successfully in the study of eventual QRS loss one would need QRS maps of the patients prior to the onset of chest pain. Even mapping all patients with chest pain in the coronary care unit we have collected very few maps prior to the ST segment elevation, and when the ST elevation has occurred after the first map most patients have been treated with thrombolytic therapy. In the study the use of a standardized normal to derive the "QRS loss" maps gives a reasonable correlation with the maps showing the initial ST elevation.

In a study on dogs, Flowers et al. [Flowers 1978] showed the importance of these different diagnostic electrocardiographic techniques in assessing infarction size. They concluded that the best correlations were available from the difference map at 16 milliseconds with a 95% confidence limits of 0.56-0.97. In terms of human studies, the problem of gold standard for infarction size makes similar estimations difficult unless they are against post mortem data. We were concerned that the selective approach would not recognize the entire QRS loss because the differences

between inferior infarction and normal persisted throughout the first 80 msec of the QRS (figure 1). Recording 80 msec also avoids the difficulty in picking the QRS onset sufficiently accurately. Our data are sampled at 1 KHz, and the onset is picked automatically and then checked manually against the individual leads, but even this leaves the QRS onset uncertain in some patients. The 0-80 msec period does not take into account minor conduction delays, which may alter the QRS morphology. From these data this does not appear to affect the correlation. All maps with prolonged QRS intervals greater than 0.10 seconds were excluded from the analysis.

The correlation coefficients used are useful for comparing the shapes of body surface maps and have been used for clustering similar shapes [Walker 1987, Bell 1989]. This form of correlation coefficient compares all values, both positive and negative. This is appropriate because it is invalid to separate ST elevation from ST depression when they arise from the same source, unless one has resolved the data back onto the heart surface and defined the separate current sinks and sources on the heart.

Some patients showed a marked change from the short term follow up to the long term follow up map. Several patients who had anterior infarction in this time period were excluded, but some patients who showed initial high correlations were seen to have a much lower correlation on the follow-up map. The reasons for this are not clear. Montague et al. [Montague 1984] demonstrated changes occurring between a mean of 79 hours and a mean of 8 months; these changes were mainly in a reduction of the infarction pattern, which is similar to the one seen in this series. No common factor separating these patients who showed QRS recovery from those who did not could be isolated.

The conclusions that can be drawn from this study are that the region of ST elevation in inferior infarction predicts the the QRS loss when compared to the

normal QRS, and that the effects of intervention can be assessed through the resultant QRS loss.

Table 1: Correlation coefficients for all groups

Correlation group	correlation coefficient	binary correlation coefficient
Good		
Mean	0.488	0.435
Median	0.577	
Poor		
Mean	0.018	0.048
Median	0.009	
Bad		
Mean	-0.099	-0.099
Median	-0.062	

Table 2: Clinical correlates by group

	Correlation group		
correlation group	good	poor	bad
number	53	11	6
mean age (years)	65 ± 10	66 ± 10	63 ± 7
% male	80	100	17
CK max (iu/L)	1793 ± 1640	1934 ± 1655	875 ± 770
First map time (hours)			
mean	11.9	11.8	24.8
median	6	8	11.5
range	1-60	4-50	4-66

CK max is the peak creatine kinase level measure following the reference inferior wall myocardial infarction

Figure 1: Comparison of the patients with a normal body surface map and patients with an acute inferior wall myocardial infarction map over the QRS complex

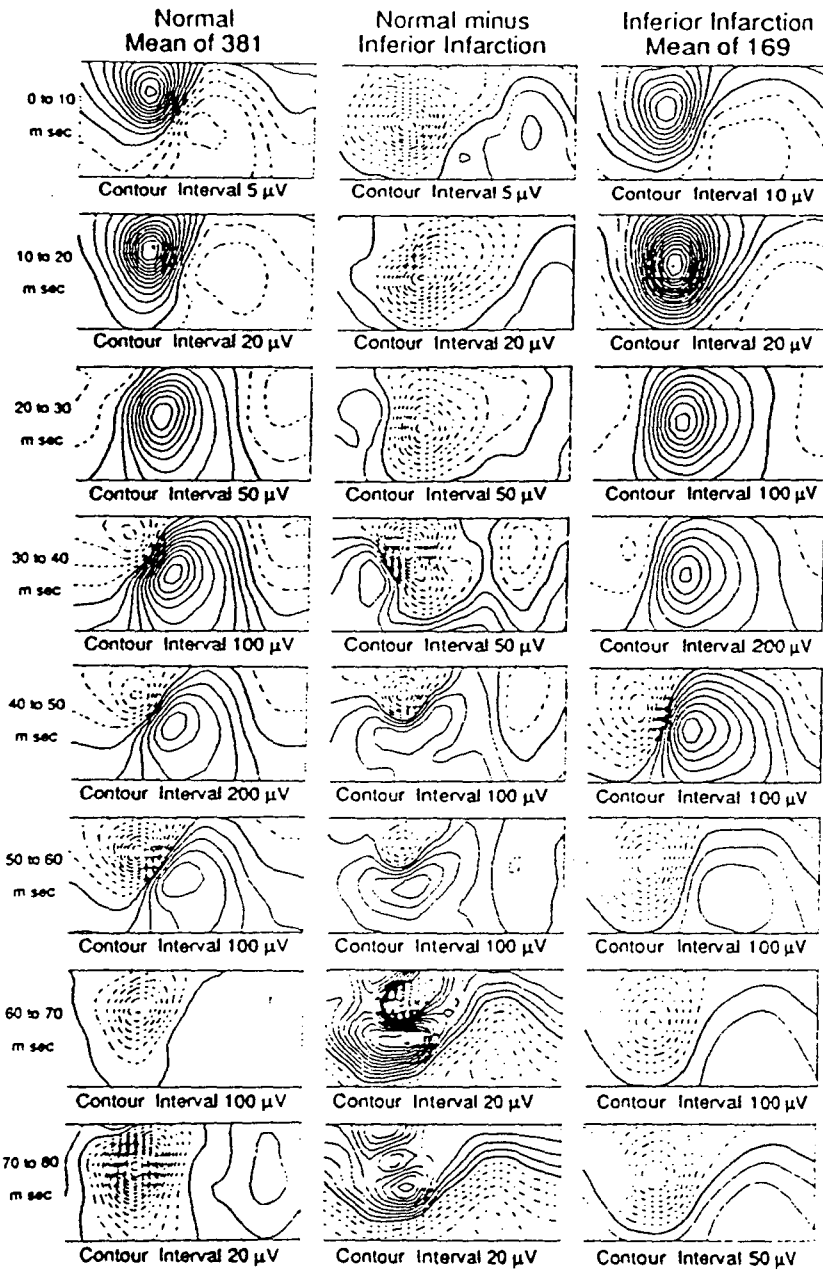

A series of maps illustrating the difference between normal (LHS) and inferior infarction (RHS) at time intervals throughout the QRS. Each map is integrated over 10 milliseconds. The difference maps are in the center. Dashed lines represent negative contours, heavy continuous lines represent the zero contour, and thin continuous lines positive contours.

Chapter 9

The prognostic significance of the ST segment in acute anterior wall myocardial infarction determined by body surface mapping

Introduction

Studies on the temporal evolution of the body surface map pattern in acute anterior wall myocardial infarction have focused on the changes occurring between days and months after the infarction. There have been few electrocardiographic mapping studies on the early evolutionary phase of acute anterior wall myocardial infarction [Montague 1986, Nakagaki 1981]. In particular the relationship of the ST potential distribution, determined by body surface mapping during the initial phase of acute anterior wall myocardial infarction, to the clinical course of the patients has not been evaluated. We examined the relationship of the spatial distribution of ST segment potentials to short and long term mortality and morbidity.

In acute inferior wall myocardial infarction the area of ST segment potential depression is related to the area of ST segment elevation in the majority of patients. In one group of patients the body surface map is dominated by ST segment depression. We have demonstrated that this pattern is associated with a higher mortality and rate of coronary artery by pass grafting than other ST segment potential distributions [Walker 1987, Bell 1989a, Bell 1989b].

In acute anterior wall myocardial infarction the presence of ST segment depression has not been studied in sufficient detail to determine if the presence of the ST segment depression is a consequence of ST segment elevation or is related to inferior ischemia occurring at the time of acute anterior wall myocardial infarction [Myers 1949, Marriott 1977]. In a study of standard electrocardiograms the presence of inferior ST segment depression with anterior wall myocardial infarction was associated with a higher mortality and morbidity and with the presence of multivessel coronary artery disease [Haraphongse 1984]. Studies done during angioplasty of the left anterior descending coronary artery have suggested that the inferior ST segment depression is an electrical phenomenon rather than a reflection

of inferior wall myocardial ischemia [Quyyumi 1984]. In the present study 162 patients in the first 36 hours of acute anterior wall myocardial infarction were studied by body surface mapping and the mapping patterns and measurements related to the clinical course of the patients.

Methods

Study population

The patients in this study had the diagnosis of acute anterior or lateral wall myocardial infarction on the basis of cardiac pain typical of acute myocardial infarction, anterior or antero-lateral ST segment elevation in the 12 lead electrocardiogram with subsequent Q wave formation and a rise and fall of creatine kinase consistent with myocardial infarction. Patients were included only if they were mapped within 36 hours of symptom onset. All patients with a history of previous myocardial infarction, with bundle branch block or a QRS duration of greater than 0.11 seconds on the initial 12 lead electrocardiograms were excluded.

All patients gave informed consent and mapping did not interfere with clinical management of the patients. No patient was excluded because of age, shock, left ventricular failure or arrhythmia. Clinical management and investigations were the responsibility of the patient's attending physician. All patients who met the selection criteria for this study were included.

Clinical observation

Detailed medical records were kept. Total creatine kinase levels were measured every 8 hours for 48 hours and the peak level used in this study as an approximation of infarct size. Patients were classified as having ventricular fibrillation if they left hospital alive after one or more episodes of ventricular

fibrillation. Patients were classified as having ventricular tachycardia only if it was sustained or recurrent and warranted cardioversion or continuing drug therapy and the patient did not have ventricular fibrillation. All patients with either second degree or complete heart block were classified as having atrioventricular block. Left ventricular failure was diagnosed if a chest X-ray showed pulmonary venous engorgement with interstitial oedema and the patient's notes recorded evidence of clinical left ventricular failure. The status of all surviving patients was determined 5 years after the onset of the study by interview with the patient or local medical officer. All deaths were confirmed by inspection of the State record of deaths.

Body surface mapping

The ST segment maps used in this study were each constructed from data averaged over a 20 millisecond interval centered on a point 140 milliseconds after the QRS onset.

Grouping of map patterns

The map patterns were compared using a calculated correlation coefficient [Walker 1987, Pham-Huy 1981]. Cluster analysis grouped individual maps on the single linkage method.

Statistical analysis

Continuous variables were compared by the Student T test [Matthews 1987]. Discrete variables were compared by chi squared test with correction for continuity where appropriate [Matthews 1987]. The distribution of a discrete variable on a continuous variable was analysed by the Mann-Whitney U test [Moses 1984]. In the tables the continuous variables have been divided into quartiles for ease of display,

but the statistical calculation is performed on the total number of comparisons. The Kaplan-Meier morbidity curves were compared using the Mantel-Haenszel test [Matthews 1987]. A p value of 0.05 or less was regarded as significant.

Results

The study group consisted of 162 patients, 38 women and 124 men with a mean age of 62 ± 11 years and range 33-78 years. Initial body surface electrocardiographic maps were performed a mean of 6.3 hours after the onset of symptoms of acute anterior infarction. The median follow up time for surviving patients was 36 months. Thirty-one percent of the patients had thrombolytic therapy. The analysis has been performed on the whole patient set, because with inclusion of the patients treated with thrombolytic therapy does not alter the results.

Clinical Significance of the magnitude ST segment potential shift

The maximum ST segment potential elevation and the relationship to the clinical course of the patients is shown in table 1. The maximum ST segment potential elevation is related to left ventricular failure. The magnitude of the elevation is not significantly related to ventricular arrhythmias or to the early death rate.

The maximum ST segment depression and the relationship to the clinical data is shown in table 2. The maximum ST segment potential depression was related to the occurrence of left ventricular failure and to ventricular fibrillation.

Clinical significance of peak creatine kinase level

The creatine kinase peak elevation is strongly related to early mortality ($p = 0.016$), left ventricular failure ($p < 0.001$) and ventricular tachycardia ($p = 0.017$).

Clinical significance of the distribution of ST segment potential shift

Figure 1 shows the mean ST segment potential distribution for each of the 6 patterns of ST segment potentials and table 3 shows the characteristics of the group patterns. The distributions are separated into 6 groups by cluster analysis. Two of the groups, 4 and 5, have insufficient patients for meaningful analysis. Groups 1 and 2, the most common patterns, are dominated by anterior ST segment elevation and differ only in the shape of the lower thoracic ST depression distribution. Group 0 is also dominated by anterior ST segment elevation but the ST segment elevation does not extend onto the lower third of the thorax. Group 3 has anterior ST segment elevation but the ST segment elevation extends only to the left mid-axillary line and there is a greater area of ST segment depression recorded on the left and posterior thoracic walls. The maximum ST segment potential elevation of group 3 patients was less than the other groups and, with groups 4 and 5, they had a higher maximum ST segment potential depression than groups 0, 1 and 2. Group 4 is dominated by antero-lateral ST segment potential elevation and is similar to group 1 but the ST segment elevation is shifted to the left side of the anterior thorax. Group 5 is different from the other group patterns with the top half of the thorax covered by the ST segment elevation and the bottom half by ST segment depression. The lowest correlation coefficient between maps in a group is 0.6, and is greater than 0.80 between average map patterns and each group pattern member.

Table 4 presents the clinical characteristics of the 6 groups. There was no difference in the age of patients, time from pain onset to map data collection, or the maximum creatine kinase peak between the groups. The clinical course and complication rates in hospital were the same in each group. Figure 2 presents the early mortality for each ST segment potential distribution group (excluding groups 4

and 5). There is no difference in mortality between groups. Figure 3 shows the late mortality for the ST segment potential groups. With time the group 3 mortality rises compared to the other groups, which are nearly constant, though this does not reach statistical significance. Figure 3 shows survival free of coronary artery by pass grafting between the groups. Group 3 has a significantly higher rate of coronary artery by pass grafting than the other groups (p =0.001) and by 15 months all but 3 patients in group 3 had had surgery or had died.

Thirty-eight patients had gated heart pool scanning. The mean values in the groups 0, 1 and 2 was 38%. No patient in group 3 had a gated heart pool scan. The gated heart pool scan ejection fraction was closely related to the creatine kinase (p=0.022) and the maximum ST segment depression (p=0.041), but not to mortality.

Relationship of ST segment potential distribution to coronary artery anatomy

Patients had coronary arteriography performed only for clinical reasons. In the first half of the study only 15% had coronary angiography, while in the second half 45% of all surviving patients had coronary angiography. The results were similar in both groups and the groups are presented combined. In group 0, 6 of 22 patients had coronary angiography. Four of the six patients had moderate (50-70%) stenosis of the left circumflex artery or the right coronary artery in addition to the infarct related lesions the left anterior descending coronary artery. One patient had diffuse non-critical coronary artery disease, and one patient had triple vessel disease requiring coronary artery by pass grafting. In group 1, 19 of 57 surviving patients had angiography and all had lesions of the left anterior descending artery. One patient had an additional 100% occlusion of non-dominant right coronary artery and another patient had a 70% right coronary artery lesion and was the only patient in the group to require coronary artery bypass grafting. Nineteen of 37 group 2 patients

had coronary angiography. All had left anterior descending artery lesions. Two patients had triple vessel disease and underwent early coronary artery bypass grafting. Three patients with left circumflex artery lesions of greater than 70% stenosis underwent coronary artery by pass grafting. One patient with left anterior descending artery disease had a failed angioplasty and underwent coronary artery by pass grafting due to complete occlusion of the artery. In group 3, 7 patients underwent coronary arteriography. Two had triple vessel disease, and four had left circumflex lesions of 70% plus as well as lesions of the infarct related left anterior descending coronary artery. All had symptoms of ongoing cardiac ischemia requiring coronary artery by pass grafting.

Discussion

This study describes the ST segment potential distribution patterns found in acute anterior wall myocardial infarction. Although the body surface electrocardiographic map has been used to describe some aspects of acute anterior wall myocardial infarction the spatial distribution of the ST segments in a large number of patients has not previously been described. This ability to record body surface electrocardiographic maps in the acutely ill patient is reliant on having a recording system that can record data quickly and with minimal interference to the patient.

Unlike the patients with inferior wall myocardial infarction this group of patients had a relatively high rate of therapy using thrombolytic agents. Analysis of the information with and without the patients treated with thrombolytic therapy made no difference to any result. Thus the treated patients were included.

ST segment potential maximums and early mortality

The maximum value of the ST segment elevation in the body surface map is not related to the prognosis, although other studies of standard electrocardiography suggest that the magnitude of ST segment elevation is related to outcome [Nielson 1973]. Also It may be that the relationship may exists early in the course of myocardial infarction [Klainman 1987] and was not detected due to the wider range of time from the infarction onset to body surface mapping used in this study. Previous studies on factors influencing the early mortality rate have demonstrated that the age of the patient and the size of the infarcted area are the main determinants of outcome in the short term [Pierard 1989]. Our study agreed with this finding and there was a strong correlation between age (data not shown), creatine kinase peak and mortality. The magnitude of the ST segment elevation was related to the peak value of creatine kinase elevation, the QRS score on the standard electrocardiogram, the ejection fraction and the rate of left ventricular failure, all measures of left ventricular damage. Thus although the maximum ST segment elevation related to the measures of left ventricular damage, the major prognostic determinant in anterior wall myocardial infarction, the maximum ST segment elevation on body surface mapping was not related to the mortality. This finding is in agreement with the finding of other groups [Montague 1986] who described the relationship between the ST segment and measures of left ventricular function.

The pattern of ST segment changes in acute anterior wall myocardial infarction did not relate to mortality. This result relates to several factors. Patients with anterior wall myocardial infarction have a high early mortality across the board. Secondly the standard electrocardiogram records information from the anterior thorax where changes due to acute anterior wall myocardial infarction occur. ST segment depression in acute anterior wall myocardial infarction is expected on the

inferior surface of the heart. This finding was demonstrated previously [Montague 1986] using subtraction or difference maps. Inferior wall ST depression is less well detected on the surface of the body due to the distance of the inferior wall from the body surface, and the distance to the recording electrodes placed on the limbs [Rudy 1980]. This can be compared to inferior wall myocardial infarction where the limb leads record the area of ST segment elevation and the changes in the anterior wall of the myocardium are close to the anterior recording electrodes and are thus detected. These changes are well recognized in the standard electrocardiogram [Roubin 1984, Shah 1980] and are of prognostic significance when examined by body surface electrocardiographic mapping [Walker 1987, Bell 1989a, Bell 1989b]. Thirdly inferior wall myocardial infarction relates either to right coronary artery occlusion, to left circumflex artery occlusion or to posterior descending artery occlusion. In contrast anterior wall myocardial infarction occurs from left anterior descending artery occlusion. This leads to consistent electrocardiographic patterns in acute anterior wall myocardial infarction. Certainly the majority of the body surface electrocardiographic maps recorded in this study are similar in the major feature of ST segment elevation, although there is variation in the ST segment depression associated with each pattern and variation in the position of the maximum ST segment elevation.

ST segment potentials and late mortality and morbidity

Factors predicting late mortality and morbidity are different from the factors predictive in the early stages after acute myocardial infarction. These factors include a low creatine kinase MB fraction, age and anterior infarction. The conclusion has been reached that patients with late death have a small or incomplete infarction with ongoing ischemia leading to death at a later time. Our study suggests

that the ST segment distribution appears to indicate the level of residual ischemia in non-infarcted areas of the myocardium. The pattern of ST segment depression appears to divide the patients into those with double or triple vessel disease and those with single vessel disease. In the groups 3 and 0 with large areas of ST segment depression coronary angiography was more likely to reveal 2 or 3 vessel disease than in the other groups. The group 3 patients with large areas of ST segment depression and a greater magnitude of ST segment depression had a significantly higher rate of coronary artery bypass grafting than the other groups. Also the ongoing late mortality (after 1 month) in group 3 is higher than in the other groups though not reaching statistical significance. This suggests that the group 3 patients had ischemia distal to the infarction area. This ischemia is indicated by the pattern of the body surface map with the area of ST segment depression representing the area of myocardial ischemia. This compares to previous studies which have related the presence of inferior ST segment depression on the standard electrocardiogram to the prognosis in acute anterior wall myocardial infarction, and to the occurrence of left ventricular failure, and the size of the infarcted area [Haraphongse 1984].

Creatine kinase peak, mortality and morbidity

In this study the peak values of creatine kinase were the best measure of assessing outcome and complications in the short term after acute anterior wall myocardial infarction. The creatine kinase did not predict long term mortality or morbidity, while the ST segment pattern of the body surface map, while not predicting early mortality did predict morbidity in the long term.

Conclusion

This is the first study using spatial analysis of body surface maps of large

numbers of patients in acute anterior wall myocardial infarction. Previous studies have used small numbers of patients and/or have mapped the patients days after the myocardial infarction [Montague 1986, Montague 1987, Mirvis 1980]. We conclude that the initial ST segment pattern associated with a smaller area of ST segment elevation and a greater area of ST segment depression is a predictor of a poor long term outcome after acute anterior wall myocardial infarction. This feature could well be used to identify patients who would benefit from post infarction angiography and possible coronary artery surgery.

To test this conclusion requires a prospective angiogram controlled study where the body surface map pattern can be compared to areas of infarction and ischaemia.

Table 1: Clinical significance of maximum ST segment elevation

	Maximum ST segment elevation (mV)				
	[0.074,0.252)	[0.252,0.371)	[0.371,0.712)	>0.712	p value*
patients	40	41	41	40	
early death	3	6	8	9	0.18
late death	2	1	4	0	0.23
VT	7	12	7	10	0.52
VF	2	4	4	4	0.41
LVF	8	10	15	17	0.01
CABG	7	4	3	2	0.078

Table 2 : Clinical significance of maximum ST segment depression

	Maximum ST segment depression (mV)				
	< 0.052	[0.052,0.080)	[0.080,0.136)	>0.136	p value*
patients	40	41	41	40	
early death	5	9	6	6	0.76
late death	0	2	2	3	0.33
VT	12	6	6	12	0.67
VF	0	3	3	8	0.002
LVF	6	14	14	16	0.03
CABG	2	3	10	1	0.21

Note: [x,y) means the range of values between x and y, including x but not including y, as per standard mathematical notation
early death indicates death in the first month following infarction
late death indicates death after 1 month but within 24 months mean follow up period
VT= ventricular tachycardia, VF= ventricular fibrillation, LVF= left ventricular failure, CABG = coronary artery bypass grafting
* p value by Mann-Whitney U test for increasing values of maximum ST segment elevation

Table 3 : Map characteristics of different ST segment distribution groups

	ST segment distribution group					
	group 0	group 1	group 2	group 3	group 4	group 5
number	24	73	41	14	5	5
correlation coefficient	0.90 ±0.01	0.90 ±0.06	0.87 ±0.08	0.85 ±0.16	0.90 ±0.05	0.81 ±0.11
Max ST elevation (microVolts)	367 ±197	592 ±356	484 ±323	246* ±105	696 ±612	394 ±282
Max ST depression (microVolts)	104 ±55	97 ±63	86 ±85	129# ±69	130# ±50	199# ±135

correlation coefficient is the mean correlation coefficient for all maps with the mean map pattern for the group

Max ST elevation is the mean maximum ST segment potential value for each group

Max ST depression is the mean maximum ST segment potential depression for each group

* less than other groups by one way analysis of variance and students t test

the three groups 3, 4, 5 are greater than the other groups

Table 4 : Clinical significance of ST segment distribution groups

	ST segment distribution group					
	group 0	group 1	group 2	group 3	group 4	group 5
number	24	73	41	14	5	5
age (years)	60±11	61±11	59±11	60±11	65±7	64±8
time to map (h)	8±8	10±9	9±8	14±9	4±2	9±8
CKmax	2391 ±1406	2509 ±1658	2041 ±1566	1953 ±1947	2900 ±2084	2178 ±839
early death (%)	2 (8)	16 (22)	4 (10)	2 (14)	1 (20)	1 (20)
VT (%)	4 (17)	13 (18)	12 (29)	3 (21)	1 (20)	3 (60)
VF (%)	0 (0)	8 (11)	3 (7)	2 (14)	1 (20)	0 (0)
LVF (%)	6 (25)	24 (33)	11 (27)	3 (21)	3 (60)	3 (60)

Time to map is the time in hours from the onset of symptoms to the recording of the map

Early death indicates death from heart failure in the first month following infarction

VT= ventricular tachycardia, VF= ventricular fibrillation, LVF= left ventricular failure

Figure 1: Average integral body surface maps for patients with acute anterior wall myocardial infarction

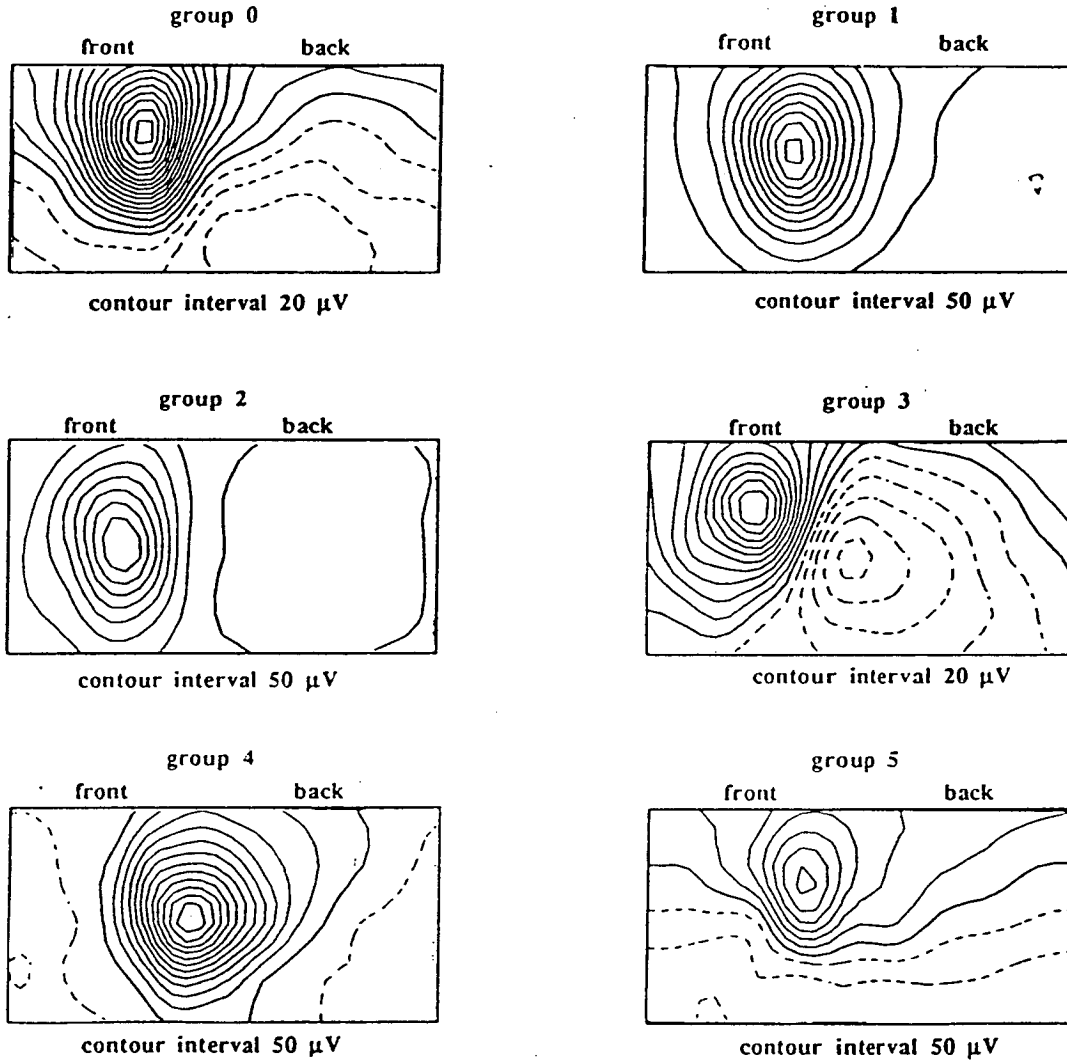

The maps are displayed in the standard format. The map onset is 120 milliseconds after the QRS onset. The integral is taken over the next 20 milliseconds. The contour interval is between contour lines in microvolts.

Figure 2: Survival curves for the ST segment map groups after acute anterior wall myocardial infarction

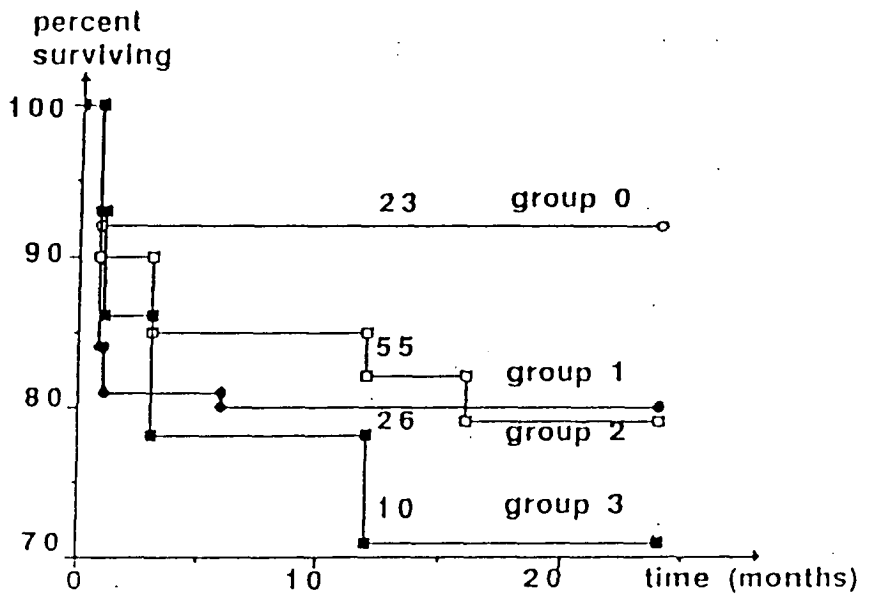

The numbers on the survival curve lines represent the number of surviving patients at 15 months following the index acute myocardial infarction. There is no difference between groups. $p > 0.05$.

Figure 3: Survival free from coronary artery surgery curves for the ST segment map groups in anterior wall myocardial infarction

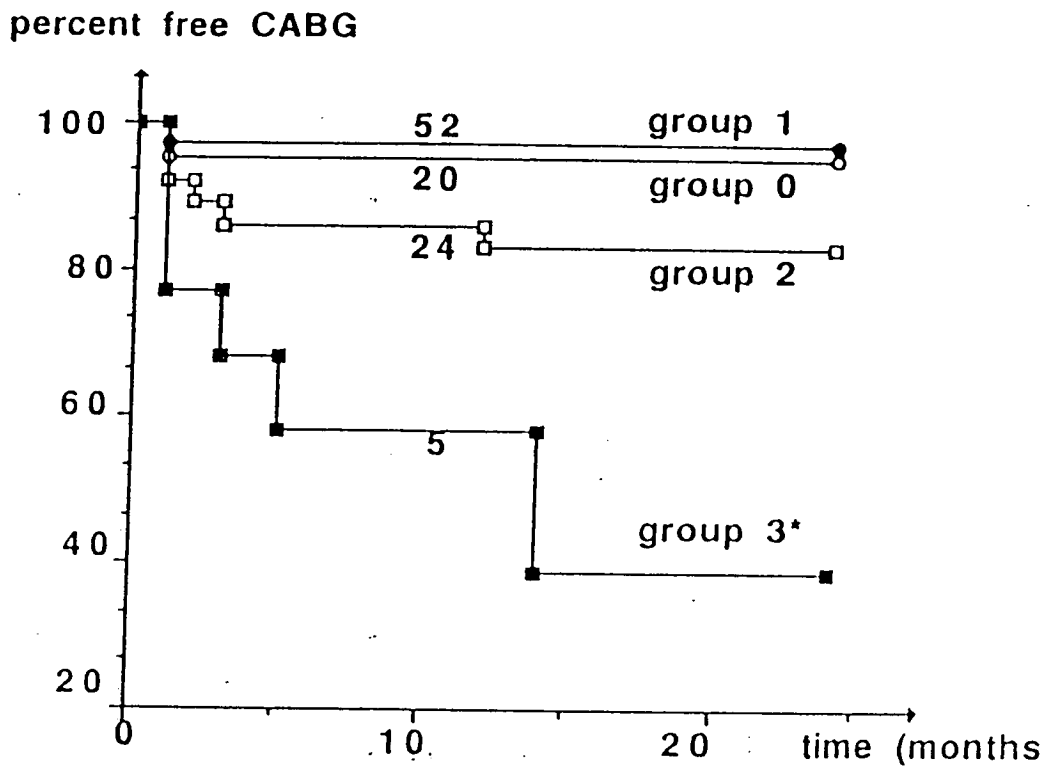

* p < 0.003

The numbers on the survival curve lines represent the number of surviving patients free from coronary artery surgery at 15 months following the index acute myocardial infarction. Group 3 has a lower rate of survival free from coronary artery by-pass grafting than the other groups combined, $p < 0.003$.

Chapter 10

The relationship of ST segment elevation to eventual QRS loss in acute anterior wall myocardial infarction

Introduction

To use the electrocardiogram to assess the effects of thrombolytic therapy, the spatial relationship between the initial ST segment elevation and eventual loss of QRS potentials is required. The eventual outcome assessed electrocardiographically could then be compared to the outcome predicted from the initial ST segment elevation.

There is a characteristic electrocardiographic pattern associated with the development of a Q wave myocardial infarction. The initial feature is ST segment elevation followed by the development of pathological Q waves in leads overlying the area of myocardial necrosis. The relationship between ST segment elevation and eventual Q wave or QRS loss has been studied in acute anterior wall myocardial infarction [Selwyn 1978, Henning 1978, Essen 1980, Zmyslinski 1979] with precordial mapping. These studies used precordial mapping and summation of the ST segment elevation compared with the sum of Q wave formation. The studies did not attempt to quantify the area of ST segment elevation compared to the area of Q wave formation. Studies of the standard electrocardiogram indicate there is inadequate quantification, and inadequate spatial features in the potential distributions, to quantify the spatial relationship of ST segment changes to area of Q wave formation [Horan 1980]. With the 12 lead electrocardiogram there is a poor correlation between initial ST segment elevation and subsequent Q wave formation in 30% of patients [Boden 1989]. Thus it is necessary to use body surface potential mapping in which a reasonable relationship between ST elevation and QRS change has been established [Selwyn 1978, Henning 1978, Essen 1980, Zmyslinski 1979, Kilpatrick 1989].

To analyze the natural history of the electrocardiogram in acute anterior wall myocardial infarction we have studied those patients with first anterior wall

myocardial infarction who might accurately represent the natural history of electrocardiographic change and analyzed the initial ST elevation in relation to the eventual early QRS loss and total QRS loss in these patients.

Methods

Study Population

The study population is 163 patients admitted to the coronary care unit with a clinical diagnosis of acute anterior or antero-lateral wall myocardial infarction. Patients were included only if they were mapped within 16 hours of symptom onset. Patients with a history of previous myocardial infarction or a QRS duration of greater than 0.11 seconds on the initial 12 lead electrocardiogram were excluded.

All patients gave informed consent and mapping did not interfere with clinical management of the patients. No patient was excluded because of age, shock, left ventricular failure or arrhythmia. Clinical management and investigations were the responsibility of the patient's attending physician. All patients who met the selection criteria for this study were included. From this group all patients who had received thrombolytic therapy were excluded. For the long term follow up study all patients who had coronary artery bypass grafting or coronary angioplasty or subsequent myocardial infarction before follow up body surface mapping were excluded.

Patients with initial body surface maps within the first 24 hours of symptom onset and second body surface maps approximately 24 hours after the initial body surface map were classed as group A. Patients with a second body surface map approximately 48 hours after the initial map were classed as group B, and if a further body surface map was recorded more than 6 months after the initial body surface map the patients were classed as group C.

Body surface mapping

The system for acquisition, display and recording of the body surface electrocardiographic data used the usual method. We constructed integral body surface maps by integrating potentials over the following time intervals in the QRS complex: QRS onset to 30 milliseconds (QRS_{0-30}), QRS onset to 40 milliseconds (QRS_{0-40}), 30 to 80 milliseconds (QRS_{30-80}), QRS onset to 80 milliseconds (QRS_{0-80}) and the 130 to 150 milliseconds (ST integral map).

Statistical Processing

We used the correlation coefficient to compare the maps.

To study the relationship between the spatial distribution of ST segment elevation and the later spatial distribution of QRS loss we correlated the initial integral ST body surface map with the integral QRS segment maps. The comparison was made several ways.

1. using the raw map data
2. with the data corrected for the normal ST segment pattern
3. with the data corrected for the normal QRS complex
4. with the data corrected for both the ST segment and QRS complex normal voltages. Correction was performed by using subtraction maps created by subtracting from the appropriate integral body surface map in the patients with myocardial infarction, the corresponding average normal body surface map constructed from data kindly loaned to us by Dr Green et al. [Green 1985] based on 208 normal men and 173 normal women and 80 patients of our own who had both normal electrocardiograms and normal coronary angiogram.

Results are displayed as density function graphs where the density function is the estimated probability density, also known as the theoretical relative frequency distribution [Snedecor 1980, Wegman 1972]. The method was discussed in chapter 4. To demonstrate the difficulty in selecting the appropriate comparison of ST segment to later QRS complex (that is the integral maps $QRS_{0\text{-}30}$, $QRS_{0\text{-}40}$, $QRS_{30\text{-}80}$ or $QRS_{0\text{-}80}$) figure 1 displays for comparison the mean map of 163 patients diagnosed as having anterior wall myocardial infarction who had a total of 552 body surface maps recorded during the 72 hours following infarction and had not receive thrombolytic therapy before the time of mapping. All maps of the 163 patients were used. The mean anterior wall myocardial infarction QRS pattern differed from the normal pattern in each 10 millisecond integral maps from 0-80 milliseconds through the QRS complex. The mean normal and anterior infarction body surface maps are displayed with corresponding normal QRS integral maps minus the myocardial infarction integral maps over the same time intervals. The subtraction maps show the variation between normal and infarction patterns was present in all the time intervals examined.

Results

Relationship of ST to QRS in normals

In 461 normal people the body surface map showed excellent correlation between the ST segment integral map and the $QRS_{0\text{-}30}$ integral, the $QRS_{0\text{-}40}$ integral, the $QRS_{0\text{-}80}$ integral and the the $QRS_{30\text{-}80}$ integral maps in figure 2. Virtually all normals have a high positive correlation between the area of ST segment elevation and the positive QRS deflection in time integral maps.

Relationship of ST to QRS in group A

Group A consisted of 70 patients with 51 male and 19 female. Their mean age was 61 ± 11 years and the mean peak creatine kinase was 2306 ± 1532 units (normal < 200 units for males and < 170 units for females). The initial maps were recorded 10 ± 6 hours after the onset of symptoms. The second maps were recorded 31 ± 9 hours after the onset of symptoms, a mean of 22 ± 8 hours after the initial map. Figure 3A-D displays the probability density function of the correlation coefficients of the different QRS segment isointegral maps and normal map corrections. The integral QRS_{0-40} map has the best negative correlation with the ST segment map and the negative correlation is not improved by correction by the normal ST segment, QRS complex or both. The integral QRS_{0-80} map also has a good negative correlation and the negative correlation is not improved by correction for the normal ST or QRS distribution. The integral QRS_{0-30} maps correlate negatively less well and the integral QRS_{30-80} maps showed no relationship to the ST segment integral maps. The patients with correlation coefficients greater than -0.30 in the integral QRS_{0-40} map were examined in detail. Four patients with poor negative correlations had the four lowest peak creatine kinase values, one patient had the highest creatine kinase value and developed a partial right bundle branch block pattern with QRS duration < 0.11 second. A further patient developed a partial right bundle branch block pattern. Review of one patient's standard electrocardiogram suggested he had previously had a silent inferior wall myocardial infarction. In two other patients no reason for the poor relationship was found. The remaining patients did not have any suggestion of previous infarction or partial bundle branch block

patterns.

Relationship of ST to QRS in group B

Group B consisted of 35 patients, 34 of whom were also in group A. The patients had initial body surface maps at 9 ± 5 hours after the onset of symptoms and a second map 57 ± 11 hours after the onset of symptoms. The mean age was 60 ± 11 years, with 28 males. Figure 4A-D displays the density function of the correlation coefficients of the different QRS segment isointegral maps. The integral QRS_{0-30} maps and the integral QRS_{0-40} maps have good negative correlations with the ST segment area of the initial body surface map and in both cases the negative correlation was slightly improved by correction with the normal integral QRS_{0-30} or QRS_{0-40} integral map as appropriate. The integral QRS_{0-80} maps and integral QRS_{30-80} maps showed no correlation to the ST segment map. Of the three patients in the integral QRS_{0-40} map with correlation coefficients greater than -0.30 one had a low creatine kinase value, one a partial right bundle branch block pattern and the last had no obvious reason for the poor correlation.

Relationship of ST to QRS in group C

Group C consisted of 37 patients (27 male) who had initial body surface maps 9 ± 5 hours after the onset of symptoms and repeat body surface maps 34 ± 17 months after the index myocardial infarction. Figure 5A-D displays the probability density function of the correlation coefficients of the different QRS segment isointegral maps. None of the integral maps shows a consistent correlation with the index infarction ST segment integral map.

Figure 6 shows the patients common to groups A and B and displays the increasing negative correlation of the ST segment and the QRS_{0-40} maps over time consistent with the original hypothesis. The initial body surface map is correlated with the initial QRS integral as well as subsequent body surface maps. The results (figure 6) shows that the major change takes place in the first 24 hours post acute myocardial infarction though not the whole change.

Discussion

These results show that in many patients the region of ST elevation during an acute anterior wall myocardial infarction correlates well with the regions of QRS loss resulting from the myocardial infarction provided the early phase of the QRS complex is used. Subjectively this had been suspected, and several studies have shown some relationship of QRS changes to ST segment elevation [Selwyn 1978, Henning 1978, Essen 1980]. No previous study has performed detailed analysis in a large group of patients.

The various QRS segments used in the study reflect the problem of assigning the electrical loss in acute myocardial infarction to any particular segment of the QRS complex. The QRS complex electrical loss, the integral QRS_{0-80} maps, can be justified by the demonstration of the alteration of the QRS complex in all integral segments after acute anterior wall myocardial infarction (figure 1) as previously suggested in body surface map studies [Kilpatrick 1989]. The classical electrocardiogram change in acute myocardial infarction is the development of the pathological Q wave. In this study we have taken the first 30 and the first 40 milliseconds of the QRS complex as representing the classical electrocardiographic Q wave. The integral QRS_{30-80} maps are inserted for completeness in attempting

to understand the relationship between the area of ST segment elevation and the loss of QRS complex electrical activity in acute anterior wall myocardial infarction. It is interesting that the best correlation occurs in the QRS_{0-30} and the QRS_{0-40}. This best correlation in the early QRS complex matches the standard electrocardiogram. The reason for this is not clear but may relate to the increasing complexity of electrical conduction due to conduction delays, inexcitability of cells and specialized conducting system damage [Mirvis 1988b].

This study includes only patients not given thrombolytic therapy. The reasons for not prescribing streptokinase were related to the time of presentation after the myocardial infarction, or the presence of recent surgery or gastrointestinal haemorrhage. Our routine practice during the time of the study was to prescribe streptokinase only to highly suitable patients. This may have caused a bias towards patients with later presentations although the time from the onset of symptoms to initial body surface map is short. The policy may also have selected against patients with higher ST segment elevation and excluded patients with a better chance of a good negative correlation.

The conclusion that can be drawn from this study is that the region of ST elevation in anterior infarction predicts the QRS loss using the integral QRS_{0-40} map and the QRS_{0-30}. This is clearly demonstrated by considering the correlation between the normal QRS complex and the normal area of ST segment elevation (figure 2) as opposed to the correlation patterns after infarction (figures 3,4,5). Any change from the consistent relationship shown in figure 2 thus may represent acute myocardial damage and thus the comparison method may allow easier diagnosis of myocardial damage. The relationship between the area of threatened damage (ST segment elevation) and the area of "fixed damage" (QRS complex voltage loss) is of

significance as a tool for measuring the effectiveness of measures to reduce myocardial infarction size. Although over time the correlation diminishes the correlation remains significantly different from normal and thus represent a diagnostic tool.

Several factors may lead to a less than perfect negative correlation between the QRS loss and ST segment elevation. Firstly there may not be a correlation between the ST segment area of elevation and the eventual QRS complex electrical loss. This seems unlikely as a relationship has previously been demonstrated by both 12 lead electrocardiography and body surface mapping [Selwyn 1978, Henning 1978, Essen 1980, Zmyslinski 1979, Kilpatrick 1989]. Alternatively some patients with a poor negative correlations had low peak creatine kinase levels. Patients with smaller areas of myocardial infarction may have less electrical activity loss and such electrical loss may be difficult to detect and to localize. There is a possibility that some patients had spontaneous reperfusion and recovery of QRS potentials thus accounting for the low creatine kinase and the poor ST segment QRS complex negative correlation. Also patients who developed partial right bundle branch block conduction defects had poor negative correlation between the ST segment elevation and the QRS complex integral maps. Thus the development of intraventricular conduction defects may lead to a poor negative correlation. The decreased correlation of the ST segment to the QRS complex over time may relate to development of ventricular distortion either physically or electrically by fibrosis and scar tissue formation with time.

Patients showed a change from the short-term follow up to the later maps. Several patients who showed initial high correlations were seen to have a lower correlation on the late follow up map. Montague et al. [Montague 1984, Montague 1986] demonstrated changes occurring between a mean of 79 hours and a mean of 8

months; these changes were mainly in a reduction of the infarction pattern voltages, which is similar to the one seen in this series. No common factor, separating these patients who showed QRS recovery from those who did not, could be isolated. The change may relate to healing or recovery of the electrical activity of the heart or due to further damage and loss of R wave.

That a correlation exists and is very different from the normal patients correlation indicated that the tool remains useful for diagnostic purposes, even if not sufficiently accurate to allow assessment of interventions to prevent myocardial damage.

Figure 1: Comparison of the patients with a normal body surface map and patients with an acute anterior wall myocardial infarction map over the QRS complex

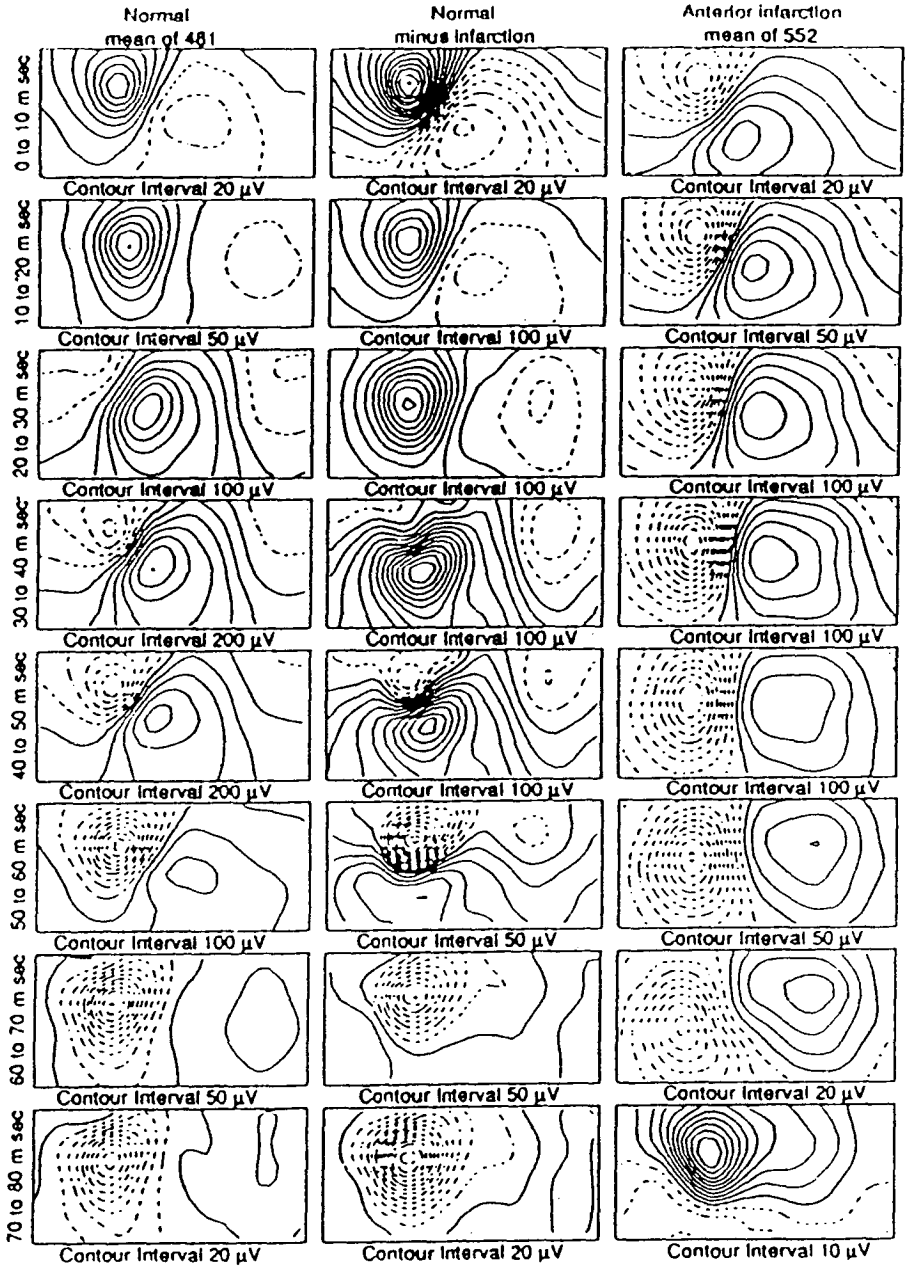

A series of maps illustrating the difference between normal (LHS) and anterior infarction (RHS) at time intervals throughout the QRS. Each map is integrated over 10 milliseconds. The difference maps are in the centre. Dashed lines represent negative contours, heavy continuous lines the zero contour, and thin continuous lines the positive contours.

Figure 2: Comparison of normal QRS integral maps with corresponding ST segment maps

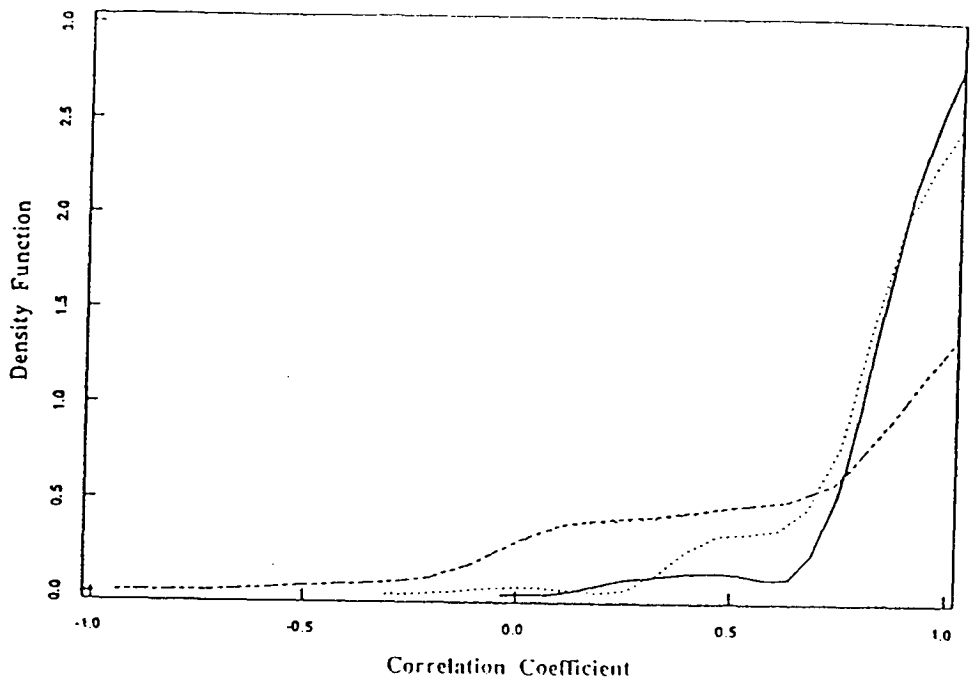

The correlation coefficient is plotted against the density function for integral ST segment maps against the maps QRS 0-30, QRS 0-40, QRS 30-80 or QRS 0-80.
The QRS 0-30 integral map density function is represented by the solid dark line.
The QRS 0-40 integral map density function is represented by the closely dotted line.
The QRS 0-80 integral map density function is represented by the dashed line.
The QRS 30-80 integral map density function is represented by the dotted line which is indistinguishable from the dashed line.

Figure 3: The QRS complex map versus corresponding ST segment map correlation coefficient plotted against the density function for group A patients.

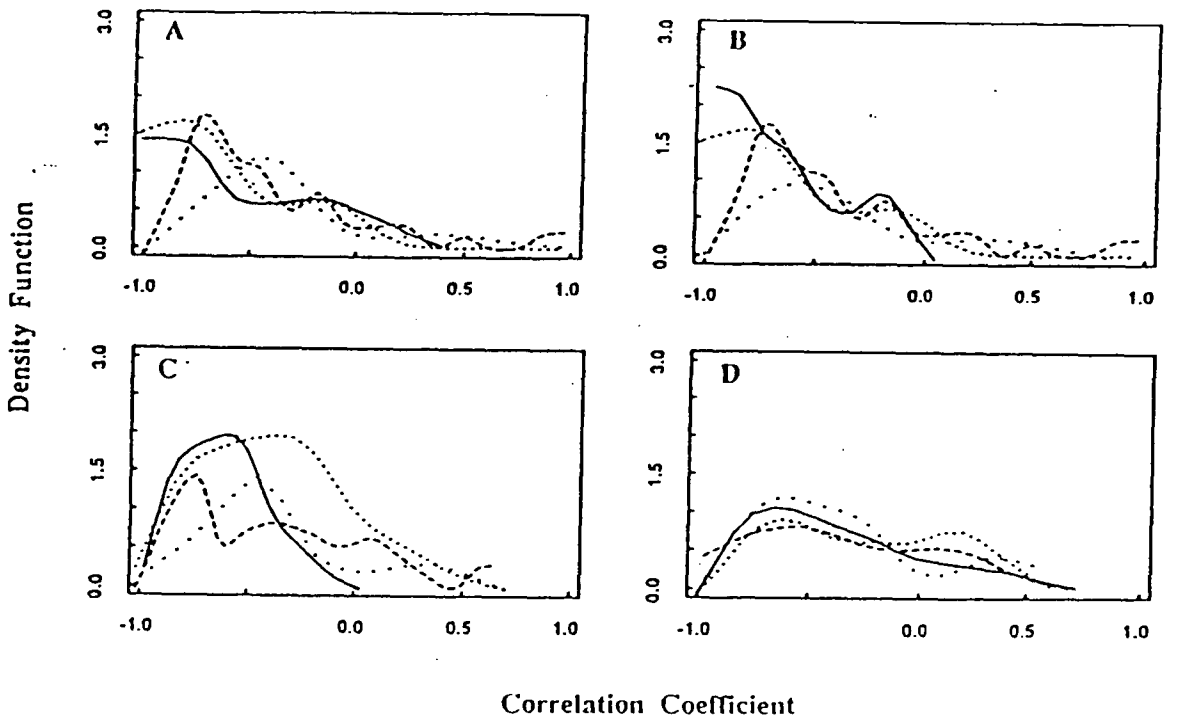

The correlation coefficient is plotted against the density function for group A patients.
Figure 3A displays the density function for QRS 0-30 integral maps.
Figure 3B displays the density function for QRS 0-40 integral maps.
Figure 3C displays the density function for QRS 0-80 integral maps.
Figure 3D displays the density function for QRS 30-80 integral maps.
In all figures A-D the solid line represents the raw data density function, the close dotted line represents the QRS complex corrected data, the dashed line represents the ST segment corrected data, and the widely dotted line represents the QRS complex and ST segment corrected data.

Figure 4: The QRS complex map versus corresponding ST segment map correlation coefficient plotted against the density function for group B patients.

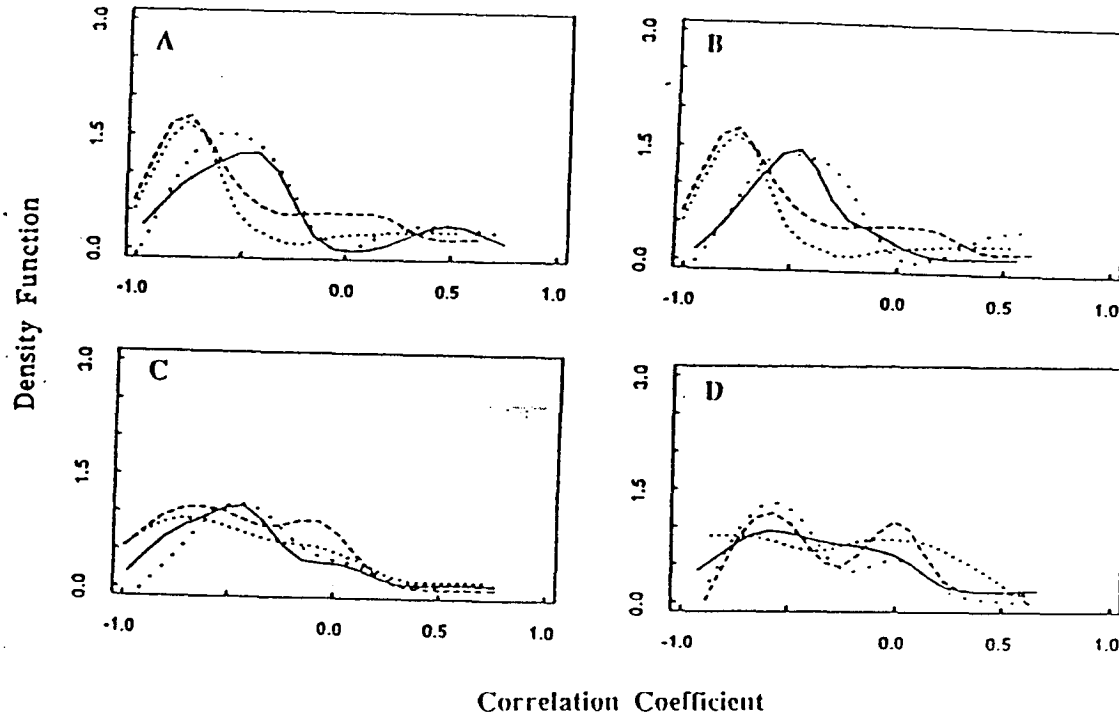

The correlation coefficient is plotted against the density function for group B patients.
Figure 4A displays the density function for QRS 0-30 integral maps.
Figure 4B displays the density function for QRS 0-40 integral maps.
Figure 4C displays the density function for QRS 0-80 integral maps.
Figure D displays the density function for QRS 30-80 integral maps.
In all figures A-D the solid line represents the raw data density function, the close dotted line represents the QRS complex corrected data, the dashed line represents the ST segment corrected data, and the widely dotted line represents the QRS complex and ST segment corrected data.

Figure 5: The QRS complex map versus corresponding ST segment map correlation coefficient plotted against the density function for group C patients.

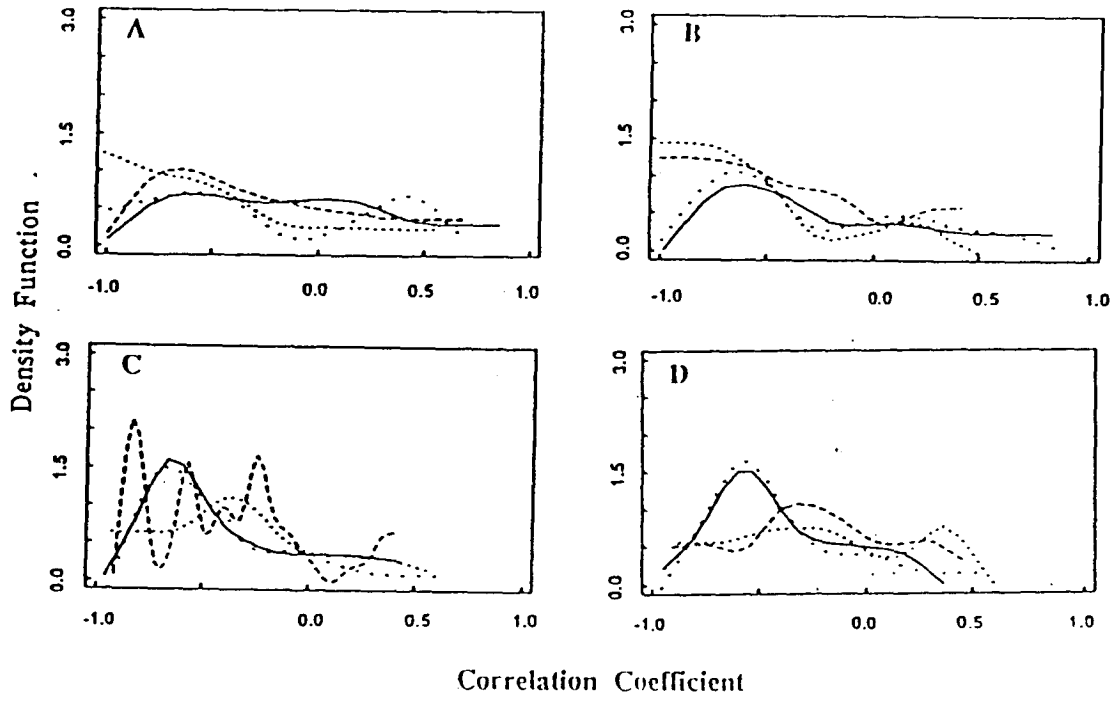

The correlation coefficient is plotted against the density function for group C patients.
Figure 5A displays the density function for QRS 0-30 integral maps.
Figure 5B displays the density function for QRS 0-40 integral maps.
Figure 5C displays the density function for QRS 0-80 integral maps.
Figure 5D displays the density function for QRS 30-80 integral maps.
In all figures A-D the solid line represents the raw data density function, the close dotted line represents the QRS complex corrected data, the dashed line represents the ST segment corrected data, and the widely dotted line represents the QRS complex and ST segment corrected data.

Figure 6: The plot of the correlation coefficient between the QRS complex maps and the corresponding ST segment maps of individual patients over time

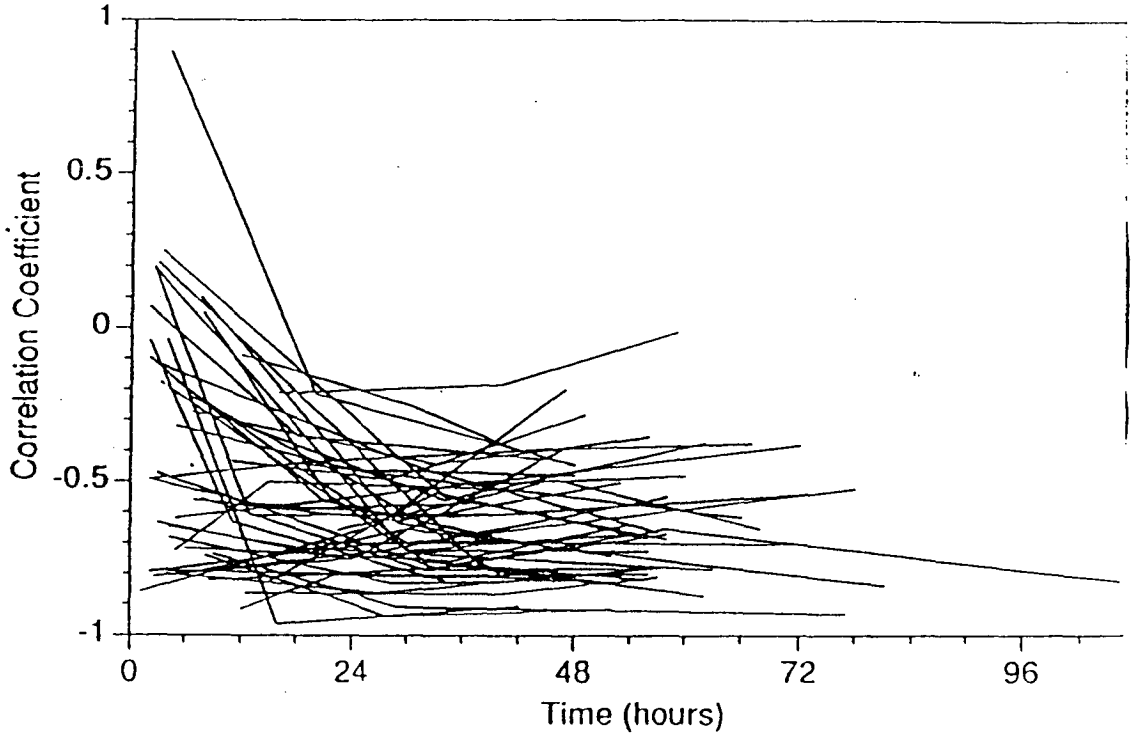

The plot of the correlation coefficient of individual patients over time. Each line represents an individual patient. The correlation is between ST segment map and the QRS 0-40 integral maps.

Chapter 11

Detection of coronary artery disease by statistical analysis of body surface maps

Introduction

In 1987 Green et al. published a paper which detailed a technique that separated patients with coronary artery disease from normals on the basis of electrocardiographic measurements from a resting body surface map [Green 1987] even if the standard electrocardiogram was normal. In the original studies resting body surface maps were recorded in a group of 41 patients having coronary arteriography and 644 presumed normal patients. An Eigenvector technique was used to reduce the body surface map data to 216 coefficients [Evans 1981, Lux 1981]. The researchers then established which of these coefficients of the Eigenvectors were the most different in the two groups of patients. Using these most significant coefficients they were able to separate the patients in the coronary artery disease group from the normal group. They also suggested that it might be possible to detect different degrees of severity and to differentiate right coronary artery disease from left coronary artery disease from the body surface distributions. We have studied a group of over 500 patients having coronary arteriography and have performed extensive analysis on this group of patients to provide independent validation of this important non-invasive technique.

Methods

Patient selection

All patients having cardiac catheterisation between May 1989 and April 1992 who had a normal or near normal 12 lead electrocardiogram were considered for this study. The patients were divided into a learning set of patient, and a test set of patients. The learning set of patients were the first half of the total number of patients admitted to the study and the test set the second half of the patients admitted to the study.

Exclusions

Patients were excluded if the coronary angiography was performed for heart disease unrelated to ischemic heart disease or if the patient had a past history of myocardial infarction. Patients with abnormal 12 lead electrocardiograms were excluded.

Definition of a normal electrocardiogram

Because this is a critical factor in this study all 12 lead electrocardiograms of the selected population were analysed independently by two experienced cardiologists who were unaware of the patient's identity. If both cardiologists thought the electrocardiograms were completely normal then the patient was allocated to group 1. If one or both readers identified non-specific abnormalities, such as minor T wave flattening, then the patient was allocated to group 2. If one or more of the readers thought the electrocardiogram showed changes which indicated ischemic heart disease the patient was excluded from further analysis.

Data collection

The system for acquisition, display and recording of the body surface electrocardiographic data has been described in chapter 3 [Walker 1983, Walker 1987].

Coronary angiography was performed on all patients using a "Siemens Bicor" laboratory system. The coronary arteriograms were reviewed by the cardiologist performing the study and the degree of stenosis taken from the reading of the cardiologist. Most studies were performed using the "Judkins" technique, although a few "Sones" studies from brachial arteriotomies were included. All studies produced

satisfactory data. Coronary arteriograms were classified on the basis of the degree of stenosis in each region and further sub-classifications performed using the criteria of Brandt and others [Brandt 1977].

Statistical analysis

The QRS onset was used as the time reference point. The body surface maps were analysed over the following integrals, all referred to the QRS onset as zero time point: 0-20 milliseconds, 20-40 milliseconds, 40-60 milliseconds, 60-80 milliseconds, 130-150 milliseconds, (ST segment map) and 190-380 milliseconds, (T wave map).

Direct visual analysis of the integral maps was used. The integral maps were also compared by correlation coefficients. Hierarchical clustering techniques with agglomerative methods (single link method and the complete linkage method) were used to fuse body surface maps into groups of similar maps [Everitt 1974].

Departure maps were constructed by calculating the difference between an individual map and an average map of a control group [Flowers 1976a, Flowers 1976b, Mirvis 1981]. The normal standard electrocardiogram with normal coronary arteries group were used for the normal control maps. For the departure maps the normal range was considered to be plus or minus 2 standard deviations. The departure maps were compared by visual inspection and correlation coefficients.

Data were reduced using an Eigenvector technique. Twelve spatial and 6 temporal Eigenvectors were derived from a set of 1352 patients including normals and patients with most electrocardiographic abnormalities. The Eigenvectors allowed a reduction of the data to 72 coefficients with a percent tract of covariance of 97.3. The 72 coefficients were derived for each patient in this study.

Multivariate discriminant function analysis using the 72 independent coefficients

derived from Eigenvector analysis was performed on a learning set to calculate the linear discriminant function. The derived linear discriminant function was applied to an independent test set to determine the general applicability of the discriminant function.

Multivariate analysis was applied to the differentiating subgroup of Eigenvector coefficients, as described in the original paper [Green 1987].

Results

Patient Groups

Three hundred and sixty four patients met the clinical criteria for the study. Patients were categorised by standard electrocardiographic findings and by angiographic findings. Group A consisted of 164 patients with normal 12 lead electrocardiograms. Group B consisted of 364 patients with normal electrocardiograms or with minor 12 lead electrocardiographic changes. Group C consisted of 256 patients of whom 164 had normal coronary arteries, 61 had proximal left anterior descending artery disease and 31 had proximal right coronary artery disease. In each group the number of patients was randomly divided into learning set and a test set of patients.

Patient data are given in table 1, and the grouping of patients for the learning and tests sets is given in table 2.

Group A

Figure 1 shows the average body surface map for the patients with coronary artery disease and without coronary artery disease and the map to map correlation coefficient. Table 3 shows the mean map maximum positive and maximum negative

potentials between corresponding integral maps. There is no significant voltage difference between any two corresponding maps. Figure 2 shows a histogram display of the correlation coefficient between the corresponding integral maps of the patients with coronary artery disease and the mean normal maps. Figure 3 shows the mean departure maps for the group of patients with coronary artery disease compared to the mean normal coronary artery, normal standard electrocardiogram group. The departure maps are less than two standard deviations different from the normal group in all sites of all the map series. There was no difference between the groups on the basis of visual inspection and correlation coefficients, with cluster analysis or with visual inspection of departure maps. The learning set of patients was separated easily by discriminant function analysis (figure 4a). The test set of patients was not separated using the developed discriminant function (figure 4b). Applying the same analysis but using only coefficients of Eigenvectors shown to be different between the two groups, again separated the patients in the learning set but did not separate the patients in the test group.

Group B

There was no difference between the groups on the basis of visual inspection, grouping by correlation coefficients with cluster analysis and visual inspection with departure maps. Discriminant function analysis separated the learning set of patients into those patients with coronary artery disease and those without coronary artery disease (figure 5a). When the discriminant equation was applied to the test sets of patients there was no separation of the groups (figure 5b). Applying the multivariate analysis using only correlation coefficients shown to be different between the two groups separated the patients in the learning set but did not separate the patients in the test group.

Group C

Using the patients with single arterial disease of a stenosis greater than 70% involving either the left anterior descending artery, the right coronary artery or having normal coronary arteries discriminant function analysis separated the learning group (figure 6a). The test set was not separated by the generated linear discriminant equation (figure 6b).

All groups

The results were not changed by using the test sets as learning sets, by different numbers of patients in the test and learning sets and by using different definitions of significant arterial disease varying from 50% narrowing to 90% narrowing. Even taking a comparison between patients with no coronary artery disease and over 90% arterial narrowing there was no detectable difference.

Discussion

This study is an appropriate test of the body surface electrocardiographic map data and analysis methods to detect occult coronary artery disease [Green 1987]. In that study the patients with coronary artery disease were compared to a normal population. In this study patients with chest pain thought to be due to coronary artery disease were classified on the basis of the "gold standard" for the detection of coronary artery disease, coronary angiography. This study tested the hypothesis that in the group of patients with chest pain who have coronary angiography resting electrocardiographic data can separate those with coronary artery disease.

A non-invasive test accurate and specific for the detection of occult but significant coronary artery disease is an aspiration of cardiologists. The recent

demonstration of detection of coronary artery disease non-invasively by body surface mapping would thus have considerable clinical application if confirmed [Green 1987]. We have taken the typical group of patients being investigated for symptoms possible related to coronary artery disease in which a coronary angiogram was performed to confirm or deny the presence of coronary artery disease. Detailed examination of the body surface maps by visual inspection, departure mapping, cluster analysis, eigenvector analysis and discriminant function analysis failed to show any difference between patients with and without coronary artery disease. This finding applied to patients with normal standard electrocardiograms and patients with minor electrocardiographic changes. Thus we believe that detailed analysis of the electrocardiographic information does not detect coronary artery disease in the absence of myocardial damage.

The statistical analysis of the information gives a clue to why previous studies showed a positive result. In these studies the initial learning set of patients could be separated by the discriminant function analysis with a high degree of certainty. When the separating equation was applied to a test set there was no separation of the diseases from non diseased groups. Thus although there are differences in the groups, the differences are not consistent and are thus of no clinical benefit. This demonstrates that statistical result derived from a set of patients should be tested in a test set of patients independent from the initial learning set.

Table 1: Patient characteristics

	number	percentage
total patients screened	505	
total patients included in study	364	
age (years)	55 ± 8	
sex (m:f)	440:65	
family history of angina	308	61
symptoms		
typical anginal pain	416	82
exertional angina	448	89
rest angina	66	33
unstable angina	86	17
history hypertension	181	36
signs		
blood pressure (mmHg)	138±21/80±11	
pulse rate	71±10	
jugular venous pressure normal	468	93
normal cardiac examination	434	86
investigations		
chest x-ray normal	446	88
positive exercise test (+ve/no.)	323/386	
medications		
beta blocker	318	63
calcium channel blocker	247	49
nitrate	182	36
digoxin	10	2

Table 2: Patient numbers for the test and learning sets

	learning set	test set
total patients screened	505	
patients with abnormal arteries	208	
patients with normal arteries	156	
group A (normal standard electrocardiography)		
normal arteries	40	47
abnormal arteries	40	37
group B (normal or non-specific standard electrocardiography)		
normal arteries	100	56
abnormal arteries	100	108
group C (normal or non-specific standard electrocardiography with specific coronary disease)		
normal arteries	100	56
left anterior descending disease	39	22
right anterior descending disease	20	11

Table 3 :Body surface map voltage measurement data

	normals coronary artery patients maps	diseased coronary artery patients maps	p value
number of maps	87	77	
QRS 0-20 integral maps			
maximum positive voltage (μV)	405 ± 274	488 ± 352	NS
maximum negative voltage (μV)	140 ± 151	136 ± 99	NS
QRS 20-40 integral maps			
maximum positive voltage (μV)	1152 ± 457	1331 ± 461	NS
maximum negative voltage (μV)	770 ± 459	690 ± 441	NS
QRS 40-60 integral maps			
maximum positive voltage (μV)	583 ± 715	590 ± 441	NS
maximum negative voltage (μV)	973 ± 994	1033 ± 407	NS
QRS 60-80 integral maps			
maximum positive voltage (μV)	133 ± 84	139 ± 104	NS
maximum negative voltage (μV)	302 ± 315	343 ± 319	NS
ST integral maps			
maximum positive voltage (μV)	154 ± 127	162 ± 99	NS
maximum negative voltage (μV)	79 ± 77	86 ± 83	NS
T wave integral maps			
maximum positive voltage (μV)	329 ± 161	121 ± 68	NS
maximum negative voltage (μV)	377 ± 192	123 ± 107	NS

μV represents microVolts

NS = not significant by two tailed Students t test between the two groups

Figure 1a : Average integral body surface maps for patients with and without coronary artery disease in the early QRS complex

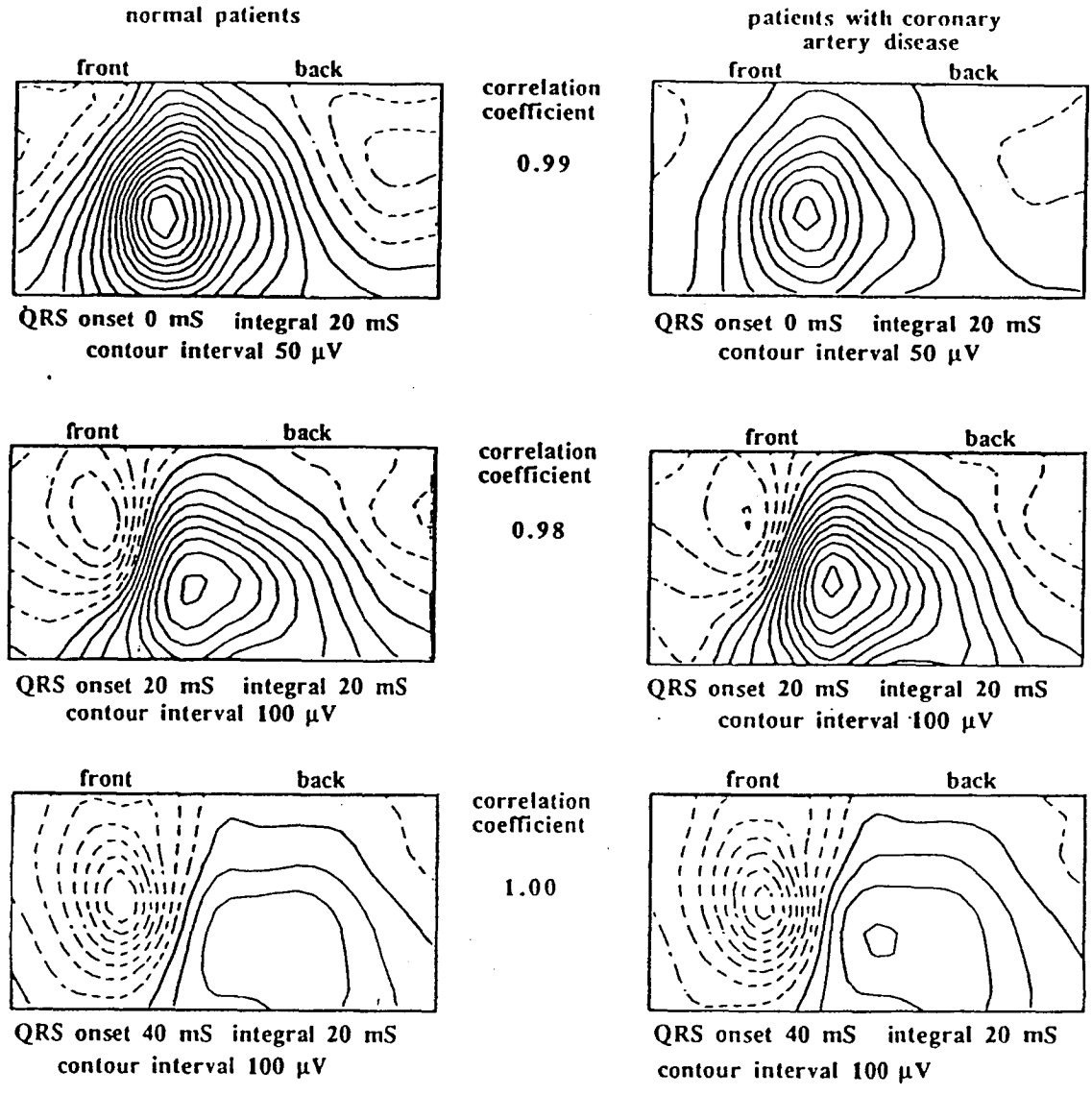

The data format is the standard unwrapped thorax format. The QRS onset is the time after the QRS onset that the integral map starts. The integral is the map integral length in milliseconds. The contour interval is in microvolts. The correlation coefficient is between the two maps at the same QRS onset time

Figure 1b : Average integral body surface maps for patients with and without coronary artery disease in the late QRS, ST and T wave integral maps

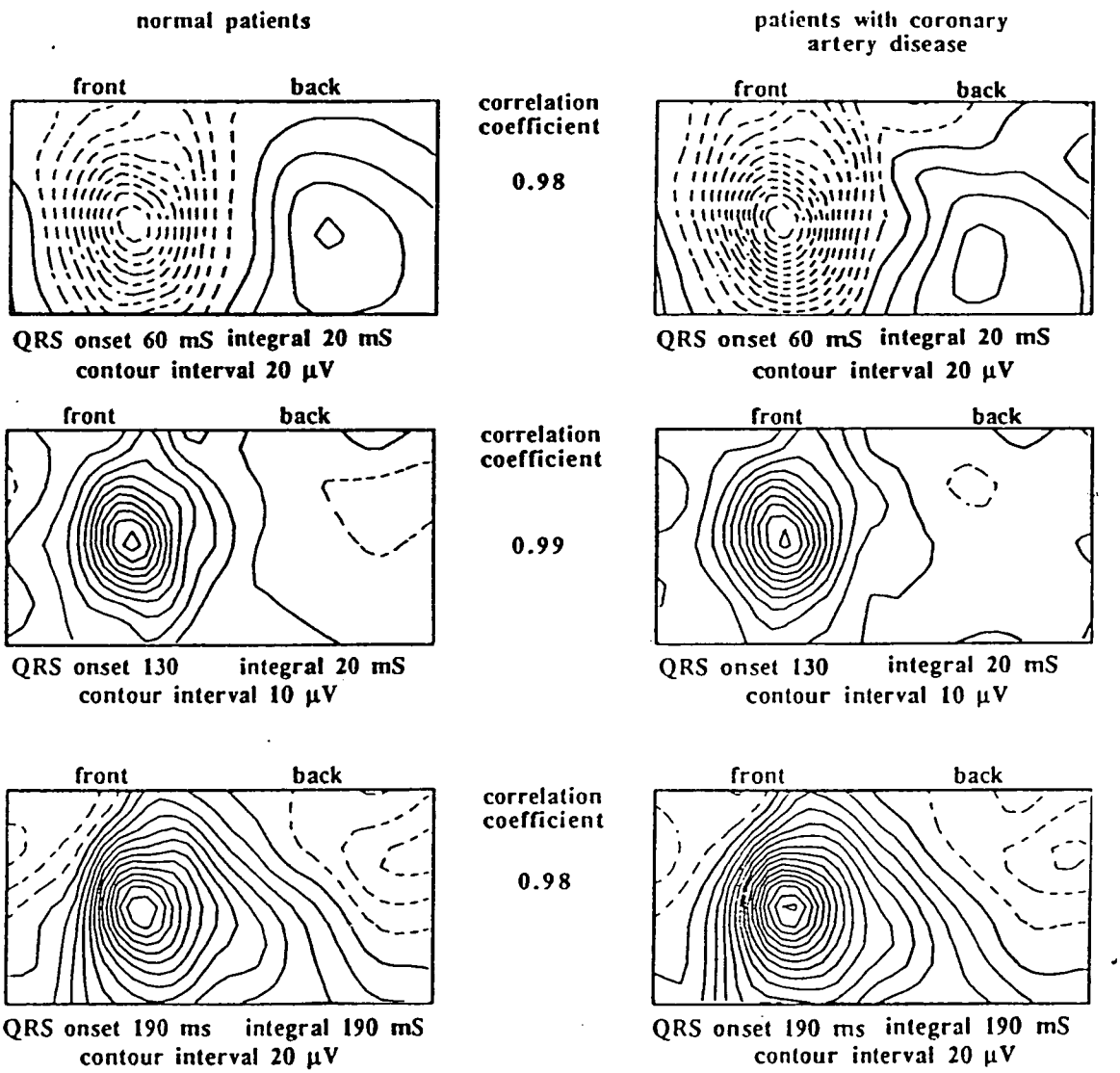

The data format is the standard unwrapped thorax format. The QRS onset is the time after the QRS onset that the integral map starts. The integral is the map integral length in milliseconds. The contour interval is in microVolts. The correlation coefficient is between the two maps at the same QRS onset time

Figure 2a: Histogram of correlation coefficient between body surface maps of patients with coronary artery disease and the mean normal body surface maps

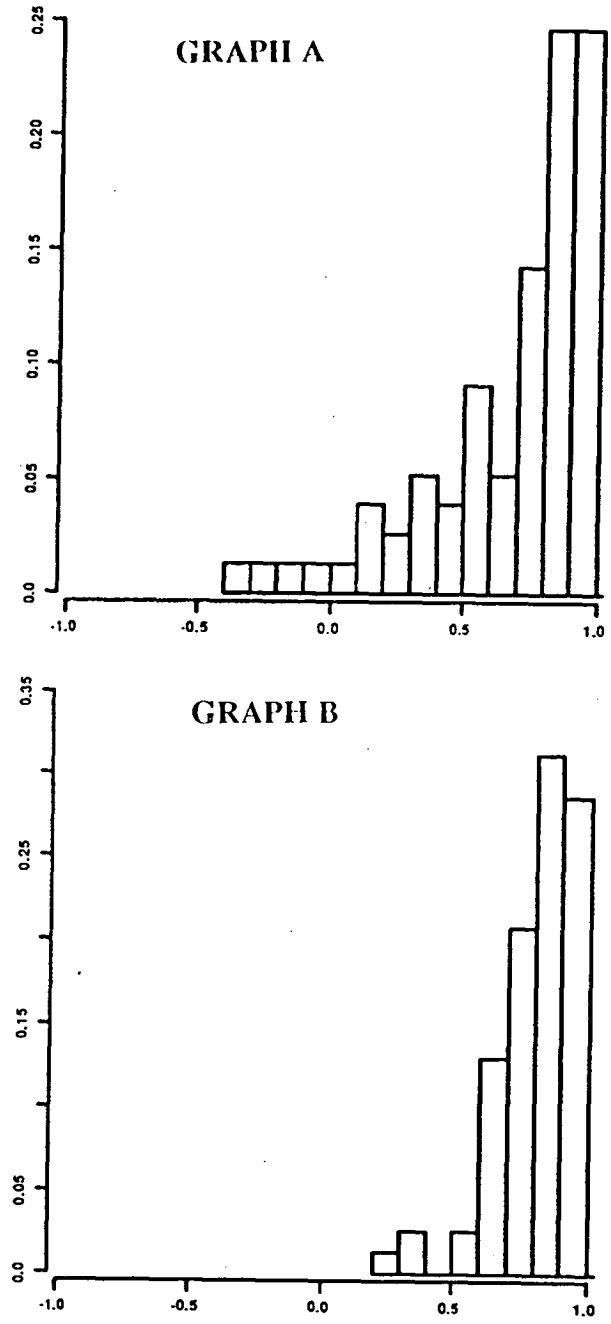

The x-axis is the correlation coefficient range -1 to 1. The y-axis is the relative frequency. Graph A is the correlation coefficient histogram for the integral 0-20 millisecond maps; graph B, 20-40.

Figure 2b: Histogram of correlation coefficient between body surface maps of patients with coronary artery disease and the mean normal body surface maps

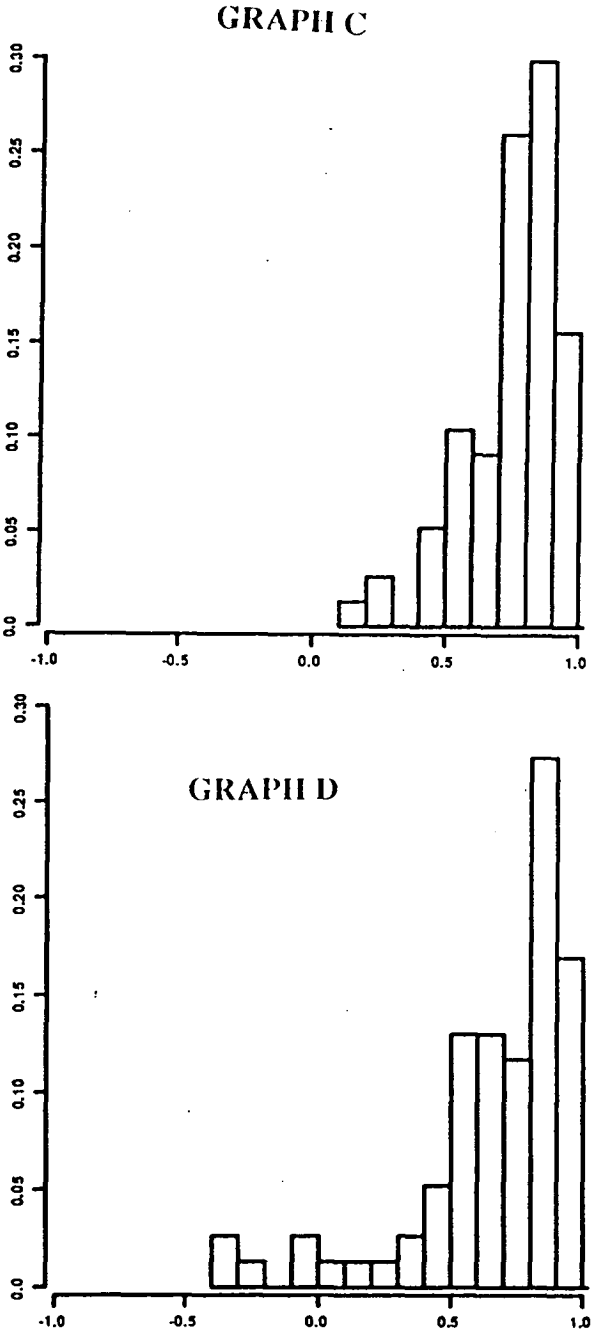

The x-axis is the correlation coefficient range -1 to 1. The y-axis is the relative frequency. Graph C is the correlation coefficient histogram for the integral 40-60 millisecond maps; graph D, 60-80.

Figure 2c: Histogram of correlation coefficient between body surface maps of patients with coronary artery disease and the mean normal body surface maps

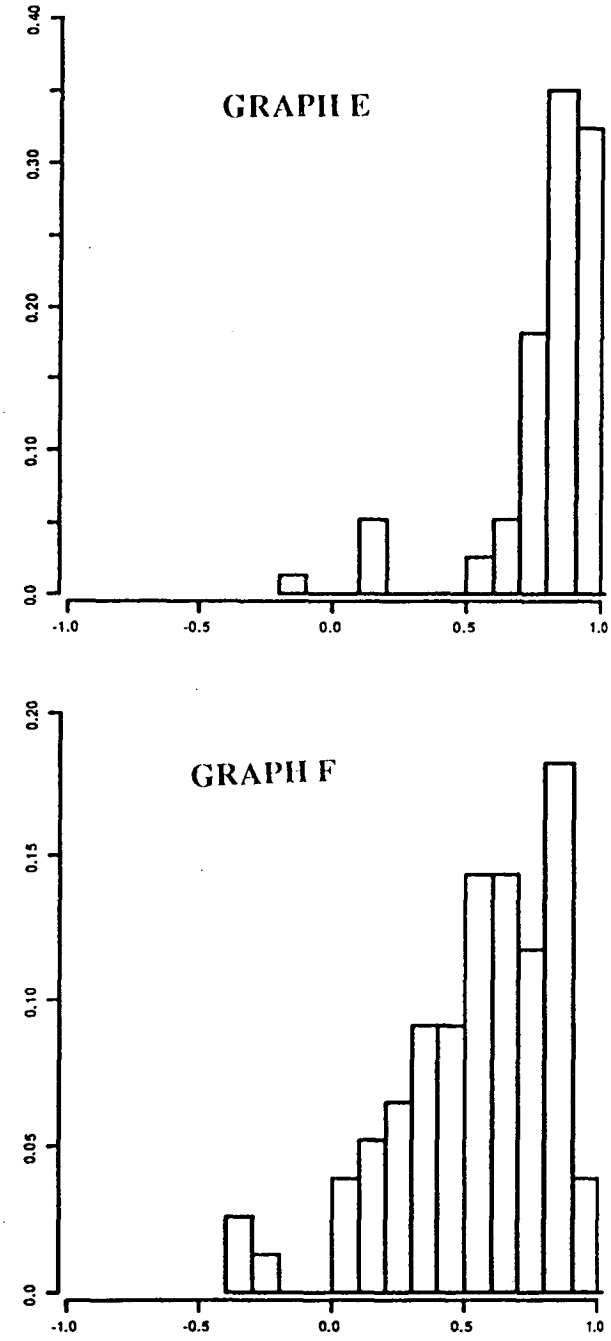

The x-axis is the correlation coefficient range -1 to 1. The y-axis is the relative frequency. Graph E is the correlation coefficient histogram for the ST segment; graph F, t wave map.

Figure 3: Average departure maps for patients with coronary artery disease

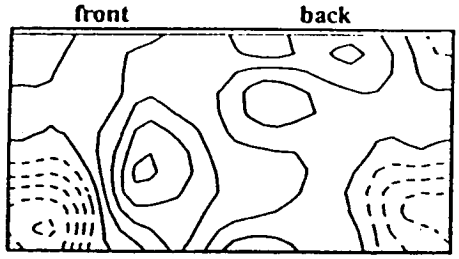

QRS onset 0 mS integral 20 mS
contour interval 0.1 standard deviations

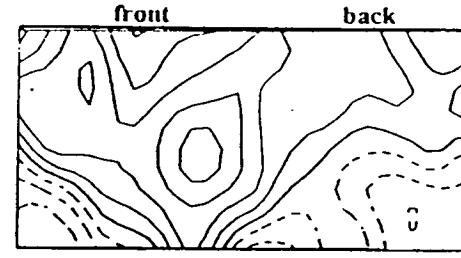

QRS onset 20 integral 20 mS
contour interval 0.1 standard deviations

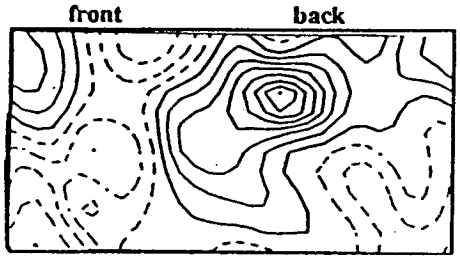

QRS onset 40 mS integral 20 mS
contour interval 0.1 standard deviations

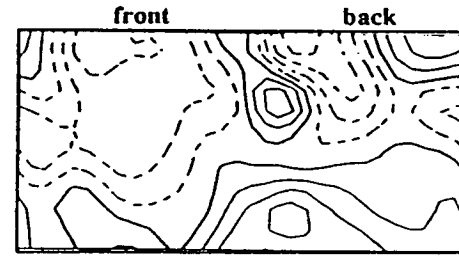

QRS onset 60 mS integral 20 mS
contour interval 0.1 standard deviations

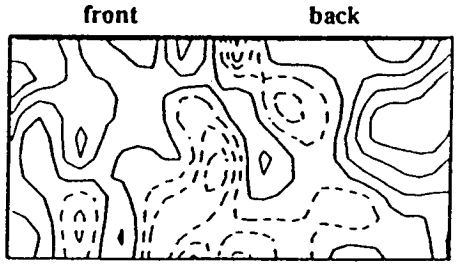

QRS onset 130 mS integral 20 mS
contour interval 0.1 standard deviations

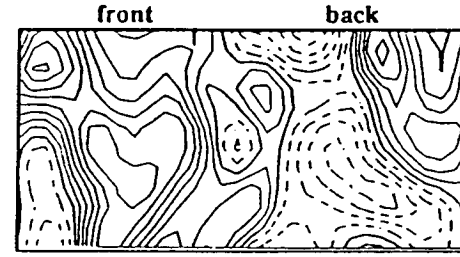

QRS onset 190 mS integral 190 mS
contour interval 0.1 standard deviations

The data format is the unwrapped thorax display. The QRS onset is the time after the QRS onset that the map starts. The integral is the map integral length. The contour lines represent standard deviations from the average normal map in the corresponding integral interval.

Figure 4: Learn and test set scatter graphs for separation of patients with and without coronary artery disease

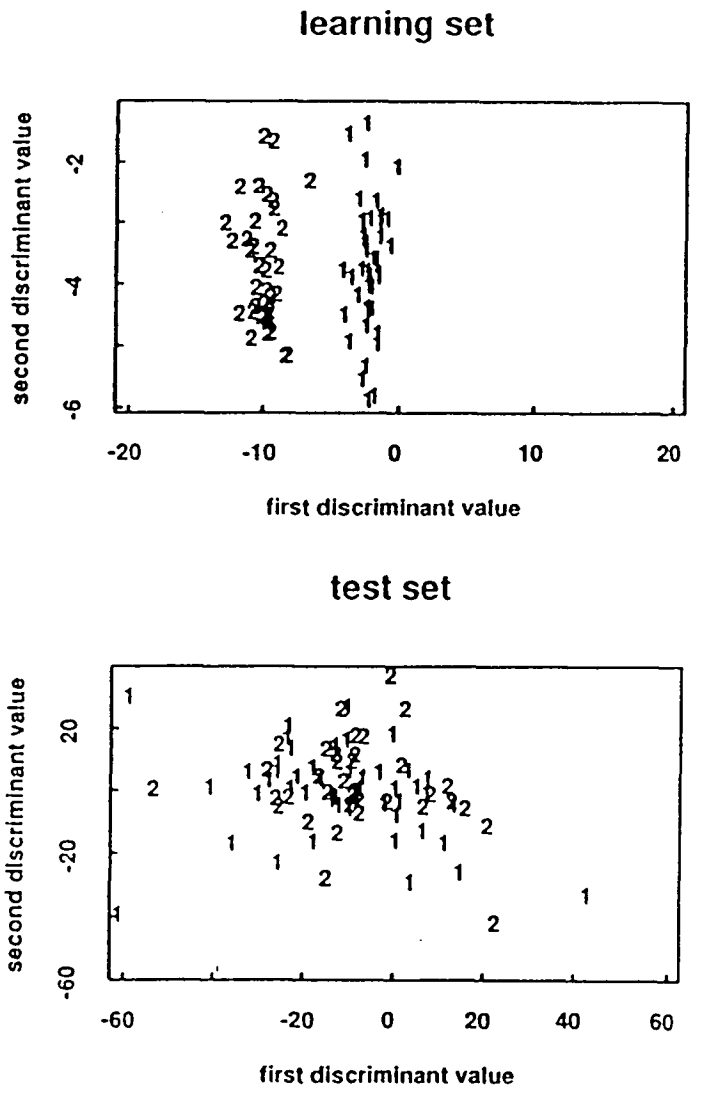

Each number 1 represents a normal patient with a normal 12 lead electrocardiogram, and each number 2 represents a patient with coronary artery disease and a normal 12 lead electrocardiogram. The learning set shows clear separation of the two groups. The test set shows no separation of the normal patients from patients with coronary artery disease

Figure 5: Learn and test set scatter graphs for separation of patients with and patients without coronary artery disease with normal or non-specific electrocardiographic abnormalities

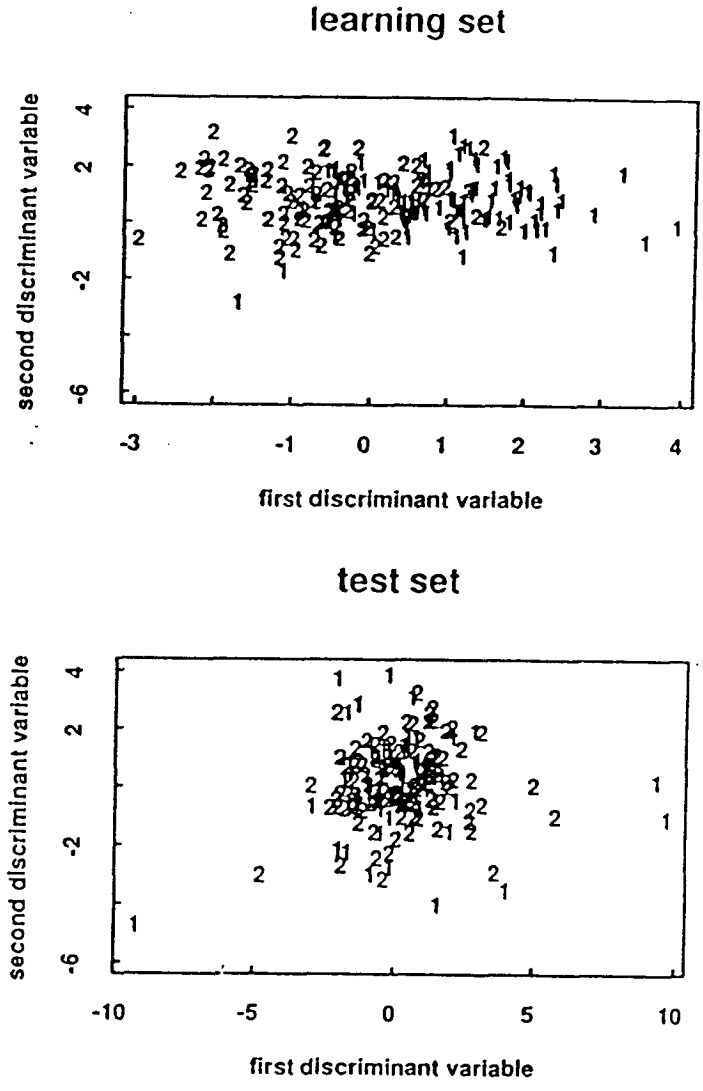

Each number 1 represents a normal patient with a normal 12 lead electrocardiogram that is normal or has only minor non-specific changes, each number 2 represents a patient with coronary artery disease and a 12 lead electrocardiogram that is normal or has minor non-specific changes. The learning set shows separation of the two groups. The test set shows no separation of the normal patients from patients with coronary artery disease

Figure 6: Learn and test set scatter graphs for separation of normal patients and patients with a specific single vessel coronary artery disease with normal or non-specific electrocardiographic abnormalities

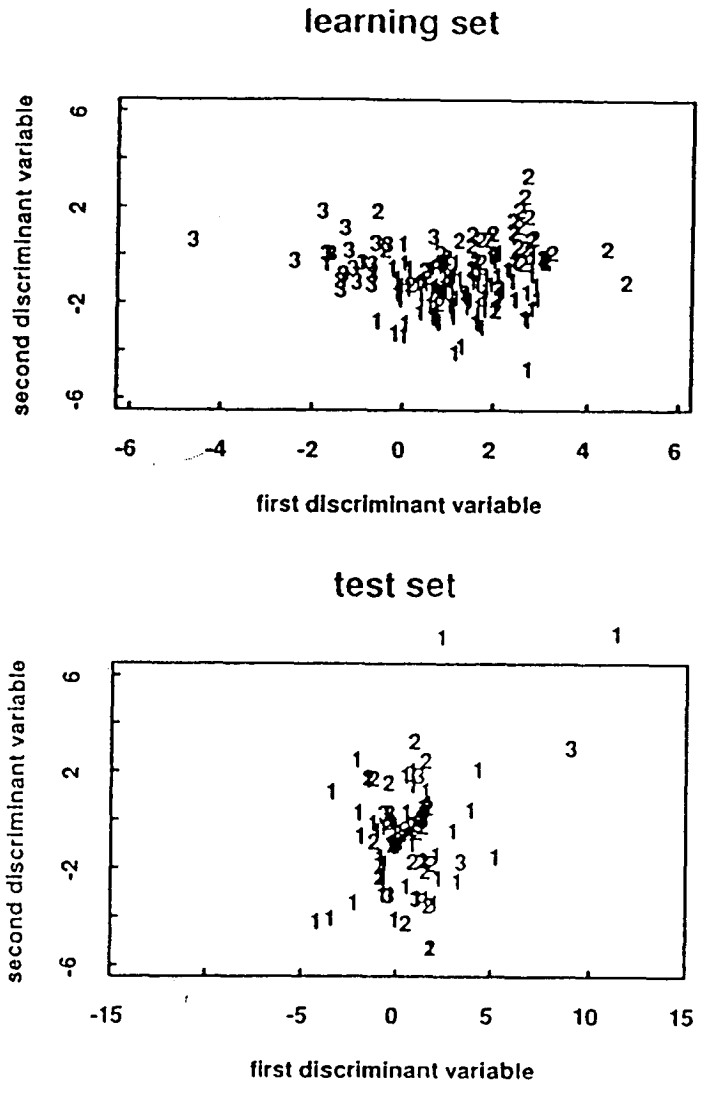

Each number 1 represents a normal patient, each number 2 represents a patient with left anterior coronary artery disease and a 12 lead electrocardiogram that is normal or has minor non-specific changes. Each number 3 represents a patient with right coronary artery disease and a 12 lead electrocardiogram that is normal or has minor non-specific changes. The learning set shows separation of the three groups. The test set shows no separation of the normal patients from patients with specific left or right coronary artery disease.

Chapter 12

Derived epicardial ST segment potential distribution compared to the resting distribution of thallium scintigraphic defect in acute myocardial infarction

Introduction

The requirement for a non-invasive measure of both myocardial infarction size and site is clear. Dr S. J. Walker developed a technique which calculates epicardial potentials from the body surface electrocardiographic data, the inverse transformation solution [Mirvis 1988]. A preliminary study on 55 patients showed that the epicardial ST segment potential could predict the artery involved in acute myocardial infarction with reasonable accuracy [Walker 1987b]. Also the derived epicardial potential was predictive of mortality in patients with acute inferior wall myocardial infarction [Kilpatrick 1989b]. To further assess the potential of this technique to analyse the size of myocardial infarction, we have analysed in detail patients who have had resting thallium scintigraphic scans after first acute myocardial infarction and before further cardiac events.

Methods

Patients Selection

Patients who had body surface electrocardiographic map data recorded during the first acute myocardial infarction and who subsequently underwent resting thallium scanning before any other cardiac event were selected. Patients were excluded if the body surface map contained only low level potentials (less than 200 microVolts difference between the most negative and the most positive recording site). This level was chosen as the equivalent of greater than 0.1 millivolts of ST segment elevation in the standard electrocardiogram. Myocardial infarction was diagnosed on the basis of a typical history of chest pain and a rise and fall of creatine kinase consistent with acute myocardial infarction. Patients with a prolonged QRS interval of greater than 0.11 seconds were excluded to maintain a homogeneous group without conduction defects. No patients were excluded due to severity of

illness.

Thallium Scanning

Following an overnight fast a symptom limited, upright bicycle stress test was performed. Two milli-Curies of thallium 201 were injected intravenously 75 seconds prior to the termination of exercise and imaging commenced within 10 minutes of radioisotope injection. Images were taken in the anterior, 45^{o} LAO and 70^{o} LAO projections; at least 300,000 counts per image were recorded in the same projection after 3 hours, maintaining an identical count time for each image.

The areas of thallium scanning were determined from the thallium data collection method. Each thallium projection available was divided into 5 sections evenly spaced around the scan picture. The epicardial distributions corresponding to the scan areas were derived as below. That is the thallium scan determined the areas for comparison in this study, the epicardial potentials corresponding to the area of thallium was estimated by the map format on a geometrical basis estimated by appearance.

Data was analysed both qualitatively and quantitatively. The myocardium was divided into regions shown in figure 1 and each region scored for the presence or absence of infarction. The scoring was done without knowledge of the results of the body surface mapping, or the clinical data of the patient. Areas were regarded as representing myocardial infarction if a defect was present on the initial scan, and remained present on the 3 hour post injection thallium scan. If thallium uptake occurred by 3 hours post thallium injection then the area was regarded as ischemic [Zaret 1974]. Areas with both a persistent defect and partial redistribution were considered to have both ischemia and infarction present and for the purpose of this study were regarded as representing myocardial infarction.

Body surface mapping

This study used the standard ST segment integral maps.

Calculation of epicardial potentials

To obtain the calculated epicardial distribution it was necessary to multiply the body surface map data recorded from any patient by the inverted derived matrix. This procedure can be done rapidly on a computer and calculated epicardial potentials are displayed within 8 minutes of data collection, although the derivation of each transfer matrix took several days when initially described [Walker 1984].

Briefly, on a nonuniform rectangular grid, the model simulates a three-dimensional resistor network that resembles the human torso both geometrically and electrically. The lungs, spine, sternum and heart are included in the model. The values used for tissue resistivity in the model are those published by Rush et al. [Rush 1963]. The torso geometry has been digitized from computed tomographic scan data obtained from a 40 year old man.

Each tomographic slice was divided into a grid with resolution of 7.5 mm in the neighbourhood of the heart, increasing to 1 cm and then 1.5 cm further from the heart.The model contained 34,914 nodes (points at which the potential calculations are performed). There were 7,237 nodes on the body surface and 807 on the epicardial surface. Intracardiac blood masses are not modeled. The epicardial surface node potentials form a closed surface surrounding the heart which envelops all cardiac chambers and transects the great vessels at the point at which they leave the heart.

With the use of the model, the epicardial potential distribution (h) and the surface potential distribution (b) were related by the following matrix equation:

$$Th=b \qquad \text{Equation 1}$$

where T is a matrix that reflects the geometry of the torso. To construct the matrix T, the epicardial nodes were first grouped to form 50 source regions of approximately equal size that covered the epicardium, and the potential was assumed to be equal at all of the nodes within any one source region. The vector h thus has 50 components- the potentials at the 50 epicardial source regions. The vector b has 160 components, corresponding to 160 potentials at the body surface sites where (interpolated) body surface map data were measured.

A regularization method was used to solve Equation 1 for h in terms of T and . The solution obtained is given by the equation

$$h = (T^tT + ßI)^{-1}T^tb \qquad \text{Equation 2}$$

where I is the appropriate sized identity matrix, and ß is the parameter that determines the amount of smoothing in the solution.

Data Display

Epicardial potentials are plotted as isopotential contour maps on the surface of the heart. These are displayed in six perspective views generated as though one were looking at the heart in situ from viewing positions anteriorly, left lateral, posterior, right lateral, inferior and superior to the heart. The solid lines are positive isopotential contours, the heavy solid line is the zero contour and the dashed lines are the negative isopotential contours. The anterior epicardial view was used to compare to the anterior thallium scan view. To derive epicardial distribution which could be made equivalent to the other projections from thallium imaging, the epicardial surfaces were rotated to LAO 45^o anterior and LAO 70^o. For this study the epicardial regions chosen to represent the thallium regions have been manually picked and are displayed in figure 2 in the 3 different projections equivalent to those of the thallium analysis. The epicardial potentials corresponding to the thallium scan

areas were averaged to calculate a thallium region epicardial potential. In this paper the ST segment has been measured over 20 millisecond periods centered 140 milliseconds after the onset of the QRS and the potentials referred to a simulated Wilson's central terminal.

Method of analysis of epicardial distribution and assessment of prediction

The epicardial distributions were analysed automatically. An abnormal area was defined as an area with a mean ST segment elevation varying from the mean value by greater than 20%. Using the 20% threshold as abnormal produced a good balance between the sensitivity and specificity of the test. Calculations using a threshold between 10% and 40% varied the specificity and sensitivity little, thus 20% was selected as an appropriate arbitrary value. Each patient thus had 15 regions for comparison against the thallium scan. Each prediction was compared with the corresponding region on the thallium scan. The total result was analysed for sensitivity and specificity of the calculated epicardial potential predicting the abnormality on thallium scanning.

Statistical Analysis

The thallium result was taken as the gold standard for scoring an area as subject to infarction or normal. The inverted transformed body surface map data was compared to the thallium scan by calculating the specificity and sensitivity for each patient over all comparisons [Rembold 1988, Sox 1986].

Results

Seventeen patients, 16 male and one female, met the selection criteria. The mean age was 52 ± 8 years. Ten patients had acute anteroseptal wall myocardial

infarction and 7 patients had acute inferior wall myocardial infarction. The mean time from the onset of symptoms to body surface electrocardiographic mapping was 12.1 ± 13.8 hours (range 3-22 hours with one patient at 60 hours) and to thallium scanning 3.6 ± 2.5 months (range 1 week to 5.8 months). The peak creatine kinase level was 1699 ± 571 iu/L for anterior wall myocardial infarction patients and 1730 ± 1050 iu/L for inferior wall myocardial infarction patients. In the anterior infarction group 5 of 10 patients had streptokinase, and in the inferior group 2 of 7 patients had streptokinase.

Anterior wall myocardial infarction

Table 1 shows the comparison of thallium scintigraph scan infarct areas with the calculated epicardial potential ST segment defined infarct region in the 10 patients with anterior wall myocardial infarction. The total sensitivity is 0.69 and the specificity is 0.75. The 45^{o} left anterior oblique and the 70^{o} left anterior oblique views demonstrate an excellent correlation between the thallium scintigraph areas of infarction and the acute ST segment elevation at the time of infarction. The anterior view is less well correlated. Overall if the pretest probability of an area being infarcted is 40% (40% of the thallium areas were regarded as positive), if the body surface map is positive for infarction there is a 0.64 chance that the area is infarcted. Angiography was performed on 5 patients, all had streptokinase, and all had lesions of the left anterior descending artery varying from 100% occlusion to 50% occlusion.

The epicardial potential distribution of the patient whose thallium scan is shown in figure 2 is illustrated in figure 3. The areas of the thallium scan with no uptake show a correlation with the areas of ST segment elevation in the calculated epicardial potentials.

Inferior wall myocardial infarction

Table 2 shows the comparison of thallium scintigraph scan infarct areas with the calculated epicardial potential ST segment defined infarct region in the 7 patients with inferior wall myocardial infarction. The total sensitivity is 0.49 and the specificity is 0.67. The three views are less well correlated than in anterior wall myocardial infarction. Only the infero-posterior areas of the thallium scan (areas denoted D, E, I, J, N, O) have a reasonable sensitivity (0.52) and specificity (0.79). Overall if the pretest probability of an area being infarcted is 40%, then if the body surface map is positive for infarction the there is a 0.50 chance that the area is infarcted. In the 5 patients with angiography all had lesions of the right coronary artery, 3 patients had associated circumflex artery lesions and 2 patients had associated left anterior descending artery lesions.

One patient, with an inferior wall myocardial infarction, unique patient number 2032 was incorrectly predicted due to normal variant ST segment elevation anteriorly.

Discussion

In this work we have shown that in calculated epicardial maps during the ST segment in acute infarction the region of ST segment elevation partially corresponds with the region of significantly reduced thallium perfusion in a post infarction redistribution thallium scan. This study was performed to validate further the inverse transform as a method which produces accurate epicardial surface distributions. A previous study showed that the epicardial ST segment distribution could be used to predict the site of infarction when compared to coronary angiography [Walker 1987b]. In inferior wall myocardial infarction the calculated epicardial potentials predict mortality [Kilpatrick 1989b]. The calculated epicardial potentials give

information about the distribution of potentials in myocardial infarction due to the great vessels altering current pathways [Kilpatrick 1990]. The thallium distribution in this study has been interpreted and compared with the automatic calculation of the mean calculated epicardial potential ST segment derived in any one equivalent region. The use of a system of region by region prediction is stringent as is the automated analysis used. The correspondence is close although some regions were wrongly diagnosed. The division of the epicardium into the 15 regions is arbitrary and includes some redundancy which is also present in the regions of the thallium scan.

We chose thallium scans because thallium uptake indicates the presence of viable myocardium [Tamaki 1982, Wackers 1977, Niess 1979]. Although the thallium scanning was done some 3 months after the myocardial infarction the correspondence was still good. It is possible that some patients had further silent myocardial infarction between the initial body surface map and the thallium scintigraph. This would tend to lessen the accuracy of the epicardial potentials in predicting the thallium scintigraphic scan accuracy, and the delay in the scintiscan should worsen the overall results.

In the group with anterior wall myocardial infarction very good correlations were obtained between the scintigraph scan and the calculated epicardial potentials in the thallium scans showing the left ventricle well. In the anterior view, which is mainly the right ventricular wall, the specificity and sensitivity of the correlation is decreased. In the inverse transformation used to calculate the epicardial potentials no account is made of the right ventricle [Kilpatrick 1990]. The heart in the inverse transformation is treated as a single solid electrical source. Thus it is possible that the poor correlation is due to the presence of the right ventricle which does not allow septal activity to be calculated. There is no solution to the electrical activity of the

septum and right ventricle problem in the field of inverse transformation electrocardiography. This may account for some of the failure of correlation between the thallium scan and the inverse transformation in this study.

In the group with inferior myocardial infarction the overall correlation is worse, and this may be due to the difficulty in detecting potentials from the inferior surface of the heart due to anatomical variables [Rudy 1980]. Although the epicardial potentials produced by the inverse transform have previously been shown to correlate well with coronary artery anatomy [Walker 1987b] and outcome in inferior wall myocardial infarction [Kilpatrick 1989b] this study is rigorous in approach, and the result affected by even the smallest errors. A further problem with the inferior group is that the 5 of 7 patients who had angiography following the thallium scintiscan all had 2 vessel disease. This may indicate that the area of ischemia and thus ST segment elevation with the acute infarction was greater than the area of final infarction. Also it is possible that subsequent events had occurred between the initial myocardial infarction and the thallium scan although there were no electrocardiographic or clinical suggestion of a myocardial infarction during that time. The thallium scan may not detect abnormal inferior areas due to anatomical reasons, again worsening the correlation between thallium scanning and calculated epicardial potentials.

That 10 patients had thrombolytic therapy is of concern. However if reperfusion lessened the area of damage then the false negative rate (thallium scintiscan negative, epicardial potential positive) would be expected to be greater.

The technique of transformation used in this paper uses a single torso model. Previous work has suggested [Kilpatrick 1990] that an individual transfer matrix for each patient would improve the accuracy of the transform. We have examined these data using separate male and female torso models to improve the accuracy but have

not shown a significant benefit. The spline interpolation method and then application to the inverse transformation matrix may lead to errors. We have found that alterations in the interpolation methods and the number of leads used cause negligible changes to the calculated epicardial results. The technique is good for detecting the region of infarction using thallium perfusion scanning as a gold standard.

Other studies comparing body surface mapping results with thallium 201 distributions have been completed. The study by Toyama et al. [Toyama 1982] derived indirectly the regions of the body surface in which q waves could be correlated with defects in the redistribution scan. They also used a subtraction technique from a normal QRS distribution to define the infarcted area. These studies have been further developed [Toyama 1985] by using the inverse solution of Yamashita [Yamashita 1981], again looking at the QRS distribution in the first 30 milliseconds of the QRS. They showed that the epicardial "Q wave" corresponded in position to the position of the infarction from scintigraphy. The method of analysis used, however, looked only at the general site of infarction whereas our study examines the correspondence between thallium and ST elevation on a precise, regional basis.

This study further confirms the potential of epicardial potential distribution to predict infarct size. This technique may have wider applications in cardiology such as the measurement of infarction size and the effectiveness of thrombolytic therapy. The advantage of this technique is that it is non-invasive and rapid; it produces a direct correlation with cardiac anatomy and and has the potential to measure the size of damaged myocardium. This rigorous study and previous work [Walker 1987, Kilpatrick 1989b, Toyama 1982] indicate that the epicardial potentials are sensibly calculated and correspond to cardiac pathology.

Table 1 : Anterior wall myocardial infarction

		thallium scan shows infarct		thallium scan is normal	
thallium scan area		map infarct	map normal	map normal	map infarction
anterior view	A	2	0	2	6
	B	3	3	3	1
	C	2	5	3	0
	D	1	2	4	3
	E	0	0	8	2
LAO 45° view	F	8	0	0	2
	G	5	4	0	1
	H	5	4	1	0
	I	0	3	6	1
	J	0	0	9	1
LAO 70° view	K	7	0	0	3
	L	8	0	2	0
	M	8	1	1	0
	N	0	0	10	0
	O	0	0	10	0
		true positive	false negative	true negative	false negative
totals		49	22	59	20

The thallium scan areas in each view are compared to the equivalent calculated epicardial potentials with each alphabet character representing a different area for comparison

LAO 45° : left anterior oblique position at 45 ° from the anterior view

LAO 70° left anterior oblique position at 70 ° from the anterior view

true positive; both thallium scan and body surface map are positive

true negative; both thallium scan and body surface map are negative

false negative; the thallium scan is positive but the body surface map is negative

false positive; the thallium scan is negative but the body surface map is positive

Table 2 : Inferior wall myocardial infarction

		thallium scan shows infarct		thallium scan is normal	
thallium scan area		map infarct	map normal	map normal	map infarct
anterior view	A	0	0	6	1
	B	0	0	5	2
	C	2	3	2	0
	D	3	2	1	1
	E	1	1	4	1
LAO 45° view	F	0	0	5	2
	G	0	0	4	3
	H	2	2	1	2
	I	2	3	2	0
	J	0	1	4	2
LAO 70° view	K	0	0	4	3
	L	0	0	3	4
	M	1	2	2	2
	N	3	2	2	0
	O	3	2	2	0
		true positive	false negative	true negative	false negative
totals		17	18	47	23

The thallium scan areas in each view are compared to the equivalent calculated epicardial potentials with each alphabet character representing a different area for comparison

LAO 45° : left anterior oblique position at 45 ° from the anterior view

LAO 70° left anterior oblique position at 70 ° from the anterior view

true positive; both thallium scan and body surface map are positive

true negative; both thallium scan and body surface map are negative

false negative; the thallium scan is positive but the body surface map is negative

false positive; the thallium scan is negative but the body surface map is positive

Figure 1: Thallium scan of patient 1

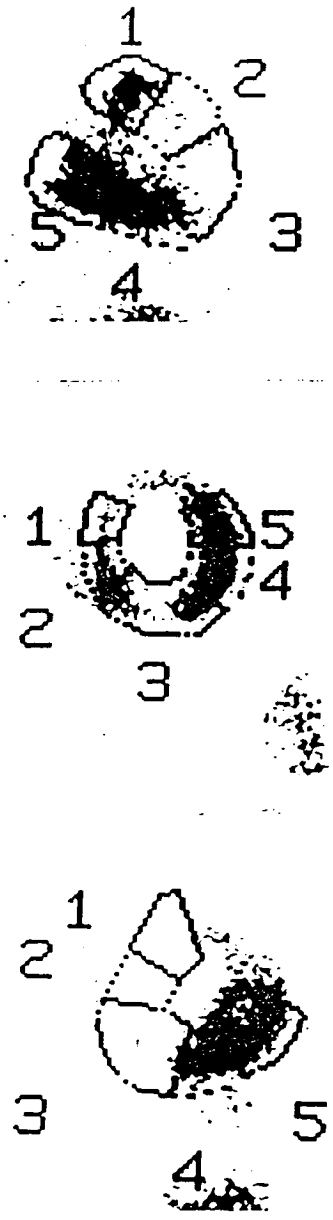

The thallium scans of patient number 1 showing in each of three views the division into regions. In the anterior view shown at the top the regions 1 to 5 correspond to regions A-E in figure 1 (appendix 1). In the centre view, the 45^{o} LAO view shows regions 1 to 5 corresponding to epicardial areas F-J respectively. Likewise in the bottom view the 70^{o} LAO view shows the regions 1-5 corresponding to epicardial areas K-O respectively.

Figure 2: Epicardial region projections

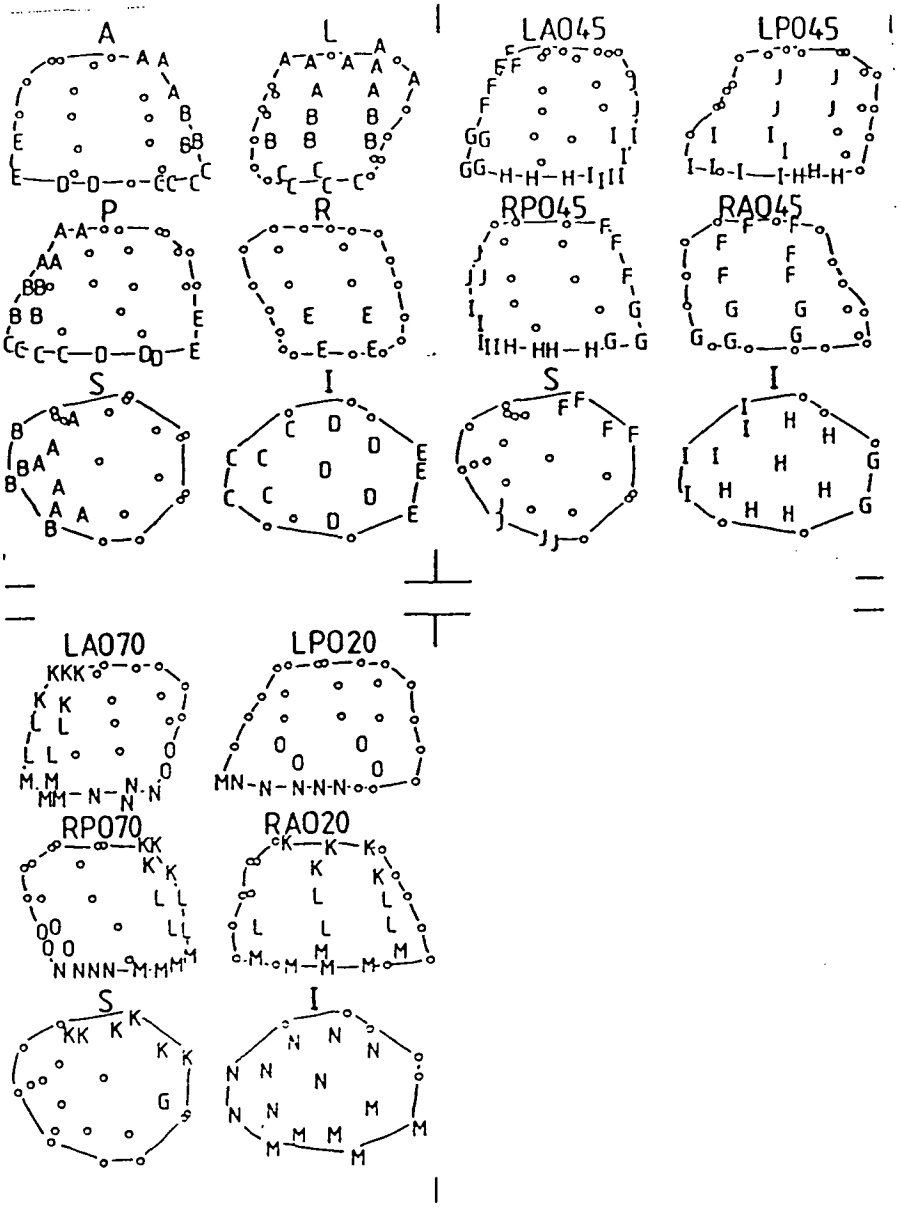

Three projections of epicardial potential regions each show six views of the epicardium. Each view shows the division of regions into sets equivalent to the thallium scan regions shown in figure 2 (appendix 2). The 15 regions are designated alphabetically. Each letter represents the point of a calculated epicardial potential. For each set of views the abbreviations are as follows : A anterior, L left lateral, P posterior, R right lateral, S superior, I inferior, LAO left anterior oblique, LPO left posterior oblique, RAO right anterior oblique, RPO right posterior oblique, numbers refer to degree rotation from antero-posterior projection. The associated number is the oblique angle in degree.

Figure 3 : Epicardial potentials of patient 1

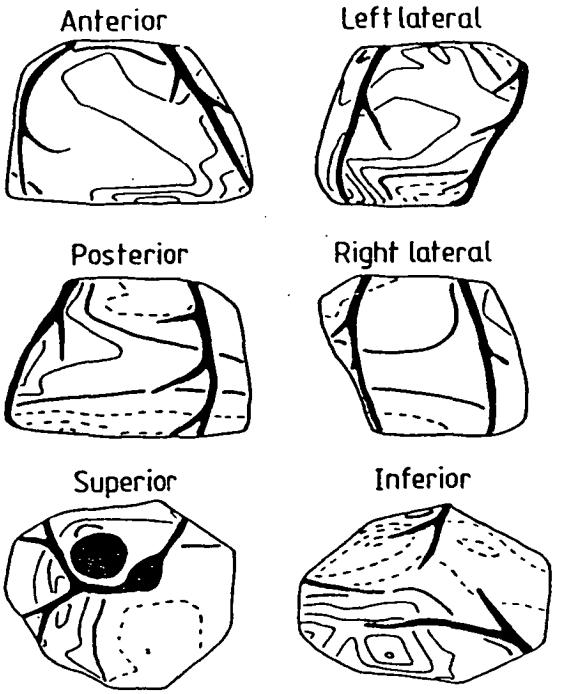

The epicardial map of patient 1 in the anterior projection corresponding to the thallium scan in figure 2. In this figure, the epicardial potential distribution is seen from 6 views and a set of coronary arteries superimposed to indicate the anatomy. In the anterior view the right coronary artery can be seen on the left and the left anterior descending coronary artery on the right. In the left lateral view the left anterior descending coronary artery is on the left and the circumflex coronary artery is on the right. In the inferior view the posterior wall is displayed at the top with the circumflex artery terminating on that surface, the right coronary artery on the right and the left anterior descending coronary artery on the left. Positive contours are shown as solid lines, negative contours as as dashed lines and the zero contour as a heavy black line. The anterior view corresponds to the anterior thallium view in figure 2. Absent thallium uptake in areas 2 and 3 in the anterior view in figure 2 correspond to the ST segment elevation in figure 3 and the epicardial areas B and C in figure 1.

Chapter 13

Conclusions and the future of body surface electrocardiographic mapping

Body surface electrocardiographic mapping and standard electrocardiogram

The body surface map is an expansion of the standard electrocardiogram. The body surface map contains the total data of the standard electrocardiogram but the display format and interpretation are different. The standard electrocardiogram does not contain all the information of the body surface map. The two methods of electrocardiography are complimentary. The standard electrocardiogram is important for the determination of the time related aspects of the cardiac electrical cycle. This is not surprising considering the standard electrocardiogram is a time potential graph. The standard electrocardiogram is also excellent for the diagnosis of other cardiac time related events, such as the classical conduction disturbances of right bundle branch block, left bundle branch block and left anterior fascicular block. Conditions where time potential relationships are important are best diagnosed by standard electrocardiography.

The body surface map, on the the other hand, is better at diagnosis when the pathological change is local causing focal electrical disturbance to the cardiac generator. Thus there is a spatial change in the cardiac potentials over the thorax which is detected by the body surface electrocardiographic map. Using ST segment mapping, isointegral mapping through the QRS complex and QRST complex the body surface map analyses spatial electrical change better than the standard electrocardiogram. In this thesis the advantages of ST segment mapping and the relationship of the spatial distribution of the ST segment changes to the resultant QRS loss in acute myocardial infarction have been demonstrated. The clinical utility of the method as a diagnostic tool and a prognostic tool is demonstrated in the studies. Furthermore analysis of the mapping data suggests that the body surface map may be useful in the assessment of thrombolytic therapy in myocardial infarction [Kilpatrick 1993] or in the prediction of ventricular arrhythmias in the same clinical setting [Briggs 1991]. To demonstrate the superiority of body surface

mapping over standard electrocardiography was not an aim of this study. Ideally any method of electrocardiography should contain the standard electrical display and the facility to display the data as a body surface map.

Problems with body surface electrocardiographic map

Advances in computer technology have removed many of the problems associated with body surface mapping. Small personal computers have the computing power to analyses and graph body surface data. The ability to reduce the data to a small number of coefficients of eigenvalues allows storage of multiple maps on a small computer disc.

The major problem with body surface mapping is not the technology but the reluctance of the medical professional. Body surface mapping is developing as an observational science. Each map is studied in relationship to the clinical state of the patient including age and sex, the results of the investigations into the cardiac function and on occasions pathological displays of the cardiac pathology. This observational process is a slow method of developing expertise. Even with over 5,000 maps recorded from the coronary care unit and cardiac catheter suite we have collected very few body surface maps on rare cardiac conditions. This, together with the enormous variation in patients, and the number of patients with complex conditions means that many maps will need to be studied before we can be confident in the clinical interpretation of the body surface maps. After a number of years of mapping patients we have become confident in the straight forward use of maps. Our colleagues who have watched and listened to our discussions on the body surface map occasionally request maps in complex diagnostic cases believing that the increased information may benefit the patient. Unfortunately, although this is an interesting process and often results in the resolution of the clinical question, it remains occasional.

A further problem with body surface maps is the lack of training and education medical practitioners have received to understand the map patterns. In the visual display form the experienced mapper is able to read and understand the map pattern, and gain clinically applicable knowledge from the body surface map. The novice is unable to interpret or even understand the map.

The statistical analysis methods used all had a similar problem, that the methods were over-inclusive. That is the methods regarded all the information as important and thus lost the important features in the nondescript features. Also the maps form a spectrum of patterns merging from normal to abnormal patterns with no clear dividing line. Thus what is an abnormal map pattern and what is a normal map pattern can be difficult to determine. Analysis by visual inspection by a trained experienced physician who can rapidly weight the appearances of the map against the clinical features and exclude unimportant features may be the best method of body surface map interpretation available. The statistical analysis appears too rigid to do such manipulations, either being over inclusive or exclusive.

The future of body surface electrocardiographic map

I believe that the body surface mapping in its present form will gradually develop as a complementary form of electrocardiography to the standard electrocardiogram. An exciting future development is the use of the inverse transformation to calculate the cardiac potential distribution on the surface of the heart. Thus the body surface electrocardiographic recording is transformed onto the surface of the heart giving a clear picture of the electrical changes associated with clinical illness. This method is discussed in chapter 2 and chapter 12. This method of interpreting body surface maps may have major application in the areas of research into the origin of the electrocardiogram and into clinical interpretation of the electrocardiogram. Indeed further studies suggest that the inverse transformation of

the body surface map will be clinically and experimentally useful [Kilpatrick 1989, Kilpatrick 1990, Bell 1991, Myerburg 1989, Kilpatrick 1993, Teh 1993]. Indeed the description of the current pathways in acute infarction [Kilpatrick 1989] and pericarditis [Teh 1993] has led to a new theory in the understanding of the standard electrocardiogram [Kilpatrick 1990] emphasizing the importance of the great vessels in the current pathways of the heart and thus the electrocardiogram.

A further advantage of the inverse transformation is that physicians may find interpretation of body surface electrocardiographic maps easier aiding the understanding of the body surface map by colleagues who are unfamiliar with the method. The inverse transformation could provide an impetus for the development of commercial machines that would record the body surface map, transform the body surface potentials onto the cardiac surface, and automatically compare the patterns to a data bank of map patterns for automatic diagnosis. Such machines could also display a standard electrocardiogram for the analysis of cardiac time cycle events.

This study

The aim of this study was to determine if there is:

1. is the additional information contained in the body surface map of clinical significance in myocardial infarction ?
2. is the display format and thus the application of topographical statistics of clinical benefit in myocardial infarction?
3. is the addition information able to detect coronary artery disease in patients presenting with chest pain ?

This study has accurately described the clinical usefulness of the body surface map in ischemic heart disease.

The studies tested capability of the body surface map to:

1. to describe the initial body surface map in inferior wall and anterior wall acute myocardial infarction including the clinical correlations,
2. to detect myocardial infarction in the initial body surface map,
3. differentiate patients with coronary artery disease from patients without coronary artery disease,
4. to examine future methods of improving body surface map.

The studies performed and the results recorded indicate that body surface mapping is a simple rapid diagnostic and prognostic tool of value in clinical medicine. Although the body surface map cannot determine the presence of coronary artery disease the use in acute myocardial infarction is clear.

Bibliography

Abildskov JA, Burgess MJ, Lux RL, Wyatt R, Vincent GM: The expression of normal ventricular repolarization in the body surface distribution of T potentials. Circulation 1976;54:901-906

Altman DG; Practical statistics for medical research. Chapman and Hall London 1991

Anon: Predictability and coronary disease. Lancet 1991:338:1364-1365

Ardissino D, Barberis P, De Servi S, Merlini PA, Bramucci E, Falcone C, Specchia G: Abnormal coronary vasoconstriction as a predictor of restenosis after sucessful coronary angioplasty in patients with unstable angina pectoris. N Engl J Med 1991;325:1053-1057

Arisi G, Macchi E, Baruffi S, Spaggiari S, Taccardi B: Potential fields on the ventricular surface of the exposed dog heart during normal excitation. Circ Res 1983;52:706-715

Armitage P, Berry G: Statistical methods in medical research, Blackwell scientific publications, Oxford, 1987;334-343

Arvan S, Varat MA: Persistent ST-segment elevation and left ventricular wall abnormalities: A 2-dimensional echocardiographic study. Am J Cardiol 1984;53:1542-1546

Bar FW, Brugada P, Dassen WR, van der Werf J, Wellens HJJ: Prognostic values of Q waves, R/S ratio, loss of R wave voltage, ST-T segment abnormalities, electrical axis, low voltage and notching: Correlation of electrocardiogram and left ventriculogram. J Am Coll Cardiol 1984;4:17-27

Barr RC, Spach MS: Construction and interpretation of body surface maps. Prog Cardiovasc Dis 1983;26:33-42

Batschelet E: Mathematics for life sciences. Springer-Verlag, Berlin. 1971:418-423

Baxt WG: Use of an artificial neural network for the diagnosis of myocardial infarction. Ann Intern Med 1991;115:843-848

Becker RA, Chambers JM: S an interactive enviroment for data analysis and graphics. Wadsworth, Belmont California 1984:191-195

Bell AJ, Loughhead MG, Walker SJ, Kilpatrick D: Prognostic significance of ST potentials determined by body surface mapping in inferior wall acute myocardial infarction. Am J Cardiol 1989a;64:319-323

Bell AJ, Nichols P, Briggs C, Kilpatrick D: Prognostic significance of ST potentials determined by body surface mapping in anterior wall acute myocardial infarction. J Electrocardiol 1993;26:177-185

Bell AJ, Ryan A, Ware R, Walker SJ, Kilpatrick D: Derived epicardial ST segment potential distribution compared to the resting distribution of thallium scintigraphic defect in acute myocardial infarction. Am J Noninvas Cardiol 1991;5:273-279

Bell AJ, Walker SJ, Kilpatrick D: Natural history of ST-segment potential distribution determined by body surface mapping in patients with acute inferior infarction. J Electrocardiol 1989b;22:333-341

Bell MR, Montarello SK, Steele PM: Does the emergency room electrocardiogram identify patients with suspected myocardial infarction who are at low risk of acute complications ? Aust NZ J Med 1990;20:564-569

Benson DW, Sterba R, Gallagher JJ, Walston A, Spach MS: Localization of the site of ventricular preexcitation with body surface maps in patients with Wolff-Parkinson-White syndrome. Circulation 1982;65:1259-1268

Berman JL, Wynne J, Cohn PF: Multiple-lead QRS changes with exercise testing. Diagnostic value and hemodynamic implications. Circulation 1980;61:53-61

Bigger JT, Coromilas J, Weld FM, Reiffel JA, Rolnitzky LM: Prognosis after recovery from acute myocardial infarction. Ann Rev Med 1984;35:127-167

Bilbao FJ, Zabalza IE, Vilanova JR, Froufe J: Atrioventricular block in posterior acute myocardial infarction: clinicopathologic correlation. Circulation 1987;75:733-736

Boden WE, Gibson RS, Schechtman KB, Kleiger RE, Schwartz DJ, Capone RJ, Roberts R, Diltiazem reinfarction study research group: ST segment shifts are poor predictors of subsequent Q wave formation in acute myocardial infarction. A natural history study of early non-Q wave infarction. Circulation 1989;79:537-548

Boden WE, Kleiger RE, Gibson RS, Reddy BR, Schechtman KB, Schwartz DJ, Capone RJ, Roberts R, and Diltiazem Reinfarction Study research Group: Favourable long term prognosis in patients with non-Q wave acute myocardial infarction not associated with specific electrocardiographic changes. Br Heart J 1989;61:396-402

Bodenheimer MM: Risk stratification in coronary artery disease: a contrary viewpoint. Ann Intern Med 1992;116:927-936

Brandt PWT, Partridge JB, Wattie WJ: Coronary arteriography; method of presentation of the arteriogram report and a scoring system. Clin Radiol 1977;28:361-365

Briggs CM, Kilpatrick D, Bell AJ: Abnormal T wave dispersion does not predict sudden death of arrhythmias following acute myocardial infarction Aust NZ J Med (suppliment) 1990;20:348a

Brush JE, Brand DA, Acampora D, Chalmer B, Wackers FJ: Use of the initial electrocardiogram to predict in-hospital complications of acute myocardial infarction. N Engl J Med 1985;312:1137-1141

Campeau L : Grading of angina pectoralis [letter] Circulation 1976;54:522-523

Carmeliet E: Myocardial ischemia: reversible and irreversible changes. Circulation 1984;70:149-151

Cedres BL, Liu K, Stamler J, Dyer A, Stamler R, Berkson DM, Paul O, Lepper M, Lindberg HA, Marquardt J, Stevens E, Schoenberger JA, Shekelle RB, Collette P, Garside D: Independent contribution of electrocardiographic abnormalities to risk of death from coronary heart disease, cardiovascular disease and all causes. Findings of three Chicago epidemiologic studies. Circulation 1982;65:146-152

Christian TF, Clements IP, Behrenbeck T, Huber KC, Cresebro JH, Gersh BJ, Gibbons RJ: Limitations of the electrocardiogram in estimating infarction size after acute reperfusion therapy for myocardial infarction. Ann Intern Med 1991;114:264-270

Cohen D, Kaufman LA: Magnetic determination of the relationship between S-T segment shift and the injury current produced by coronary artery occlusion. Circ Res 1975;36:414-424

Cohen M, Blanke H, Karsh KR, Holt J, Rentrop P: Implications of precordial ST-segment depression during acute inferior myocardial infarction. Arteriographic and ventriculographic correlations during the acute phase. Br Heart J 1984;52:497-501

Cooper JK : Electrocardiography 100 years ago. N Engl J Med 1986:315;461-464

Cooper MJ, Barrett PA, Reid GC, Lyons NR: Diagnosis of inferior myocardial infarction in the presence of left anterior hemiblock. Aust NZ J Med 1987;17:47-50

Cox J, Naylor CD: The Canadian cardiovascular society grading scale for angina pectoralis: is it time for refinements ? Ann Intern Med 1992;117:677-683

Croft CH, Woodward W, Nigod P, Corbett JR, Lewis SE, Willerson JT, Rude RE: Clinical implications of anterior S-T segment depression in patients with acute inferior myocardial infarction. Am J Cardiol 1982;50:428-436

Crow RS, Rautaharju PM, Prineas RJ, Connett JE, Furberg C, Broste S, Stamler J, and the Multiple Risk Factor Intervention Trial Research Group: Risk factors, exercise fitness and electrocardiographic response to exercise in 12,866 men at high risk of symptomatic coronary heart disease. Am J Cardiol 1986;57:1075-1082

David D, Naito M, Mitchelson E, Watanabe Y, Chen CC, Morganroth J, Shaffenburg M, Blenko T: Intramyocardial conduction: a major determinant of R-wave amplitude during acute myocardial ischemia. Circulation 1982;65:161-167

DeAmbroggi L, Bertoni T, Locati E, Stramba-Badiale M, Schwartz PJ: Mapping of body surface potentials in patients with idiopathic long QT syndrome. Circulation 1986a;74:1334-1345

DeAmbroggi L, Bertoni T, Rabbin C, Locati E, Nador F: Usefulness of time-integral analysis of body surface potential maps, in van Dam RTh, van Oosterom A eds, Electrocardiographic body surface mapping. Martinus, Nijhoff, 1986b;203-207

DeAmbroggi LD, Bertoni T, Rabbia C, Landolina M: Body surface potential maps in old myocardial infarction. Assessment of diagnostic criteria. J Electrocardiol 1986c;19:225-234

DePace NL, Iskandrian AS, Nadell R, Colby J, Hakki A-H: Variation in the size of jeopardized myocardium in patients with isolated left anterior descending coronary artery disease. Circulation 1983;67:988-994

Dunn RF, Freedman SB, Kelly DT, Bailey IK, McLaughlin A: Exercise-induced ST-segment elevation in leads V1 or aVL. A predictor of anterior myocardial ischemia and left anterior descending coronary artery disease. Circulation 1981;63:1357-1363

Eddleemon CO, Ruesta VJ, Horan LG, Brody DA: Distribution of heart potentials on the surface of the body in five normal young men. Am J Cardiol 1968;21:860-870

Ehrenberg ASC: Data reduction Analysing and interpreting statistical data. John Wiley & Sons Chichester 1975:263-273

Einthoven W, Fahr G, de Waart A : Uber die Richtung und die manifeste Grosse der Potentialschwankungen im imenschlichen Herzen und uber den Einfluss der Herzlage auf die Form des Elektrokardiogramms. Pfluegers Arch 1913:150:275-315. (Translation: Hoff HE, Sekelj P : Am Heart J 1950;40:163-194)

Essen Rv, Merx W, Doerr R, Effert S, Silny J, Rau G: QRS mapping in the evolution of acute anterior myocardial infarction. Circulation 1980;62:266-276

Evans AK, Lux RL, Burgess MJ, Wyatt RF, Abildskov JA: Redundancy reduction for improved display and analysis of body surface potential maps; II: temporal compression. Circ Res 1981;49:197-203

Everitt B; Cluster analysis. Heinemann Educational Books, London, 1974

Faugere G, Savard P. Nadeau RA, Derome D, Shenasa M, Page PL, Guardo R: Characterization of the spatial distribution of late ventricular potentials by body surface mapping in patients with ventricular tachycardia. Circulation 1986;74:1323-1333

Ferguson DW, Pandian N, Koschos JM, Marcus ML, White CW: Angiographic evidence that reciprocal ST-segment depression during acute inferior myocardial infarction does not indicate remote ischemia: analysis of 23 patients. Am J Cardiol 1984;53:55-62

Flowers N, Hand C, Sridharan M, Horan LG, Sohi GS: Surface reflections of cardiac excitation and the assessment of infarct volume in dogs. A comparison of methods. Circ Res 1978:43:406-413

Flowers NC, Horan LG, Johnson JC: Anterior infarctional changes occurring during mid and late ventricular activation detectable by surface mapping techniques. Circulation 1976a;54:906-913

Flowers NC, Horan LG, Sohi GS, Hand RC, Johnson JC: New evidence for inferoposterior myocardial infarction on surface potential maps. Am J Cardiol 1976b;38:576-581

Freedman SB, Dunn RF, Berstein L, Morris J, Kelly DT: Influence of collateral blood flow on the development of exertional ischemia and Q wave infarction in patients with severe single-vessel disease. Circulation 1985;71:681-686

Fuchs RM, Achuff SC, Grunwald L, Yin FCP, Griffith LSC: Electrocardiographic localization of coronary artery narrowings: studies during myocardial ischemia and infarction in patients with one-vessel disease. Circulation 1982;66:1168-1176

Gardner MJ, Montague TJ, Armstrong CS, Horacek BM, Smith ER: Vulnerability to ventricular arrhythmia: assessment by mapping of body surface potential. Circulation 1986;73:684-692

Gelman JS, Saltups A: Precordial ST segment depression in patients with inferior myocardial infarction : clinical implications. Br Heart J 1982;48:560-565

Gewirtz H, Horacek BM, Wolf HK, Rautaharju PM, Smith ER: Mechanisms of persistent S-T segment elevation after anterior myocardial infarction. Am J Cardiol 1979;44:1269-1275

Gibson RS, Crampton RS, Watson DD, Taylor GJ, Carabello BA, Holt ND, Beller GA: Precordial ST-segment depression during acute inferior myocardial infarction: clinical, scintigraphic and angiographic correlations. Circulation 1982;66:732-741

Goldberg HL, Borer JS, Jacobstein JG, Kluger J, Scheidt SS, Alonso DR: Anterior S-T segment depression in acute inferior myocardial infarction: indicator of posterolateral infarction. Am J Cardiol 1981;48:1009-1015

Goldman L, Cook EF, Mitchell N, Flatley M, Sherman H, Rosati R, Harrell F, Lee K, Cohn PF: Incremental value of the exercise test for diagnosing the presence or absence of coronary artery disease. Circulation 1982a;66:945-953

Goldman L, Weinberg M, Weisberg M, Olshen R, Cook EF, Sargent RK, Lamas GA, Dennis C, Wilson C, Deckelbaum L, Fineberg H, Stiratelli R, and the medical house staffs at Yale-New Haven Hospital and Brigham and Women's Hospital: A computer-derived protocol to aid in the diagnosis of emergency room patients with acute chest pain. New Engl J Med 1982b;307:588-596

Green LS, Lux RL, Haws CW: Detection and localization of coronary artery disease with body surface mapping in patients with normal electrocardiograms. Circulation 1987a;76:1290-1297

Green LS, Lux RL, Haws CW, Williams RR, Hunt SC, Burgess MJ: Effects of age, sex, and body habitus on QRS and ST-T potential maps of 1100 normal subjects. Circulation 1985;71:244-253

Green LS, Lux RL, Stilli D, Haws CW, Taccardi B: Fine detail in body surface maps using a limited lead array and spatial and temporal data representation. J Electrocardiol 1987b;20:21-26

Greenberg H, Gillespie J, Dwyer EM, Multicenter post-infarction research group: A new electrocardiographic classification for post-myocardial infarction clinical trials. Am J Cardiol 1987;59:1057-1063

Guerriere MRJ, Detsky AS: Neural networks: what are they ? Ann Intern Med 1991;115:906-908

Haraphongse M, Tanomsup S, Jugdutt BI: Inferior ST segment depression during acute anterior myocardial infarction: clinical and angiographic correlations. J Am Coll Cardiol 1984;4:467-476

Havelda CJ, Sohi GS, Flowers NC, Horan LG: The pathologic correlates of the electrocardiogram: complete left bundle branch block. Circulation 1982;65:445-451

Hedges JR, Koberneck MS : Detection of myocardial ischemia infarction in the emergency department patient with chest discomfort. Emer Med Clin North Am 1988;6:317-340

Henning H, Hardarson T, Francis G, O'Rourke RA, Ryan W, Ross J: Approach to the estimation of myocardial infarct size by analysis of precordial S-T segment and R wave maps. Am J Cardiol 1978;41:1-8

Herlitz J, Hjalmarson A, Waldenstrom J: Relationship between electrocardiographically and enzymatically estimated size in anterior myocardial infarction. J Electrocardiol 1984;17:361-370

Herlitz J, Sillfors L, Hjalmarson A: Experiences from the use of twenty-four precrodial chest leads in suspected acute myocardial infarction. J Electrocardiol 1986;19:381-388

Hindman NB, Wagner GS: Enhancement of an old diagnostic tool, the standard 12-lead ECG. J Electrocardiol 1987;20:93-97

Hinsen R, Silny J, Rau G, von Essen R, Merx W, Effert S: Technical aspects of precordial ECG-mapping, in Meyer J, Schweitzer P, Erbel R eds. : Advances in non-invasive cardiology. Martinus, Nijhoff and Boston 1983:157-172

Hirai M, Ohta T, Kinoshita A, Toyama J, Nagaya T, Yamada K: Body surface isopotential maps in old anterior myocardial infarction undetectable by 12-lead electrocardiograms. Am Heart J 1984;108:975-982

Hlatky MA, Califf RM, Lee KL, Pryor DB, Wagner GS, Rosati RA: Prognostic significance of pre cordial ST-segment depression during inferior acute myocardial infarction. Am J Cardiol 1985;55:325-329

Horan LG, Flowers NC, Brody DA: Body surface potential distribution: Comparison of naturally and artificially produced signals as analyzed by digital computer. Circ Res 1963;13:373-387

Horan LG, Flowers NC, Johnson JC: Significance of the diagnostic Q wave of myocardial infarction. Circulation 1971;43:428-436

Horan LG, Hand RC, Flowers NC, Johnson JC, Sridharan MR: The influence of electrode placement in the reconstruction and analysis of body surface maps from limited thoracic arrays. J Electrocardiol 1980;13:311-312

Horan LG, Sridharan MR, Killam HAW, Flowers NC: Patterns of body surface potential and ventriculograms specific to occlusion of subdivisions of the coronary arteries. Circ Res 1990;67:683-693

Ikeda K, Kawashima S, Kubota I, Igarashi A, Yamaki M, Yasumuri S, Tsuiki K,Yasui S: Non-invasive detection of coronary artery disease by body surface mapping after diryridamole infusion. J Electrocardiol 1986;19:213-224

Ikeda K, Kubota I, Igarashi A, Yamaki M, Tsuiki K, Yasui S: Detection of local abnormalities in ventricular activation sequence by body surface isochrome mapping in patients with previous myocardial infarction. Circulation 1985;72:801-809

Ishikawa T, Watabe S, Yamada Y, Miyachi K, Sakai Y, Ito A, Sotobata I: New diagnostic evidence on the T wave map indicating involved coronary artery in patients with angina pectoris. Circulation 1988;77:301-310

Jagger JD: Long term follow-up of inferior myocardial infarction. Prognostic significance of precordial ST segment depression. Aust NZ J Med 1985;15:681-684

Janse MJ, Kleber AG: Electrophysiological changes and ventricular arrhythmias in the early phase of regional myocardial ischemia. Circ Res 1981;49:1069-1081

Justis DL, Hession WT: Accuracy of 22-lead ECG analysis for diagnosis of acute myocardial infarction and coronary artery disease in the emergency department: a comparison with 12-lead ECG. Ann Emerg Med 1992;21:1-9

Kamakura S, Shimomura K, Ohe T, Matsuhisa M, Toyoshima H: The role of initial minimum potentials on body surface maps in predicting the site of accessory pathways in patients with Wolff-Parkinson-White syndrome. Circulation 1986;74:89-96

Kambara H, Phillips J: Long term evaluation of early repolarization syndrome (normal variant RS-T segment elevation). Am J Cardiol 1976;38:122-128

Kilpatrick D, Ball AJ, Briggs CM: Assessment of reperfusion in myocardial infarction by body surface electrocardiographic mapping. J Electrocardiol 1993;26:1-11

Kilpatrick D, Bell AJ, Briggs CM: Assessment of reperfusion in myocardial infarction by body surface electrocardiographic mapping. J Electrocardiol 1993;26:279-289

Kilpatrick D, Bell AJ: The relationship of ST elevation to eventual QRS loss in acute inferior myocardial infarction. J Electrocardiol 1989;22:343-348

Kilpatrick D, Bell AJ, Walker SJ: Derived epicardial potentials differentiate ischemic ST depression from ST depression secondary to ST elevation in acute inferior myocardial infarction in humans. J Am Coll Cardiol 1989;14:695-702

Kilpatrick D, Bell AJ, Walker SJ: Importance of the great vessels in the genesis of the electrocardiogram. Circ Res 1990;66:1081-1087

Klainman E, Sclarovsky S, Lewin RF, Topax O. Farbstein H, Pinchas A, Fohoriles L, Agmon J: Natural course of electrocardiographic components and stages in the first twelve hours of acute myocardial infarction. J Electrocardiol 1987;20:98-109

Kleber AG, Janse MJ, van Capelle FJ, Durrer D: Mechanisms and time course of S-T and T-Q segment changes during acute regional ischemia in the pig determined by extracellular and intracellular recordings. Circ Res 1978;42:603-613

Klocke FJ: Measurements of coronary flow reserve: defining pathophysiology versus making decisions about patient care. Circulation 1987;76:1183-1189

Kornreich F, Montague TJ, Rautaharju PM: Identification of first acute Q wave and non-Q wave myocardial infarction by multivariate analysis of body surface maps. Circulation 1991;84:2442-2453

Laks MM, Startt/Selvester RH: Computerized electrocardiography - an adjunct to the physician. N Engl J Med 1991;325:1803-1804

Lance GW, Williams WT : Computer programs for hierarchical polythetic classification. Comp J 1966;9:60-66

Lau J, Antman EM, Jimenez-Silva J, Kupelnick B, Mosteller F, Chalmers TC: Cumulative meta-analysis of therapeutic trials for myocardial infarction. N Engl J Med 1992;327:248-254

Lembo NJ, Starling MR, Dell'Italia LJ, Crawford MH, Chaudhuri TK, O'Rourke RA: Clinical and prognostic importance of persistent precordial (V1 -V4) electrocardiographic ST segment depression in patients with inferior transmural myocardial infarction. Circulation 1986;74:56-63

Lepeschkin E, Surawicz B: The duration of the Q-T interval and its components in electrocardiograms of normal persons. Am Heart J 1953;46:9-20

Liao Y, Liu K, Dyer A, Schoenberger JA, Shekelle RB, Collette P, Stamler J: Sex differential in the relationship of electrocardiographic ST-T abnormalities to risk of coronary death: 11.5 year follow-up findings of the Chicago heart association detection project in industry. Circulation 1987;75:347-352

Liebman J, Rudy Y, Diaz P, Thomas CW, Plonsey R: The spectrum of right bundle branch block as manifested in electrocardiographic body surface potential maps. J Electrocardiol 1984;17:329-346

London MJ, Hollenberg M, Wong MG, Levenson L, Tubau JF, Browner W, Mangano DT, SPI research group: Intraoperative myocardial ischemia: localization by continuous 12-lead electrocardiography. Anesthesiology 1988;69:232-241

Lux RL, Burgess MJ, Wyatt RF, Evans AK,Vincent GM, Abildskov JA: Clinically practical lead system for improved electrocardiography: Comparison with precordial grids and conventional lead systems. Circulation 1979;59:356-363

Lux RL, Evans AK, Burgess MJ, Wyatt RF, Abildskov JA: Redundancy reduction for improved display and analysis of body surface potential maps; I: spatial compression. Circ Res 1981;49:186-196

Lux RL, Smith CR, Wyatt RF, Abildskov JA: Limited lead selection for estimation of body surface potential maps in electrocardiography. IEEE Trans Biomed Eng 1978;25:270-276

MacDonald RG, Hill JA, Feldman RL : ST segment response to acute coronary occlusion: Coronary hemodynamic and angiographic determinants of direction of ST segment shift. Circulation 1986;74:973-979

Macfarlane PW, Laurie TDV: The normal electrocardiogram and vectorcardiogram, in Macfarlane PW, Laurie TDV eds. Comprehensive electrocardiograph. Theory and practice in health and disease. Pergamon Press, New York, 1989;1:218-229

Madias JE: A comparison of serial 49-lead precordial ECG maps and standard 6-lead precordial ECGs in patients with acute anterior Q wave myocardial infarction. J Electrocardiol 1989;22:115-124

Marcus EB, Yano K, MacLean CJ: Regression of Q waves following acute myocardial infarction. Am J Epidemiol 1989;129:105-111

Mark DB, Hlatky MA, Lee KL, Harrell FE, Califf RM, Pryor DB: Localizing coronary artery obstructions with the exercise treadmill test. Ann Intern Med 1987;106:53-55

Maroko PR, Libby P, Covell JW, Sobel BE, Ross JJr, Braunwald E: Precordial S-T segment elevation mapping: An atraumatic method for assessing alterations in the extent of myocardial ischemic injury. Am J Cardiol 1972;29:223-230

Marriott HJL, ed. Myocardial infarction, in : Practical electrocardiography. Williams and Wilkins, Baltimore, 1977;232-55

Matthews DE, Farewell VT: Using and understanding medical statistics, Krager, Basel, 1987

McPherson DD, Horacek BM, Johnstone DE, Lalonde LD, Spencer CA, Montague TJ: Q-wave infarction: pathophysiology of body surface potential map and ventriculographic patterns in anterior and inferior groups. Can J Cardiol (supplement A) 1986;91A-98A

McPherson DD, Horacek BM, Spencer CA, Johnstone DE, Lalonde LD, Cousins CL, Montague TJ: Indirect measurement of infarct size. Correlative variability of enzyme, radionuclear angiography, and body-surface-map variables in 34 patients during the acute phase of myocardial infarction. Chest 1985;88:841-848

Melin JA, Piret LJ, Roland JM, Vanbutsele RJM, Rousseau MF, Cosyns J, Brasseur LA, Beckers C, Detry J-MR: Diagnostic value of exercise electrocardiography and thallium myocardial scintigraphy in patients without previous myocardial infarction: a bayesian approach. Circulation 1981;63:1019-1024

Merri M, Benhorin J, Alberti M, Locati E, Moss AJ: Electrocardiographic quantitation of ventricular repolarization. Circulation 1989;80:1301-1308

Mikell FL, Petrovich J, Snyder MC, Taylor GJ, Moses HW, Dove JT, Batchelder JE, Schneider JA, Wellons HA: Reliability of Q-wave formation and QRS score in predicting regional and global left ventricular performance in acute myocardial infarction with sucessful reperfusion. Am J Cardiol 1986;57:923-926

Miller WT, Kertzer R, Bunk CL, Alexander LA: Normal variations in body surface electrocardiographic potential distributions during QRS: effects of exercise and exercise training. J Electrocardiol 1985;18:239-250

Miller WT, Spach MS, Warren RB: Total body surface mapping during exercise: QRS-T-wave changes in normal young adults. Circulation 1980;62:632-645

Mills RM, Young E, Gorlin R, Lesch M: Natural history of S-T segment elevation after acute myocardial infarction. Am J Cardiol 1975;35:609-614

Mirvis DM: Body surface distribution of electrical potential during atrial depolarization and repolarization. Circulation 1980a;62:167-173

Mirvis DM: Body surface distribution of repolarization forces during acute myocardial infarction. I. Isopotential and isoarea mapping. Circulation 1980b;62:878-887

Mirvis DM: Body surface distributions of repolarization potentials after acute myocardial infarction. II. Relationship between isopotential mapping and ST-segment potential summation methods. Circulation 1981;63:623-631

Mirvis DM: Current status of body surface electrocardiographic mapping. Circulation 1987;75:684-688

Mirvis DM, Ingram L, Holly MK, Wilson JL, Ramanathan KB: Electrocardiographic effects of experimental nontransmural myocardial infarction. Circulation 1985;71:1206-1214

Mirvis DM: Methods for body surface electrocardiographic mapping, in Mirvis DM edt. Body surface electrocardiographic mapping. Kluwer Academic Publishers, Bostin, 1988a;43-62

Mirvis DM: Methods for body surface electrocardiographic mapping, in Mirvis DM edt. Body surface electrocardiographic mapping. Kluwer Academic Publishers, Bostin, 1988b;137-142

Montague TJ, Gardner MJ, McPherson DD, Johnstone DE, Spencer CA, Lalonde LD, Horacek BM, Black SA, Tremayne HK, Trider PJ : Electrocardiographic and ventriculographic recovery patterns in Q wave myocardial infarction. J Am Coll Cardiol 1986a:8:521-528

Montague TJ, Johnstone DE, Spencer CA, Lalonde LD, Gardner MJ, O'Reilly MG, Horacek BM: Non-Q-wave acute myocardial infarction: Body surface potential mapping and ventriculographic patterns. Am J Cardiol 1986b;58:1173-1180

Montague TJ, Smith ER, Cameron DA, Rautaharju PM, Klassen GA, Felmington CS, Horacek BM: Isointegral analysis of body surface maps surface distribution and temporal variability in normal subjects. Circulation 1981:63;1166-1172

Montague TJ, Smith ER, Johnstone DE, Spencer CA, Lalonde LD, Bessoude RM, Gardner MJ, Anderson RN, Horacek BM: Temporal evolution of body surface map patterns following acute inferior myocardial infarction. J Electrocardiol 1984:17:319-328

Montague TJ, Smith ER, Spencer CA, Johnstone DE, Lalonde DE, Bessoudo RM, Gardner MJ, Anderson RN, Horacek BM.: Body surface electrocardiographic mapping in inferior myocardial infarction. Manifestations of left and right ventricular involvement. Circulation 1983;67:665-673

Morace G, Padeletti L, Porciana MC, Fantini F: Effects of isoproterenol on the "early repolarization" syndrome. Am Heart J 1979;97:343-347

Moses LE, Emerson JD, Hosseini H: Analysing data from ordered categories. N Engl J Med 1984;331:442-448

Muller JE, Maroko PR, Braunwald E: Evaluation of precordial electrocardiographic mapping as a means of assessing changes in myocardial ischemic injury. Circulation 1975;52:16-27

Muller JE, Maroko PR, Braunwald E: Precordial electrocardiographic mapping. A technique to assess the efficacy of interventions designed to limit infarct size. Circulation 1978;57:1-8

Musso E, Stilli D, Macchi E, Regoliosi G, Brambilla C, Francescon P, Bo M, Rolli A, Botti G, Taccardi B: Body surface maps in left bundle branch block uncomplicated or complicated by myocardial infarction, left ventricular hypertrophy or myocardial ischemia. J Electrocardiol 1987;20:1-20

Myerburg RJ, Castellanos A: Resolution of nonspecific repolarization patterns from body surface signals: a new horizon of clinical electrocardiography. J Am Coll Cardiol 1989;14:703-704

Myers GB, Klein HA, Hiratzka T: Correlations of electrocardiographic and pathologic findings in anteroposterior infarction. Am Heart J 1949;37:205-236

Nahum LH, Mauro A, Chernoff HM, Sikand RS: Instantaneous equipotential distribution on surface of the human body for various instants in the cardiac cycle. J Appl Physiol 1951;3:454-464

Nakagaki O, Yano H, Mitsutake A, Kikuchi Y, Takeshita A, Kanaide H, Nakamura M: Re-elevation of ST segment on precordial mapping in natural time course following acute anterior myocardial infarction. Jap Circ J 1981;45:562-568

Nattel S, Warnica JN, Ogilvie RI : Indications for admission to a coronary care unit in patients with unstable angina. Can Med Assoc J 1980;122:180-184

Nelson CV: Human thorax potentials. Ann NY Acad Sci 1957;65:1014-1050

Nichols TL, Mirvis DM: Frequency count of the electrocardiogram. Spatial features and effects of myocardial infarction. J Electrocardiol 1985;18:185-194

Nielson BL: ST-segment elevation in acute myocardial infarction. Prognostic importance. Circulation 1973;48:338-345

Niess GS, Logic JR, Russell RO, Rackley CE, Rogers WJ: Usefulness and limitations of thallium-201 myocardial scintigraphy in delineating location and size of prior myocardial infarction. Circulation 1979;59:1010-1020

Niggemann B, Gann D: The electrocardiogram in patients with acute myocardial infarctions treated with intracoronary streptokinase. J Electrocardiol 1984;17:263-270

Ohta T, Toyama J, Ohsugi J, Kinoshita A, Isomura S, Takatsu F, Ishikawa H, Nagaya T, Yamada K: Correlation between body surface isopotential maps and left ventriculograms in patients with old anterior myocardial infarction. Jap Heart J 1981;22:747-761

Oliva PB: Unstable rest angina with ST-segment depression. Pathophysiologic considerations and therapeutic implication. Ann Intern Med 1984;100:424-440

Olliff BC, Horan LG, Flowers NC: Correlative analysis of vectorcardiograms and serial instantaneous surface potential maps in normal young men. Am Heart J 1972;83:780-790

Osugi J, Ohta T, Toyama J, Takatsu F, Nagaya T, Yamada K: Body surface isopotential maps in old inferior myocardial infarction undetectable by 12 lead electrocardiograms. J Electrocardiol 1984;17:55-62

Ouyang P, Brinker JA, Mellits ED, Weisfeldt ML, Gerstenblith G: Variables predictive of sucessful medical therapy in patients with unstable angina: selection by multivariate analysis from clinical, electrocardiographic, and angiographic evaluations. Circulation 1984;70:367-376

Patterson DLH, Treasure T: The culprit coronary artery lesion. Lancet 1991;338:1379-1381

Paulin S: Assessing the severity of coronary lesions with angiography. N Engl J Med 1987;316:1405-1407

Perloff JK: The recognition of strictly posterior myocardial infarction by conventional scaler electrocardiography. Circulation 1964;30:706-714

Pham-Huy H, Gulrajani RM, Roberge FA, Nadeau RA, Mailloux GE, Savard P: A comparative evaluation of three different approaches for detecting body surface isopotential map abnormalities in patients with myocardial infarction. J Electrocardiol 1981;14:43-55

Pichler M, Shah PK, Peter T, Singh B, Berman D, Shellock F, Swan HJC: Wall motion abnormalities and electrocardiographic changes in acute transmural myocardial infarction: implications of reciprocal ST segment depression. Am Heart J 1983;106:1003-1009

Pierard LA, Chapelle J-P, Albert A, Dubois C, Kulbertus HE : Characteristics associated with early (≤ 3 months) versus late (> 3 months to ≤ 3 years) mortality after acute myocardial infarction. Am J Cardiol 1989;64:315-318

Pipberger HV, Doyle JT, Schlesselman S, Pipberger HA, Halperin M, McManus Cd, Appel M, Yamamoto WS: The orthogonal electrocardiogram as risk indicator for the prediction of myocardial infarction and/or cardiac death. J Electrocardiol 1986:19:327-336

Pozen MW, D'Agostino RB, Selker HP, Sytkowski PA, Hood WB: A predictive instrument to improve coronary-care-unit admission practices in acute ischemic heart disease. A prospective multicenter clinical trial. New Engl J Med 1984:310:1273-1278

Quyyumi AA, Rubens MB, Rickards AF, Crake T, Levy RD, Fox KM: Importance of "reciprocal" electrocardiographic changes during occlusion of left anterior descending coronary artery. Studies during percutaneous transluminal coronary angioplasty. Lancet 1986;8471:347-350

Rautaharju PM, Warren JW, Jain U, Wolf HK, Nielsen CL: Cardiac infarction injury score: an electrcardiographic coding scheme for ischemic heart disease. Circulation 1981;64:249-256

Reid PR, Taylor DR, Kelly DT, Weisfeldt ML, Humphries JO'N, Ross RS, Pitt B: Myocardial-infarct extension detected by precordial ST-segment mapping. N Engl J Med 1974;290:123-128

Rembold CM, Watson D : Posttest probability calculation by weights. Ann Intern Med 1988;108:115-120

Roubin GS, Shen WF, Nicholson M, Dunn RF, Kelly DT, Harris PJ: Anterolateral ST segment depression in acute inferior myocardial infarction: angiographic and clinical implications. Am Heart J 1984;107:1177-1182

Rudy Y, Ploinsey R: A comparison of volume conductor and source geometry effects on body surface and epicardial potentials. Circ Res 1980;46:283-291

Sane U : Early diagnosis of acute myocardial infarction with special reference to the diagnosis of the intermediate coronary syndrome : a clinical study. Acta Med Scand (supplement) 1972;45:1-76

Savage RM, Wagner GS, Ideker RE, Podolsky SA, Hackel DB: Correlation of postmortem anatomic findings with electrocardiographic changes in patients with myocardial infarction. Retrospective study of patients with typical anterior and posterior infarcts. Circulation 1977;55:279-285

Schor S, Behar S, Modan B, Barell V, Drory J, Kariv I : Deposition of presumed coronary patients from an emergency room : a follow-up study. JAMA 1976;236:941-943

Schuster EH, Bulkley BH: Ischemia at a distance after myocardial infarction: a cause of early post infarction angina. Circulation 1980;62:509-515

Seager QB : Cardiac enzymes in the evaluation of chest pain. Ann Emerg Med 1980;9:346-349

Selwyn AP, Fox K, Welman E, Shillingford JP: Natural history and evaluation of Q waves during myocardial infarction. Br Heart J 1978;40:383-387

Selwyn AP, Shillingford JP: Praecordial mapping of Q waves and RS ratio changes in acute myocardial infarction. Cardiovasc Res 1977;11:167-171

Shah PK, Pichler M, Berman DS, Maddahi J, Peter T, Singh BN, Swan HJC: Noninvasive identification of a high risk subset of patients with acute inferior myocardial infarction. Am J Cardiol 1980;46:915-921

Snedecor GW, Cochran WG: Statistical methods, Iowa State University Press, Ames, 1980;175-191

Sohi GS, Flowers NC, Horan LG, Sridharan MR, Johnson JC: Comparison of total body surface map depolarization patterns of left bundle branch block and left-axis deviation. Circulation 1983;67:660-664

Sohi SG, Flowers NC: Body surface map patterns of altered depolarization and repolarization in right bundle branch block. Circulation 1980;61:634-640

Sox HC: Probability Theory in the use of diagnostic tests. Ann Intern Med 1986;104:60-66

Spach MS, Barr RC, Benson DW, Walston AII, Warren RB, Edwards SB: Body surface low-level potentials during ventricular repolarization with analysis of the ST segment. Variability in normal subjects. Circulation 1979a;59:822-836

Spach MS, Barr RC: Physiological correlates and clinical application of isopotential surface maps, in Hoffman I, Hamby RI and Glassman E, eds. Vectorcardiography 2. North Holland Publishing,Amsterdam, 1971;131-141

Spach MS, Barr RC, Warren RB, Benson DW, Walston AII, Edwards SB: Isopotential body surface mapping in subjects of all ages: Emphasis on low-level potentials with analysis of the method. Circulation 1979b;59:805-821

Spach MS, King TD, Barr RC, Boaz DE, Morrow MN, Herman-Giddens S: Electrical potential distribution surrounding the atria during depolarization and repolarization in the dog. Circ Res 1969;24:857-873

Spodick DH: Differential characteristics of the electrocardiogram in early repolarization and acute pericarditis. N Engl J Med 1976:295:523-526

Stafford AN, Lloyd BL, Thompson PL: Anterior ST segment depression in inferior myocardial infarction: effects on complications and long term survival. Aust NZ J Med 1986;16:378-384

Stanley PC, Pilkington TC, Morrow MN: The effects of thoracic inhomogeneties on the relationship between epicardial and torso potentials. IEEE Trans Biomed Eng 1986:33:273-280

Sugishita Y, Koseki S, Matsuda M, Ajisaka R, Iida K, Ito I, Ooshima M, Takeda T, Akisada M: Significance of ST-segment and T wave changes in the resting electrocardiograms of patients with exertional angina, studied by exercise radionuclide angiocardiograms. J Electrocardiol 1985;18:175-184

Surawicz B, Lasseter KC: Electrocardiogram in pericarditis. Am J Cardiol 1970;26:471-474

Suzuki K, Toyama S, Yoshino K, Fudemoto Y: Relationship between the location of the infarcted area in body surface isopotential mapping and the location of myocardial infarction in ventriculography. J Electrocardiol 1984;17:47-54

Sylven JC, Horacek BM, Spencer CA, Klassen GA, Montague TJ: QT interval variability on the body surface. J Electrocardiol 1984;17:179-188

Tamaki S, Nakajima H, Murakami T, Yui Y, Kambara H, Kadota K, Yoshida A, Kawai C, Tamaki N, Mukai T, Ishii Y, Torizuka K: Estimation of infarction size by myocardial emission computed tomography with thallium 201 and its relation to creatine kinase-MB release after myocardial infarction in man. Circulation 1982;60:994-1001

Teh BS, Walsh J, Bell AJ, Walker SJ, Kilpatrick D: Electrical current paths in acute pericarditis. J Electrocardiol 1993;26:291-300

Ticcardi B: Body surface distribution of equipotential lines during atrial depolarization and ventricular repolarization. Circ Res 1966;19:865-878

Ticcardi B: Distribution of heart potentials on dog's thoracic surface. Circ Res 1962;11:862-869

Ticcardi B: Distribution of heart potentials on the thoracic surface of normal human subjects. Circ Res 1963;12:341-352

Toyama J, Suzuki K, Koyama M, Yoshino K, Fujimoto K: The body surface isopotential mapping of the QRS wave in myocardial infarction: A comparative study of the scintigram with thallium-201. J Electrocardiol 1982;15:241-248

Toyama J, Suzuki K, Yoshino K, Fujimoto K: A comparative study of body surface isopotential mapping and the electrocardiogram in diagnosis of myocardial infarction. J Electrocardiol 1984;17:7-13

Toyama S, Suzuki K, Koyama M: The isopotential mapping of the T wave in myocardial infarction. J Electrocardiol 1980;13:323-330

Toyama S, Suzuki K, Takahashi T, Yamashita Y: Epicardial isopotential mapping from body surface isopotential mapping in myocardial infarction. J Electrocardiol 1985;18:277-286

Toyama S, Suzuki K, Takahashi T, Yamashita Y: Myocardial infarction size and location: a comparative study of epicardial isopotential mapping, thallium-201 scintigraphy, electrocardiography and vectorcardiography. J Electrocardiol 1987;20:203-211

Varat MA: Non-transmural infarction: clinical distinction between patients with ST depression and those with T wave inversion. J Electrocardiol 1985;18:15-20

Vincent GM, Abildskov JA, Burgess MJ, Miller K, Lux RL, Wyatt RF: Diagnosis of old inferior infarction by body surface isopotential mapping. Am J Cardiol 1977;39:510-515

Wackers FJT, Becker AE, Samson G, Sokole EB, van der Schoot JB, Vet AJTM, Lie KI, Durrer D, Wellens H: Location and size of acute transmural myocardial infarction estimated from thallium 201 scintiscan: a clinicopathological study. Circulation 1977;56:72-78

Walker SJ, Bell AJ, Loughhead MG, Lavercombe PS, Kilpatrick D: Spatial distribution and prognostic significance of ST segment potentials in acute inferior infarction determined by body surface mapping. Circulation 1987;76:289-297

Walker SJ, Kilpatrick D: A validation of derived epicardial potential distributions by prediction of the coronary artery involved in acute myocardial infarction in humans. Circulation 1987;76:1282-1289

Walker SJ, Lavercombe PS, Loughhead MG, Kilpatrick D: A body surface mapping system with immediate interactive data processing, in Ripley KL eds: Computers in Cardiology. IEEE Computer Society Press, Washington DC, 1983:305-308

Waller AD: A demonstration on man of electromotive changes accompanying the heart's beat. J Physiol 1887;8:229-234

Warner R, Hill NE, Sheehe PR, Mookherjee S, Fruehan CT, Smulyan H: Improved electrocardiographic criteria for diagnosis of inferior myocardial infarction. Circulation 1982;66:422-428

Wasserman AG, Bren GB, Ross AM, Richardson DW, Hutchinson RG, Rios JC: Prognostic implications of diagnostic Q waves after myocardial infarction Circulation 1982;65:1451-1455

Wasserman AG, Ross AM, Bogaty D, Richardson DW, Hutchinson RG, Rios JC: Anterior ST segment depression during acute inferior myocardial infarction: evidence for the reciprocal change theory. Am Heart J 1983;106:516-520

Wegman EJ: Nonparametric probability density estimation : 1. a summary of the available methods. Technometrics 1972;14:533-546

Willems JL, Abreu-Lima C, Arnaud P, von Bemmel JH, Brohet C, Degani R, Denis B, Gehring J, Graham I, van Herpen G, Machado H, Macfarlane PW, Michaelis J, Moulopoulos SD, Rubel P, Zywietz C: The diagnostic performance of computer programs for the interpretation of electrcardiograms. N Engl J Med 1991;325:1767-1773

Wilson FN, Macleod AC, Barker PS: Electrocardiographic leads which record potential variations of the heart at a single point. Proc Soc Exp Biol Med 1932;29:1011-1012

Yamada K, Toyama J, Sugenoya J, Wada M, Sugiyama S: Body surface isopotential maps. Clinical application to the diagnosis of myocardial infarction. Jap Heart J 1978;19:28-45

Yamaki M, Ikeda K, Kubota I, Nakamura K, Hanashima K, Tsuiki K, Yasui S: Improved diagnostic performance on the severity of left ventricular hypertrophy with body surface mapping. Circulation 1989;79:312-323

Yamashita Y: Inverse solution in electrocardiography: determining epicardial from body surface maps by using the finite element method. Jap Circ J 1981;45:1312-1322

Yasumura S, Kubota I, Ikeda K, Tsuiki K, Yasui S: Using body surface mapping to detect vulnerability to ventricular arrhythmias in patients with coronary artery disease. J Electrocardiol 1987;20:114-120

Young BD, Macfarlane PW, Lawrie TDV: Normal thoracic surface potentials. Cardiovasc Res 1974;8:187-193

Zaret BL, Martin ND, Flamm MD: Myocardial imaging for non-invasive evaluation of regional perfusion at rest and after exercise, in Strauss HW eds. Cardiovascular nuclear medicine, CV Mosby Co, St Louis, 1974:151-210

Zmyslinski RW, Akiyama T, Biddle TL, Shah PM: Natural course of the S-T segment and QRS complex in patients with acute anterior myocardial infarction. Am J Cardiol 1979;43:29-34